PIEZOELECTRIC ENERGY HARVESTING FROM LOW AND VARIABLE FREQUENCY VIBRATIONS

PHOSY PANTHONGSY

A THESIS SUBMITTED IN PARTIAL FULFILLMENT

OF THE REQUIREMENTS FOR THE DEGREE OF

DOCTOR OF ENGINEERING IN ELECTRICAL ENGINEERING

FACULTY OF ENGINEERING

KING MONGKUT'S INSTITUTE OF TECHNOLOGY LADKRABANG

2019

KMITL-2019-EN-D-018-051

PIEZOELECTRIC ENERGY HARVESTING FROM LOW AND VARIABLE FREQUENCY VIBRATIONS

PHOSY PANTHONGSY

A THESIS SUBMITTED IN PARTIAL FULFILLMENT

OF THE REQUIREMENTS FOR THE DEGREE OF

DOCTOR OF ENGINEERING IN ELECTRICAL ENGINEERING

FACULTY OF ENGINEERING

KING MONGKUT'S INSTITUTE OF TECHNOLOGY LADKRABANG

2019

KMITL-2019-EN-D-018-051

Thesis Title	Piezoelectric Energy Harvesting from Low and Variable Frequency Vibrations
Student	Mr. Phosy Panthongsy
Student ID.	59601028
Degree	Doctor of Engineering
Program	Electrical Engineering
Year	2019
Thesis Advisor	Asst. Prof. Dr. Don Isarakorn

ABSTRACT

With plenty of vibrations available in the surrounding environment, converting kinetic energy into useable electricity for powering the low-powered wireless electronic devices has received tremendous attention over the last decade and continues to grow rapidly. In general, many energy harvesters have to face the challenge of low and variable frequency vibrations especially of human movement, i.e., the frequency of a vibration source usually does not match with the resonant frequency of a harvester, resulting in low energy conversion efficiency. To address this problem, three kinds of approaches, frequency self-tuning, broadband and frequency up-conversion strategies have been recently investigated, which will be practical depending on the application. In this thesis, the energy harvesting floor tile specifically targeted to convert kinetic energy from human footsteps into useable electricity is focused. After the general introduction of research scope, the relevant parameters for the design of mechanism are analyzed. The operating principle of the tile is based on frequency up-conversion in which low frequency input vibrations are converted into high frequency vibrations of an electromechanical transduction. The piezoelectric cantilevers are used as transducers, the operational frequency of which is converted up by an interaction between a permanent magnet and an iron bar. Vertical displacement of the oscillating cantilevers is localized with a stopper preventing damage to the piezoelectric layer from shock or over-displacement excitation. The magnetic field density is investigated

through finite element analysis simulation in order to define the optimal magnetizing gaps. Experimentally, the following structure is initially configured as a test bench to characterize the performance of PZT cantilever, verify the optimal parameters setup and validate the design. The prototype is then scaled up by accommodating 24 PZT cantilevers followed by the experiments to evaluate its energy harvesting performance in both laboratory and real word scenarios. The results show a successful piezoelectric energy harvesting floor tile, which can be further used to power up a low-power wireless sensor node. The energy conversion efficiency reaches 17.12 % demonstrating the potential of harvesting energy from human footstep.

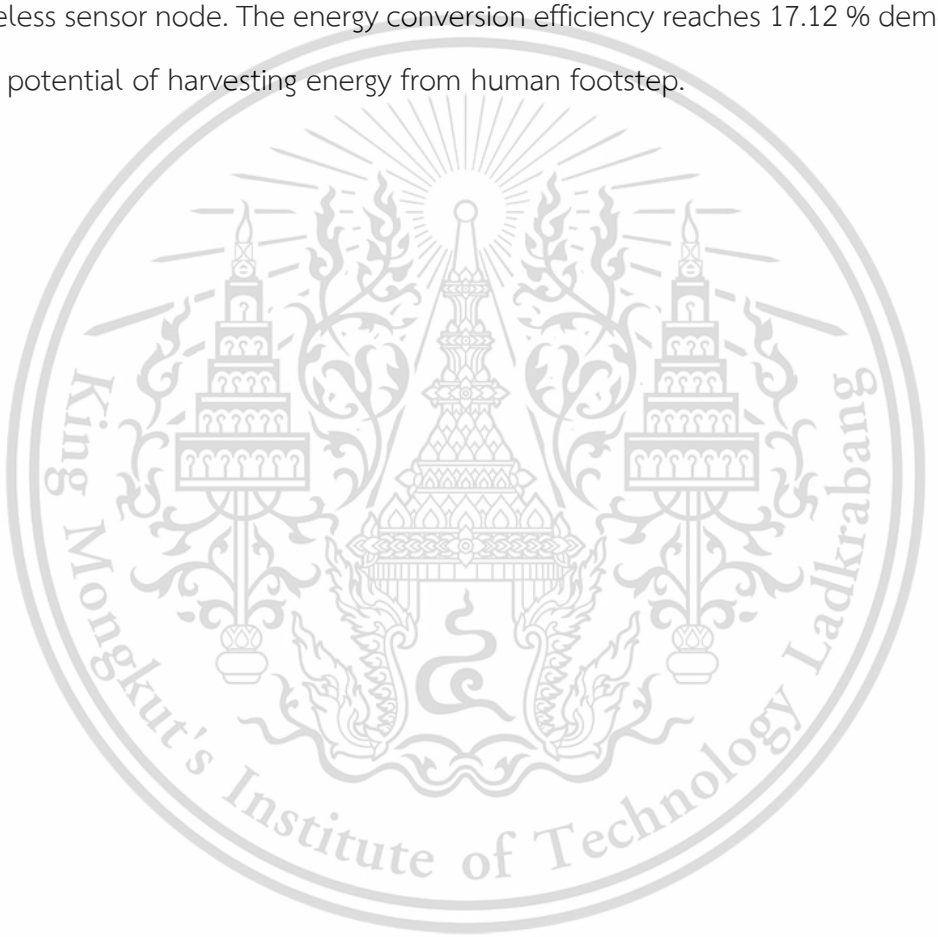

ACKNOWLEDGEMENTS

There are many people I need to thank for their advice, help and encouragement throughout the completion of this thesis as well as sharing the hardships and the great movements with me.

Foremost, I would like to express my sincerest gratitude to my advisor and co-advisor, Asst. Prof. Dr. Don Isarakorn and Prof. Dr. Kazuhiko Hamamoto, respectively. Working with my both supervisors has been a great pleasure as I have enjoyed the liberty to choose my own paths and consistently received their professional guidance and support when in doubt. Their incredible patience, expertise and suggestions are useful not only for dealing with the challenges of project I have worked on, but also for inspiring me in almost every aspect of life.

I was lucky to work with and learn from amazing researchers. Among them, I would like to thank to Dr. Pattanaphong Janphuang, Mr. Songmoung Nundrakwang and Mr. Somphong Suphachiaraphan for fruitful discussion, sharing the useful information on the mechanism design of the energy harvesting floor tile and their help in choosing piezoelectric cantilevers and my thanks also goes to Asst. Prof. Dr. Noppadol Maneerat for providing the mechanical parts contributed in configuration of a test bench.

I gratefully acknowledge the AUN/SEED-Net for full financial support for my sandwich-PhD studies at the host institution in Thailand, King Mongkut's Institute of Technology Ladkrabang (KMITL) and the Japanese supporting university, Tokai University. I also want to extend my grateful to the National Research Council of Thailand for their financial support.

I am not exaggerating when I say that the Multi-Scale Electromechanical System Laboratory is the best working environment I have ever been in. Everyone in this laboratory is very kind, friendly and helpful, sharing their idea and techniques in carrying out the research even many lunches and coffee/tea breaks. My acknowledge

goes to all those, Mr. Subhawat Jayasvasti, Mr. Vorapong Sutthisaksri and Mr. Thapanun Sudhawiyangkul.

I greatly appreciate the support from program officers (JICA Project for AUN/SEED-Net), especially Mrs. Arunee Suvarnatarn, Mr. Krit Manator and Ms. Waranuch Tanubamrungsuk.

Finally, I am deeply grateful to my beloved family for their unconditional and constant love, continued support and encouragement during the entire study period.

Phosy Panthongsy

CONTENTS

CONTENTS (Cont.)

LIST OF TABLES

LIST OF FIGURES

LIST OF FIGURES (Cont.)

LIST OF FIGURES (Cont.)

NOMENCLATURE

P	Polarization
S_j	Mechanical strain
E_i	Electric field
d_{ij}	Piezoelectric constant
T_j	Stress
s_{ij}^E	Elastic compliance coefficient
D_i	Electric displacement
ε_{ij}^T	Permittivity
ε_e	Dielectric permittivity
ε_r	Relative permittivity
ε_0	Permittivity in free space
u_e	Electrical density
F	Applied force
$f(t)$	Driving force
d	Piezoelectric coefficient
A	Area of piezoelectric element
m	Proof mass
k	Spring constant
c_m	Mechanical damping
c_e	Electrical damping
$z(t)$	Displacement
F_e	Electrical damping force
W	Energy dissipated in the damper every cycle
$\dot{z}$	Velocity of a moving mass
z_{act}	Initial mass displacement
ω_n	Natural frequency

NOMENCLATURE (Cont.)

ω_d	Damped natural frequency
P_{total}	Total power output
ς_T	Combined mechanical and electrical damping ratio
ς_e	Electrical damping ratio
γ	Frequency ratio
d_1	Air gap between the plastic stopper and the PZT cantilever
d_2	Air gap between the permanent magnet and the iron bar
F_{iM}	Attracting force from the permanent magnet
B	Magnetic flux density
A_i	Cross section of the area of the pole
μ_0	Permeability of the air
F_L	Compressive force
F_{jS}	Restoring force of the spring
F_{iZ}	Resultant force in the z-axis
F_{iC}	Restoring force
F_{ix}	Force in the x-axis
m_L	Mass of the pedestrian
g	Gravitational acceleration
k_{jS}	Spring constant
k_{iC}	Effective spring constant
h	Displacement from the equilibrium position of the spring
θ	Top surface angle of permanent magnet
m_{iT}	Total mass of the magnet and the stainless-steel mass
$(EI)_{Cantilever}$	Effective bending modulus of the unimorph piezoelectric cantilever
l	Length of the piezoelectric and elastic layers

NOMENCLATURE (Cont.)

E_p	Young's modulus of the piezoelectric
E_e	Young's modulus of the elastic layers
I_p	Moments of inertia of the piezoelectric
I_e	Moments of inertia of the elastic layers
w_p	Widths of the piezoelectric
w_e	Widths of the elastic layers
t_p	Thicknesses of the piezoelectric
t_e	Thicknesses of the elastic layers
t_n	Distance of the neutral plane in the piezoelectric layer
$P(t_m)$	Instantaneous power
$V_L(t_m)$	Transient voltage across the resistive load
t_m	Particular time identifying the voltage sample
t_N	Entire time of voltage sampling
P_{Avg}	Average power
N	Number of voltage samples
R_L	Resistance of the resistive load
E_{input}	Input mechanical energy
k_{eff}	Effective spring constant
z_0	Tip displacement of a PZT cantilever
T_P	Time period of oscillation
M	Seismic mass
T_d	Step time interval
d_3	Distance between stainless steel masses along x-axis
d_4	Distance between stainless steel masses along y-axis

Chapter 1

Introduction

This chapter is purposed to briefly set the scope of this thesis and to outline the research goals as well as the thesis's structure. The playing role and main challenge of the wireless electronic devices relying on battery are identified, the promising solution methods of which are roughly offered before a motivation is created.

1.1 Wireless Sensor Applications and Energy Harvesting

Wireless sensor node emerged decades ago has been continuously important in a variety of fields including industry, agriculture, infrastructure, disaster prediction and environment monitoring due to its ability to track information in a hard-to-reach location at a lower cost than wire solution. Following the feature of communication without wiring and recent trend of electronics technology that electronic components are reduced in size and power consumption, many existed wireless sensor nodes are powered by battery. However, there are several issues on battery use such as limited energy storage capacity, battery lifespan, and inconvenient maintenance of depleted batteries in unreachable location especially implanted sensors. Therefore, harvesting ambient environment energy to supply sustainable electrical power to devices such as an energy autonomous system is highly desirable. Energy powering small embedded device is typically harvested from light, thermal or vibration sources. Environmental vibration has particularly attracted many researchers because of its ubiquity.

1.1.1 Transduction Mechanisms for Vibrational Energy Harvester

The main transduction approaches employed for vibrational energy harvesting have generally been divided into three different categories [1]: electrostatic, electromagnetic and piezoelectric transductions as shown in figure 1.1.

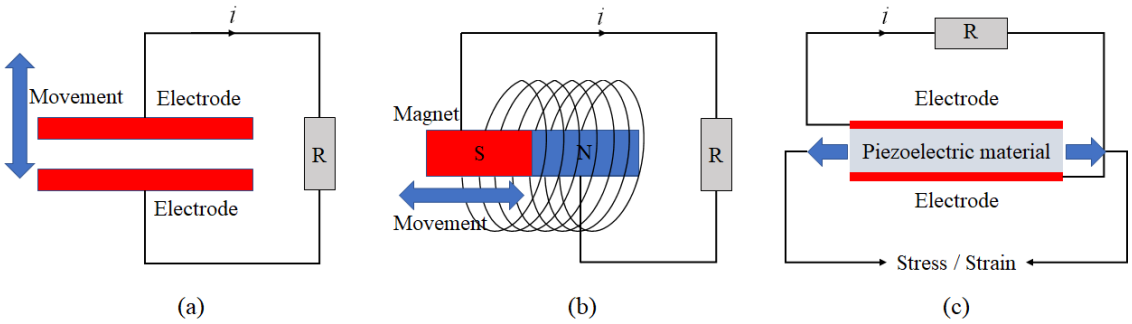

Figure 1.1 Vibration-to-electric energy conversion; (a) electrostatic, (b) electromagnetic, and (c) piezoelectric transductions.

• **Electrostatic Transduction:** the generators based on this principle are fundamentally capacitive structure, which are configured from two plates separated by air, vacuum or any dielectric materials. Being applied the external vibration, the plates of a charged variable capacitor is separated from each other, and mechanical energy is turned into electrical energy. Advantageously, these designs are fabricable as miniature scale with good performance which are appropriate for integration in Micro-Electro-Mechanical Systems (MEMS). However, the drawback can be found that the high priming voltage is required for their operation. Although the use of electret materials can eliminate the priming voltages requirement, it has a shorter lifetime [2]–[4].

• **Electromagnetic Transduction:** a relative motion between a coil and a permanent magnet is used to convert the kinetic energy of the vibrations into electrical energy, following the Faraday's law of induction. The electromagnetic generators are efficient at larger scale applications and commercially available as well. The problem with these generators is the micro-scale applications. The miniature scale device limits the number of coils turns and the moving magnitude of coil turn or permanent magnet, resulting a low output voltage.

• **Piezoelectric Transduction:** this type of transduction mechanism uses the piezoelectric material that give the ability to produce the electrical energy when it is deformed by the appliance of external stress or vice versa. This transduction mechanism should be the simplest technique due to the direct energy conversion

with a relative high-power density. Otherwise, it has the low-profile structure, which is easy to configuration and is suitable for micro-scale applications. The downside is that the piezoelectric materials are the brittle ceramic, the lifespan of which can be reduced by the long-term vibration and high kinetic force. Moreover, the energy conversion efficiency depends on the material and mechanical properties.

1.1.2 Comparison of Vibration-to-Electric Energy Conversion Mechanisms

While each type of transduction mechanisms presents the best depending on the applications, the quick comparison among them is possible due to the likely energy density. This approach has been reported by Roundy *et al.* [5]. They summarized the maximum energy densities of three kinds of transducers as shown in Table 1.1. It is noticed that the piezoelectric generators can produce the highest power output for a given size.

Table 1.1 Comparison of energy density among three kinds of mechanisms

Type	Practical maximum (mJ/cm^3)	Aggressive maximum (mJ/cm^3)	Assumptions
Electrostatic	4.0	44	3×107 V m^{-1}
Electromagnetic	24.8	400	0.25 T
Piezoelectric	35.4	355	PZT-5H

From the advantage and drawback of transduction mechanisms mentioned previously and a given compassion, the piezoelectric transduction is of much interest due to its high energy generation capability with a simple structure, highest output energy density and simplicity of configuration. Therefore, it will be focused on this thesis.

1.2 Motivation

As known in the field of energy harvesting, the piezoelectric energy harvesters are most effective at much high frequencies. Commonly, their resonant frequency is closely matched to the frequency of the surrounding vibration sources in order to achieve maximum power generation. However, this means is not a good option for conversion of low frequency and variable vibration over time. The generated electrical energy drops significantly when the resonant frequency of the harvesters deviates far from the frequency of the vibration source. Furthermore, the vibrations created by both natural source and man-made means rely on the random or semi-random phenomena, and their energy is spread over a certain band, for instance, human motion (< 10 Hz), car vibrations (< 20 Hz) and guard rail on the street (< 50 Hz) [6]. In addition to these data, more examples can be found in [7], [8]. Therefore, to address these challenges, the piezoelectric energy harvesters based on frequency self-tuning, broad band and frequency up-conversion principles have been investigated recently; a more detail will be explained in chapter 2. Among of them, the frequency up-conversion strategy presents a good deal with very low frequency like human movement in which to make the cantilever or buzzer disk of a piezoelectric harvester deflect initially and then leave it to oscillate freely. An initial deflection can be implemented by mechanical contact or by non-contact magnetic interaction. The integration of contact frequency up-conversion mechanism to a harvester offers the effective induction of initial deflection, but the core challenge is the decrease in life span of the piezoelectric cantilever. Otherwise, the main advantage of non-contact frequency up-conversation mechanism is that the piezoelectric cantilevers do not have to suffer repeated damaging physical contact with anything, making their operation more reliable than that of the contact frequency up-conversation mechanism. However, the energy generated by a non-contact generator drops significantly at high speed of magnetic plucking. For these reasons, an efficient energy harvester with frequency up-conversion mechanism that has a long operational lifetime and suffers

no effect of high plucking speed is of much interest, which will be investigated in this thesis.

1.3 Research Objectives

With a great number of pedestrians flowing in public places every day such as in train station, shopping center, sightseeing etc., (e.g., a few busy places in Thailand; the total number of tourists to Siam Paragon mall is in a range of 180,000-200,000 people per day in 2017 [9]; the passenger stranding at Suvarnabhumi airport is approximately 195,000 per day in 2017 [10]; and the average daily ridership of 10 stations of BTS Skytrain is 660,790 people during 2017-2018 [11]. These numbers are continuing to increase every year), converting the kinetic energy of human footstep into usable electric energy is a very attracting topic. It should enable the battery-less systems in the future due to a huge energy source available. Therefore, the objectives of this research are to design, realize and evaluate the piezoelectric energy harvesting floor tile using the frequency up-converting mechanism. To this end, the specific goals in this thesis can be addressed as follows:

- Develop a test bench for characterization of piezoelectric cantilever based on frequency up-converting energy harvester.
- Develop the frequency up-converting technique that make no effect on lifetime of piezoelectric cantilever for a long-term use.
- Develop the finite element (FE) models used to study the magnetic interaction in optimization of structural configuration.
- Investigate the energy harvesting performance and reliability of piezoelectric cantilever targeted to use in the energy harvesting floor tile.
- Verify the feasibility of designed mechanism.
- Evaluate the scaled-up prototype in both simulated and real scenarios.

1.4 Structure of Thesis

Regarding to the framework of this project, the thesis is structured with five chapters and the outline of each one is as follows:

- Chapter 2 introduces the piezoelectricity, piezoelectric material selection and literature review of current strategies for low and variable frequency vibration energy harvesting. The advantage and drawback of such strategies are clarified to identify an appropriate one for human motion energy harvesting and then adapt it to the energy harvester designed in chapter 3.
- Chapter 3 describes the concept of energy harvesting floor tile combined with the frequency up-conversion principle. The following structure is configured as a test bench for characterizing the performance of piezoelectric cantilever and validation of the designed mechanism in chapter 4 as well. The magnetic coupling used to up-convert the operational frequency of piezoelectric cantilever is determined by the finite element analysis simulation. The method to compute the performance of a piezoelectric cantilever based on frequency up-converting energy harvester is given and the testing results are introduced and discussed.
- Chapter 4 provides the experimental validation to verify the feasibility of the designed mechanism by examining its energy harvesting behavior with simulated human footstep and the magnetic interaction effecting on the oscillating piezoelectric cantilever. The energy harvesting floor tile is then prototyped and emulated in the laboratory and real word experiments. Its capability to power up a low-power wireless sensor node is considered.
- Chapter 5 summarizes the finding of this research and gives the recommendations for future work.

Chapter 2

Piezoelectric Energy Harvesting

This chapter presents a more detail of piezoelectric conversion. The criterion for piezoelectric material selection in this research is provided. Moreover, the literature review of low frequency and random vibration energy harvesting strategies will be discussed to find an optimal technique for a very low frequency excitation like human movement. The finding of this chapter will contribute to the design of energy harvesting floor tile.

2.1 Piezoelectricity

The piezoelectricity was originally discovered by Pierre and Jacque Curie in 1880, which results from an electromechanical coupling between mechanical and electrical states in quartz. When the certain types of crystals are compressed or tensed, the internal generation of the electrical charge is offered. Reversely, if subjected to an electrical field, such materials will produce the internal strain affecting on mechanical deformation. These phenomena are named as the piezoelectric direct and reverse effects as shown in figure 2.1, respectively.

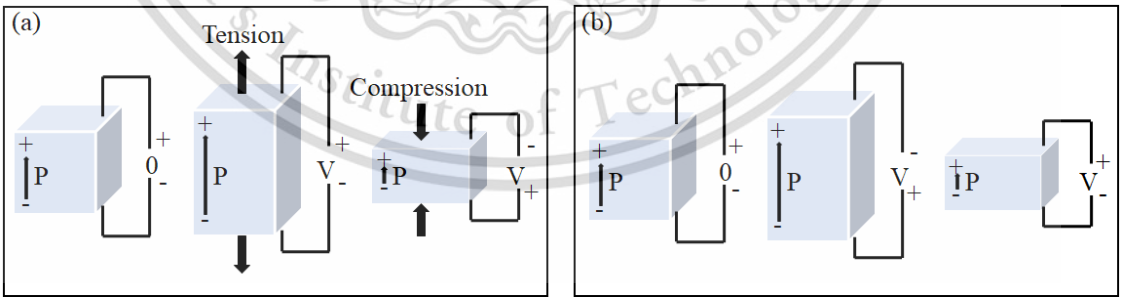

Figure 2.1 (a) Direct piezoelectric effect and (b) reverse piezoelectric effect where P represents the direction of polarization.

Naturally, the crystals have many molecules and each one has an individual polarization (P) with random direction as illustrated in figure 2.2. One end is negative

charged and other end is positives charged, called a dipole. To produce the piezoelectric effect, the process called poling is implemented to lie the polarization of all dipoles in one direction. The polar axis is an imaginary line running through the center of both positive and negative charged of molecule. For the poling process, the piezoelectric substance is heated under the application of a strong electric field. The heat lets the molecules to move more freely and the electric field forces all the dipoles in the crystal to line up and face in nearly the same direction.

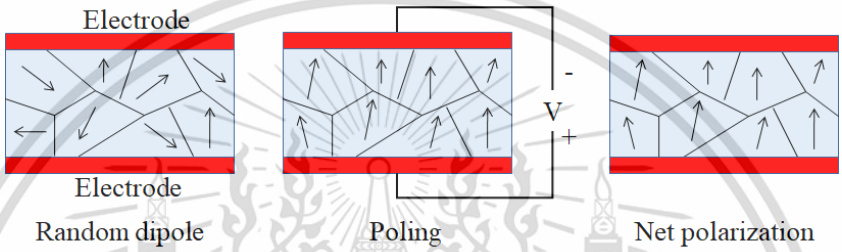

Figure 2.2 Poling process for regulating direction of dipoles.

Theoretically, a relation between stress, strain, and electric field for the reverse piezoelectric effect can be expressed as follows:

$$S_j = d_{ij}E_i + s_{ij}^{E}T_j \tag{2.1}$$

where S_j is the mechanical strain resulting from an applied electric field (E_i); d_{ij} is the piezoelectric constant interacting to the mechanical strain produced by the applied electric field or stress (T_j); and s_{ij}^{E} is the elastic compliance coefficient at constant electric field. In addition, a relation between electric displacement, electric field for the direct piezoelectric effect is given as:

$$D_i = d_{ij}T_j + \varepsilon_{ij}^{T}E_i \tag{2.2}$$

where D_i is the electric displacement produced by an applied stress, and ε_{ij}^{T} is the permittivity at constant mechanical strain.

From the equations (2.1) and (2.2), the subscript i = 1, 2, and 3 identifies the electrical direction and the subscript j = 1, 2, 3, 4, 5 and 6 identifies the mechanical

direction as shown in the figure 2.3 (a). For example, d_{31} is the piezoelectric constants concerning the mechanical strain produced in the 1- direction by an applied the electric field in the 3-direction. In the other way, when the applied electric field and the obtained strain are along the 3-direction, the piezoelectric constant is d_{33} as figure 2.3 (b) and (c).

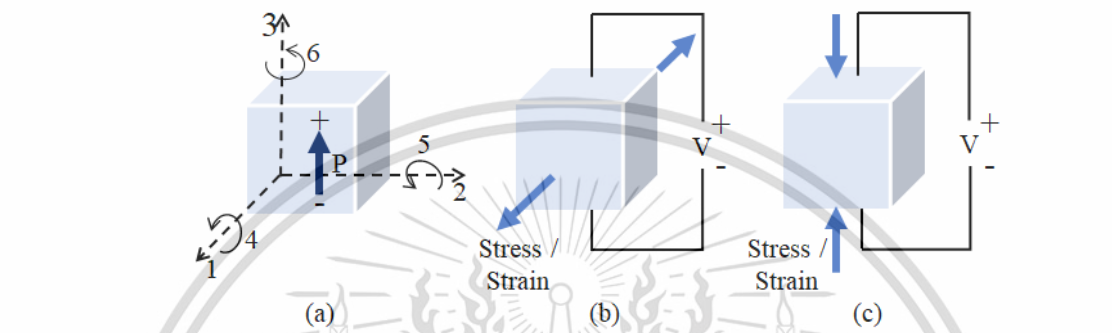

Figure 2.3 (a) Piezoelectric effect direction, (b) 31 (transverse) mode, and (c) 33 (longitudinal) mode.

2.2 Piezoelectric Material Selection

As the piezoelectric technology becomes ubiquitous in a variety of applications, various piezoelectric materials are recently available. The selection of piezoelectric materials in the design of energy harvesting devices is crucial, which has considerable influence with the characteristics and performances of harvester. While the decision criteria on piezoelectric materials can includes the output voltage, energy density, operational bandwidth and cost, an energy conversion efficiency is the most important one that is evaluable through a relatively figures of merit (FOMs). The FOM for each application, i.e. MEMs or Bulk piezoelectric energy harvests, should be much different from others [12]. This works is focused on bulk piezoelectric component, the FOM of which was considered by Priya *et al.* [13]. With eliminating the input mechanical energy in coupling factor, such FOM is given as

$$FOM = \frac{d^2}{\varepsilon_e} \tag{2.3}$$

where $\varepsilon_e = \varepsilon_r\varepsilon_0$; ε_e is the dielectric permittivity; ε_r is the relative permittivity; ε_0 is the is the permittivity in free space; and d is the piezoelectric coefficient. This FOM is the product governed by the effective piezoelectric strain constant and the effective piezoelectric voltage constant ($d \times g$) in the electrical density formula:

$$u_e = \frac{1}{2}(d \times g) \cdot \left(\frac{F}{A}\right)^2 \tag{2.4}$$

where F is the applied force; and A is the area of piezoelectric element. From this equation, it is noticeable that the electrical energy density in piezoelectric materials is directly proportional to such FOM.

Table 2.1 summarizes the widely used piezoelectric materials [12]. By substituting the given materials properties into the equation (2.1), the FOM values were obtained as listed in table 2.2, which were normalized to be easily compared. The results show that PMN-PT is the superior materials. PZN-PT can present the transduction coefficient far below that attainable with PMN-PT. Both PVDF and PZT seem reasonable. Moreover, AlN and $BaTiO_3$ might be not a good option for the milli-scale piezoelectric energy harvesters. Among of them, PZT is a popular choice for energy conversion devices due to the acceptable energy conversion efficiency, easier fabrication, good robustness and reasonable price [14]–[18].

Table 2.1 Properties of piezoelectric materials

Parameter	PVDF	AlN	$BaTiO_3$	PZT	PZN-PT	PMN-PT
d_{33} (m/V)	$-3.30e^{-11}$	$3.40e^{-12}$	$1.49e^{-10}$	$3.60e^{-10}$	$2.00e^{-09}$	$2.82e^{-09}$
ε_r	12	10.4	1700	1700	5200	8200

Table 2.2 Piezoelectric materials comparison

Figures of merit	PVDF	AlN	$BaTiO_3$	PZT	PZN-PT	PMN-PT
d^2/ε_e	0.0936	0.0011	0.0135	0.0786	0.7932	**1.0000**

2.3 Strategies for Variable and Low Frequency Vibration Energy Harvesting

Many piezoelectric vibration energy harvesters face the challenge of low and variable frequency vibrations. The resonant frequencies of such the vibration sources usually deviates from the frequency of the harvesters resulting in low energy conversion efficiency as investigated by Miller *et al.* [19]–[21]. To address this problem, several strategies for variable-frequency vibration energy harvesting have been investigated, which can be mainly classified into three different techniques including the frequency self-tuning, broadband and frequency up-conversion techniques:

2.3.1 Frequency Self-tuning Technique

Various frequency-tunable harvesters have been studied, which present potential solutions [22]. However, most of the designed tuning mechanisms need some form of energy to operate, thus the high output power is required to compensate for the energy supplied into the tuning itself. The referred tuning mechanisms include the use of magnetic potential wells proposed by Mukherjee *et al.* [23] as a harvesting system shown in figure 2.4. The shaped pole-pieces on a pair of permanent magnets were employed to vary the effective spring constant of cantilever, shifting the resonant frequency. Roundy drawn the distinction between the active tuning device that has to continuously supply power to execute the resonant frequency adjustment and the passive tuning device that are able to turn off after a new resonant frequency obtained [24].

To address a challenge mentioned above, the passive self-tuning devices that can tune the resonance without the need of supply energy to the actual tuning were introduced. For instances, the use of spring stiffening to make a difference to a microelectromechanical device as proposed by Marzencki [25]. Miller *et al.* [26] presented the system allowing the passive self-tuning of device by incorporating a proof mass that is able to slide along a beam with ends clamped as illustrated in figure 2.5. The approach is alike to work intruded by Boudaoud *et al.* [27], where a freely

sliding bead on a string was employed. Miranda and Thomson showed a spring-suspended slider used with a simple cantilevered beam [28]. Kozinsky [29] studied a resonator with a steel bead that can freely move inside a cylinder. Furthermore, in [30], [31] Gu and Livermore examined passively self-tuning systems to apply in rotational applications.

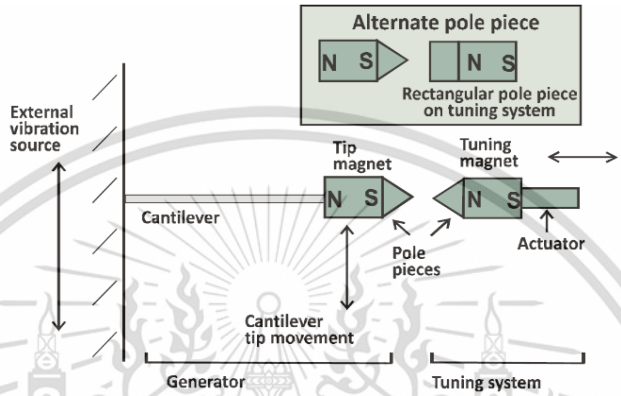

Figure 2.4 Frequency tuning concept consisting of magnetic potential well.

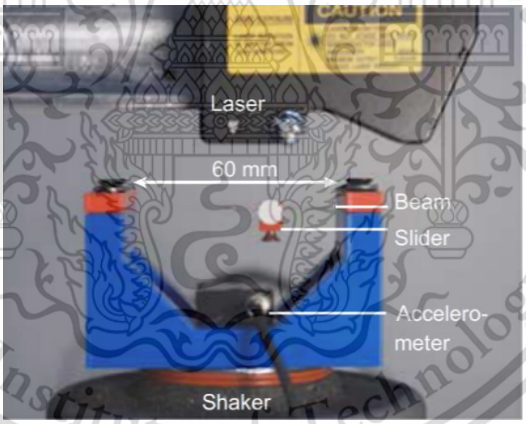

Figure 2.5 Passive self-tuning device using the sliding proof mass.

Throughout the relatively frequency self-tuning works, it is noticeable that the shortcomings can come with the tunable range and the response time of the frequency tuning. When the frequency of vibration sources changes very quickly and randomly, the self-tuning mechanism might not be able to follow.

2.3.2 Broadband Technique

The design of a system that has a broadband frequency response and can efficiently operate with changes in vibration is an alternative [22]. An obvious topical review was presented by Zhu *et al.* [22], which consist of two main approaches. The one means is to mount several harvesting devices with different natural frequencies on one platform, e.g. using multiple bimorph cantilevers as discussed by Ferrari *et al.* [32] and using fractal-inspired multi-frequency plates as investigated by Castagnetti [33]. The piezoelectric cantilever is targeted to conform to such plates as shown in figure 2.6.

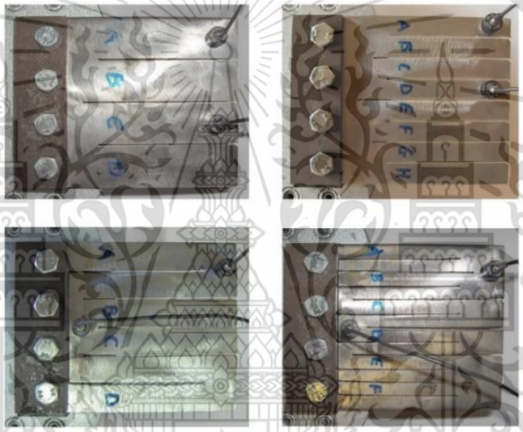

Figure 2.6 Different fractal-inspired multi-frequency plates.

The second means is to implement the nonlinearity and bistability on system to vary the frequency response. A review on existing bistable systems is given by Harne and Wang [140] and Beeby *et al.* [34] introduced the comparison of the power outputs produced by the linear and non-linear systems. Abdelkefi *et al.* used a couple of asymmetric tip masses to make a unimorph cantilever beam vibrate torsionally [35]. Zhu *et al.* [36], Jones *et al.* [37], and Ferrari *et al.* [38] induced the nonlinearity through a permanent magnet coupling. Figure 2.7 illustrates an example of such system. When objected to excite by the random vibration, the piezoelectric boned on harmonic steel substrate will be bounced between two stable states under a single-magnet coupling [39]. Otherwise, the pre-stressing or buckling beams has been focused such as the

works presented by Marinkovic and Koser [40], Hajati *et al.* [41]–[43], and Cottone *et al.* [44]. The general nonlinear response of buckled beams can be found in [45], introduced by Emam and Nayfeh. Blackburn and Cain investigated the nonlinear piezoelectric resonance with high power generation [46].

Broadband energy harvesters offer work well in many situations, but one of the problems is found that their mechanical quality factor (Q-factor) is decreased deteriorating the peak power output. Although the use of several piezoelectric cantilevers with different resonant frequency has no effect on the Q factor, only single piezoelectric cantilever contributed to the generated power resulting in low output power density.

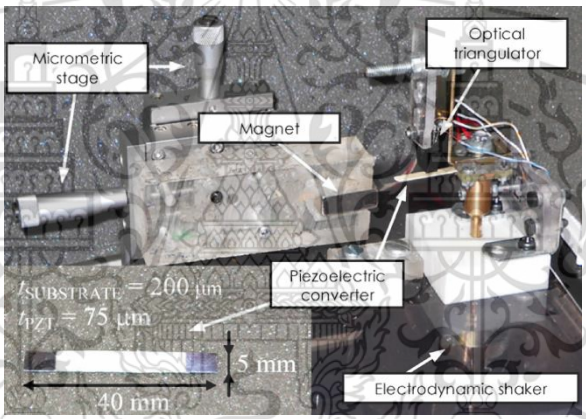

Figure 2.7 Single-magnet nonlinear converter

2.3.3 Frequency Up-Converting Technique

The frequency self-tuning and broadband strategies are suitable to scope with varying frequency. In order to harvest energy from a very low excitation frequencies as a few Hertz, especially the human motion, the frequency up-conversion strategy has recently seen much of interest. The energy harvesters combined with this strategy are always exited to oscillate at their resonant frequency through a direct impact, mechanical plucking or magnetic plucking, regardless of the input excitation frequency, thus a wide range of operational frequency is achievable. As the acceleration of input excitations are generally low, a piezoelectric cantilever of harvesters usually needs a

proof mass in motion to increase the energy conversion efficiency. The direct impact devices include a work presented by Galchev *et al.* [47]; they realized the mechanism that up-convert the frequency of piezoelectric beams through a magnetic latching with a large tungsten carbide inertial mass as shown in figure 2.8. Umeda *et al.* [48], [49] investigated the generated energy from a piezoelectric beam impacted by a steel ball. Zhang *et al.* [50] designed a multi-impact harvester using teeth with an attached roller to impact two stiff piezoelectric cantilever beams. Ranaud *et al.* [51], [52] used a moving mass to strike one of two piezoelectric cantilevers located at each end of a harvester container while the harvester was being shaken from side to side. The impact from the moving mass increased the operational frequency of the piezoelectric enabling it to harvest energy from low-frequency and high-amplitude input and then provide the output power to wearable gait monitoring device. Moreover, Gu *et al.* [53], [54] and Jacquelin *et al.* [55] used a low frequency resonator to impact a high frequency energy harvesting resonator.

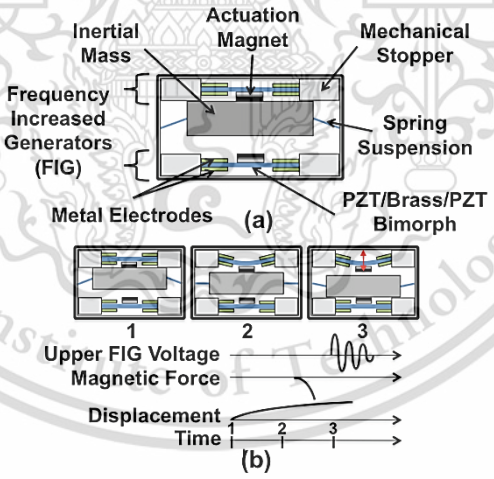

Figure 2.8 Schematic drawing of a piezoelectric frequency-increased power generator; (a) structure and (b) operational sequences.

The mechanisms plucking piezoelectric cantilevers and then leaving them to oscillate naturally have been widely studied, e.g. Pozzi *et al.* [56]–[59] applied a plucking based on the frequency up-conversion strategy to a piezoelectric wearable energy harvester in order to convert energy from knee-joint motion. This mechanically

plucking deflected the piezo-electric beams through a plectrum and then rapidly left them free to vibrate. An analogous set-up is proposed by Janphuang *et al.* [60]. The teeth of the rotating gear wheel were used to pluck an atomic force microscope (AFM)-like piezoelectric beam as shown in figure 2.9. The drawbacks with the use of direct impact or mechanically plucking are that the brittle piezoceramic materials can be damaged and the considerable noise was made.

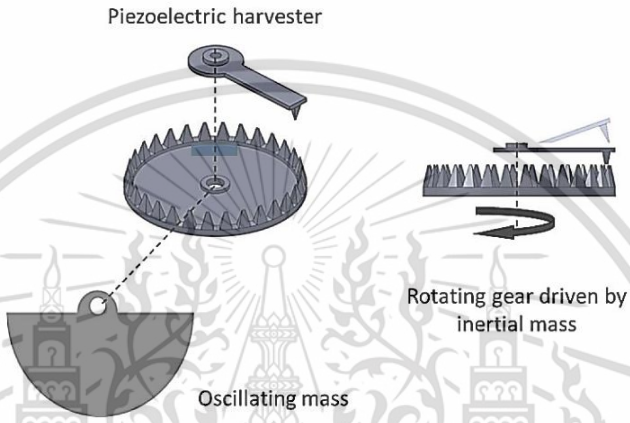

Figure 2.9 Schematic drawing of a concept for harvesting energy from the rotating gear.

To overcome the aforementioned limitations, the frequency up-converting mechanisms based on non-contact magnetic plucking have been recently investigated. For example, Kuang *et al.* [61] reported the knee-joint energy harvester using the non-contact magnetic interaction instead of mechanical contact to excite the bimorph. The knee-joint motion actuated a primary magnet to pluck the bimorph through a secondary magnet attached on the bimorph tip as illustrated in figure 2.10. Pillatsch *et al.* [62] demonstrated a body-movement energy harvesting device that used a rotational system. In this device, magnetic coupling with a rotating proof mass was used to pluck the piezoelectric cantilever. Luong *et al.* [63] used magnetic force interaction between permanent magnets to excite a piezocomposite generating element (PCGE) in a small-scale windmill. The primary magnet was attached to the input rotor, and the secondary magnet was attached to the free end of the PCGE. The further linear systems that operate by opposing permanent magnets are introduced by Yang and Tang *et al.* [64]–[66] and Wickenheiser *et al.* [67], [68].

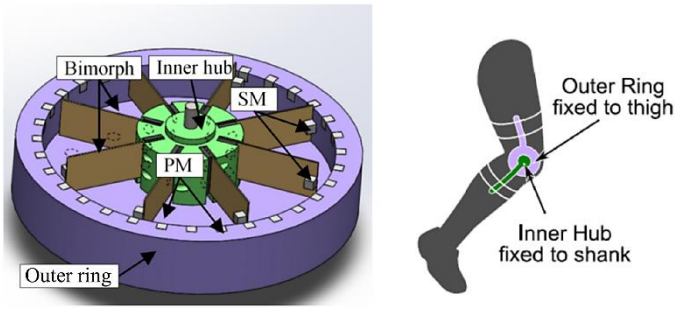

Figure 2.10 A schematic of the piezoelectric knee-joint energy harvester using magnetic plucking mechanism for frequency up-conversion; where PM is a primary manet and SM is a secondary magnet.

From a literature review of strategies for low frequency energy harvesting, it was found that the frequency up-conversion technique seems to be the most promising for human motion applications. This technique will be applied on the energy harvesting floor tile in chapter 3.

2.4 Summary

The fundamental of piezoelectricity including the piezoelectric effect, polarization and directional identification of electromechanical respond in piezoelectric material was presented first in this chapter. Then, the criterion of piezoelectric material selection for energy harvesting application using the figure of merit (FOM) was introduced. A few types of piezoelectric material were compared. The result shows that a piezoelectric PZT material is a reasonable one. In addition, the literature review of low-frequency vibration energy harvesting strategies was given. The frequency up-conversion principle should be suitable for harvesting energy from human motion.

Chapter 3

A configuration to Characterize Piezoelectric Cantilever Used in Energy Harvesting Floor Tile

This chapter is meant to introduce a concept of energy harvesting floor tile based on the frequency up-conversion principle and a configuration to test the performance of piezoelectric cantilever, optimizing the parameters setup of the sign. The frequency up-conversion through interaction between permanent magnet and iron bar will be studied. The magnetic force exciting on piezoelectric cantilever is going to be considered by the finite element method. Additionally, the data measurement and performance analysis of piezoelectric cantilever will be explained.

3.1 Theory on Frequency Up-converting Energy Harvester

To design the energy harvesting floor tile based on the frequency up-conversion principle, the relevant parameters need to be analyzed first. They can be considered from the operating principle of frequency up-converting energy harvester as depicted in figure 3.1. This simple model is presented by Galchev *et al.* [69], which is based on a simple mass-spring damper system.

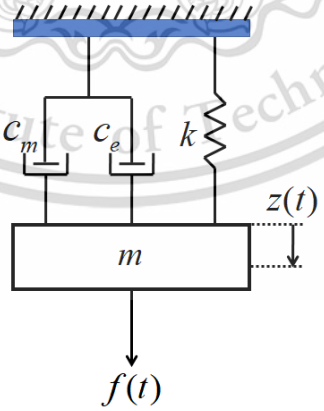

Figure 3.1 A simple model of a frequency up-converting energy harvester.

In this case, the driving force $f(t)$ excite directly on a proof mass m supported on a suspension with a spring constant k and a damping element including the mechanical

damping c_m and electrical damping c_e to provide a motion with a displacement $z(t)$. Its differential equation is given by

$$m\ddot{z}(t)+(c_m+c_e)\dot{z}(t)+kz(t)=f(t). \tag{3.1}$$

The mechanical damping is a result of friction, air resistance etc., while the electrical damping is occurred from the energy transduction. The electrical damping force F_e in electrical energy conversion is defined by $F_e = c_e\dot{z}$ where $\dot{z}$ is the velocity of a moving mass as a function of time, as the case herein, the energy dissipated in the damper every cycle can be calculated by integrating the F_e over a full cycle as

$$W=\oint F_e dz. \tag{3.2}$$

The integral is taken over the period of the external excitation to account for the entire time that a mass is oscillating freely after having been excited. The velocity of a moving mass can be written as

$$\dot{z}(t)=-z_{act}\omega_n\frac{e^{-\varsigma_T\omega_n t}}{\sqrt{1-\varsigma_T^2}}\sin(\omega_d t) \tag{3.3}$$

where z_{act} represents the initial mass displacement just after released; ω_n is the natural frequency of the harvester; ς_T is the combined mechanical and electrical damping ratio of the harvester; and ω_d is the damped natural frequency of the harvester ($\omega_d=\omega_n\sqrt{1-\varsigma_T}$). With dividing the energy dissipated in the harvester per input excitation cycle by the period of the external excitation and multiplying by two to account for the fact that the harvester will be excited once per cycle, the total power output can be given by

$$P_{total}=\frac{1}{2}\frac{m\varsigma_e\omega\omega_n^3 z_{act}^2}{1-\varsigma_T^2}\left[\left(\frac{1-e^{-4\pi\varsigma_T\frac{\omega_n}{\omega}}}{2\varsigma_T\omega_n}\right)-\left(\frac{e^{-4\pi\varsigma_T\frac{\omega_n}{\omega}}(2\omega_d\sin(4\pi\frac{\omega_d}{\omega})-2\varsigma_T\omega_n\cos(4\pi\frac{\omega_d}{\omega})}{4(\varsigma_T^2\omega_n^2+\omega_d^2)}\right)\right] \tag{3.4}$$

where ς_e is the electrical damping ratio of the harvester; and ω is the frequency of input excitation. Assuming that ς_e (ignoring mechanical damping ratio) is large enough such that the harvester can be completely damped per excitation cycle $2\pi/\omega$, the total power output equals to

$$P_{total} \sim m\gamma^2\omega^3 z_{act}^2 \tag{3.5}$$

where $\gamma = \omega_n / \omega$. Increasing the frequency ratio γ can lead the power output increase. This point can be a guideline for an optimization of the frequency up-converting energy harvester [31]. The γ is directly proportional to the resonant frequency ω_n of the harvester, which can be increased with reducing the mass or increasing the spring constant. However, there is a trade-off between γ, m, and z_{act}. The z_{act} is influenced directly by the spring constant of the harvester, which therefore should be optimized first.

3.2 Concept of Energy Harvesting Floor Tile

The schematic diagram of the energy harvesting floor tile with the frequency up-conversion mechanism is illustrated in figure 3.2.

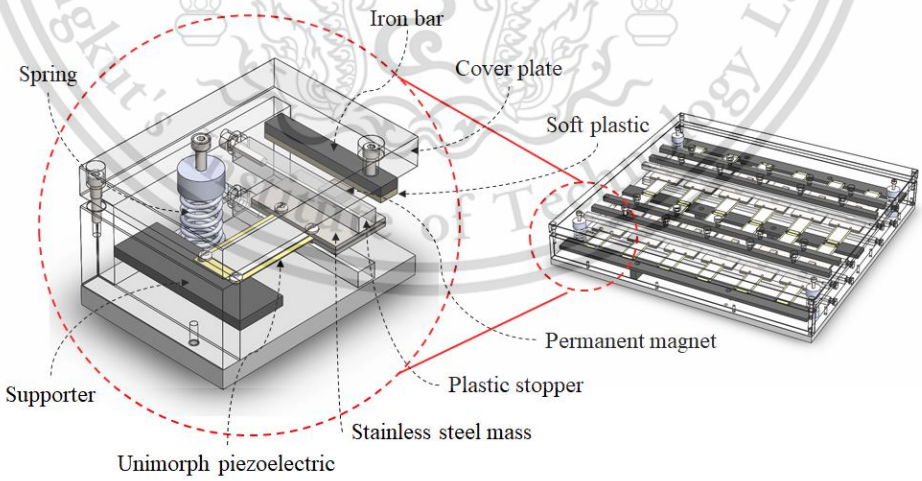

Figure 3.2 Schematic drawing of energy harvesting floor tile.

The piezoelectric cantilevers are mounted on a supporter, the free ends of which are attached to a stainless-steel mass to increase the strain in the piezoelectric

substance causing the increase of electrical output power during oscillation. The permanent magnets are glued to the top surface of the mass for attracting the iron bar underneath the cover plate when the floor tile is stepped on. The soft plastic is used to absorb the impact force between the iron bar and the permanent magnet. Four springs are installed at each corner pulling up the cover plate. A stopper is used to protect the piezoelectric layer from damage from over-displacement excitation.

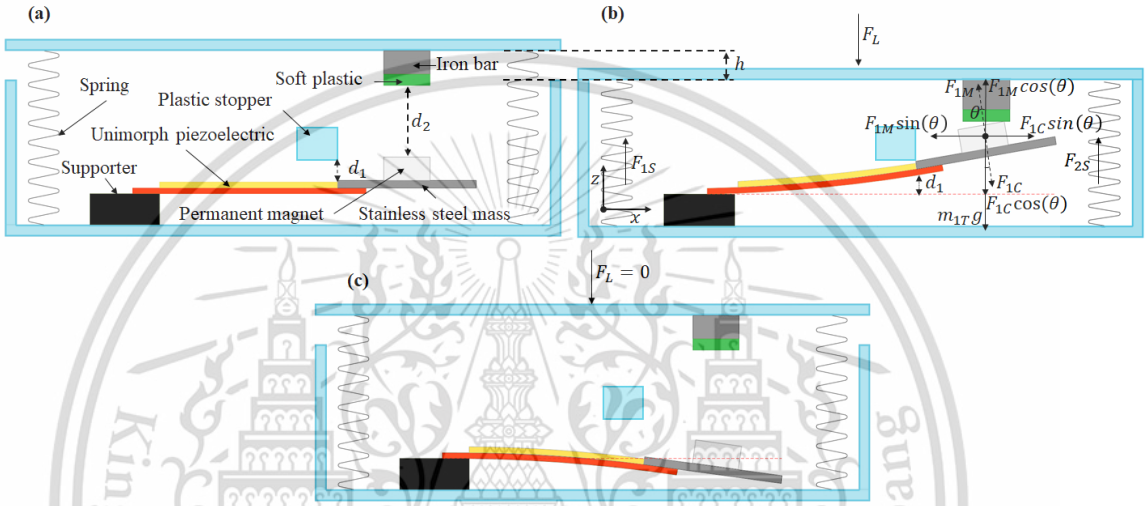

Figure 3.3 (a) Waiting for load; (b) and (c) Loaded and unloaded states of energy harvesting floor tile.

Figure 3.3 illustrates the frequency up-converting sequences of energy harvesting floor tile. In the waiting for load state (Figure 3.3 (a)), the air gap between the permanent magnet and the iron bar (d_2) should be optimized to ensure that the attracting force from the permanent magnet (F_{iM}) to the iron bar is not going to stop vibrating cantilever; therefore, the iron bar should be located where F_{iM} = 0. The attractive force exerted by the permanent magnet at the air gap is given by the following Maxwell's equation:

$$F_{iM} = \frac{B^2 A_i}{2\mu_0} \tag{3.6}$$

where the subscript i identifies a particular permanent magnet and unimorph cantilever. B represents the magnetic flux density, A_i is the cross section of the area of the pole, and μ_0 is the permeability of the air.

For the loaded state shown in figure 3.3 (b), when the energy harvesting floor tile is stepped on, springs are compressed by a compressive force (F_L) from the weight of the pedestrian. The compressive force F_L should be larger than the restoring force of the spring (F_{jS}); $F_L \rangle \sum_{j=1}^{a} F_{jS}$ where a is the total number of the springs used. From Newton's second law and Hooke's law, F_L and F_{jS} can be calculated by the equations below,

$$F_L = m_L g \tag{3.7}$$

$$F_{jS} = -k_{jS} h \tag{3.8}$$

where the subscript j identifies a particular spring; m_L is the mass of the pedestrian; g is the gravitational acceleration; k_{jS} is the spring constant; and h represents the displacement from the equilibrium position of the spring. The loaded state is also a state that the iron bar comes close to a location where the magnetic field density is high so that the bar will be attracted by the permanent magnet. Thus, the permanent magnet deflects the piezoelectric cantilever underneath the iron bar. The resultant force in the z-axis (F_{iZ}) deflecting the unimorph piezoelectric cantilever is equal to

$$F_{iz} = F_{iM} \cos\theta - (F_{iC} \cos\theta + m_{iT} g) \tag{3.9}$$

where F_{iC} is the restoring force of the unimorph piezoelectric cantilever; θ is the top surface angle of permanent magnet, and m_{iT} represents the total mass of the magnet and the stainless-steel mass at tip of piezoelectric unimorph cantilever. The restoring force F_{iC} can be calculated from the equation below: [70]

$$F_{iC} = k_{iC} d_1 \tag{3.10}$$

where k_{iC} is the effective spring constant of the unimorph piezoelectric cantilever; d_1 is the displacement of the unimorph piezoelectric cantilever from its rest position; and k_{iC} is calculated by the following equation,

$$k_{iC} = \frac{3(EI)_{Cantilever}}{l^3} = \frac{3(E_p I_p + E_e I_e)}{l^3} \tag{3.11}$$

where $(EI)_{Cantilever}$ is the effective bending modulus of the unimorph piezoelectric cantilever; l is the length of the piezoelectric and elastic layers; E_p and E_e are the Young's modulus of the piezoelectric and elastic layers; and I_p and I_e are the moments of inertia of the piezoelectric and elastic layers. The moments of inertia of the piezoelectric and elastic layers can be determined by the following equations [53]:

$$I_p = \frac{w_p t_p^3}{l^3} + w_p t_p \left(\frac{t_p}{2} - t_n\right)^2, \text{ and} \tag{3.12}$$

$$I_e = \frac{w_e t_e^3}{l^3} + w_e t_e \left(\frac{t_e}{2} - t_n\right)^2 \tag{3.13}$$

where w_p and w_e are the widths of the piezoelectric and elastic layers; t_p and t_e are the thicknesses of the piezoelectric and elastic layers; and t_n is the distance of the neutral plane in the piezoelectric layer, shown in figure 3.4, which can be calculated by the equation below,

$$t_n = \frac{E_p t_p^2 - E_e t_e^2}{2(E_p t_p + E_e t_e)}. \tag{3.14}$$

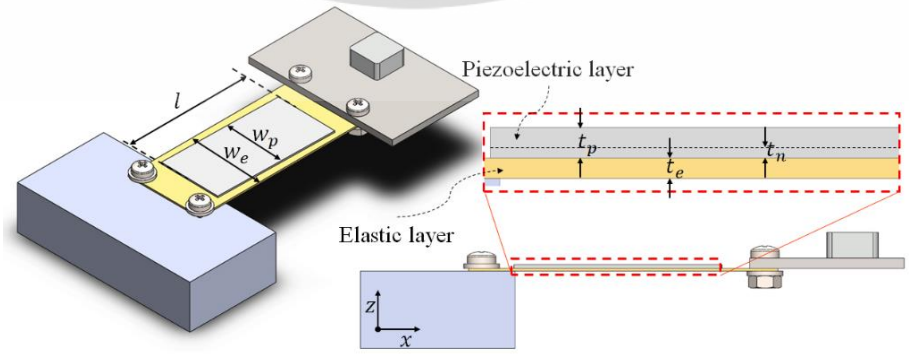

Figure 3.4 Schematic of a unimorph piezoelectric cantilever with a proof mass.

Furthermore, the compressive stress in the unimorph piezoelectric cantilever is induced by the resultant force in the x-axis,

$$F_{ix} = F_{iM}\sin\theta - F_{iC}\sin\theta . \tag{3.15}$$

In the unloaded state, when the foot moves up and away from the energy harvesting floor tile; F_L= 0 as shown in figure 3.3(c) and the total restoring force of the spring is higher than the total force in the z-axis; $\sum_{j=1}^{a} F_{jS} \rangle \sum_{i=1}^{b} F_{iz}$ where *b* is the number of the cantilevers with an attached permanent magnet; the springs will push the cover plate and the iron bar up and away from the permanent magnet. This step will rapidly separate the permanent magnet from the iron bar allowing the unimorph piezoelectric cantilever to freely oscillate at a high frequency.

3.3 Design of a Test Bench

Following to a concept in section 3.2, a test bench for examining performance of piezoelectric cantilever targeted to integrate to the prototype of floor tile can be designed. The general system of such device is shown as a block diagram in figure 3.5, which consists of an oscilloscope (Tektronix TD 3032B) and frequency up-converter. The oscilloscope is used to measure the output electricity from piezoelectric cantilever having been excited by the frequency up-converter. The frequency up-converter is mainly divided into mechanism and control circuit parts. The structure of mechanism part is illustrated in figure 3.6. A motor shaft with a snail cam is used to excite the follower for transforming the rotary motion exerted from motor into the linear motion of a cover plate. When a greatest radial dimension of snail cam rotates to match the follower, the iron bar attached underneath of a cover plate is moved closer to a permanent magnet at where high magnetic field. Meanwhile, a permanent magnet will attach the iron bar with bending a piezoelectric cantilever through magnetic attractive force. The displacement of piezoelectric cantilever is localized by the stopper. After that, when a snail cam leaves a follower, the spring will suddenly pluck the cover

plate up. It releases the iron bar far from permanent magnet and then let the piezoelectric cantilever oscillate freely at resonant frequency. In addition, a motor is controlled by the microcontroller (ATmega32) with an integrated circuit chip (L293D driver motor), while the matching between a greatest radial dimension of a snail cam and a follower is tracked by a limit switch to unsure that the permanent magnet obviously attach to the iron bar.

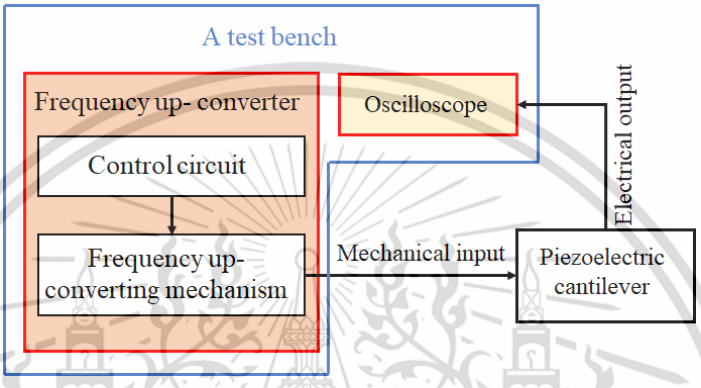

Figure 3.5 Block diagram of overall system of a test bench.

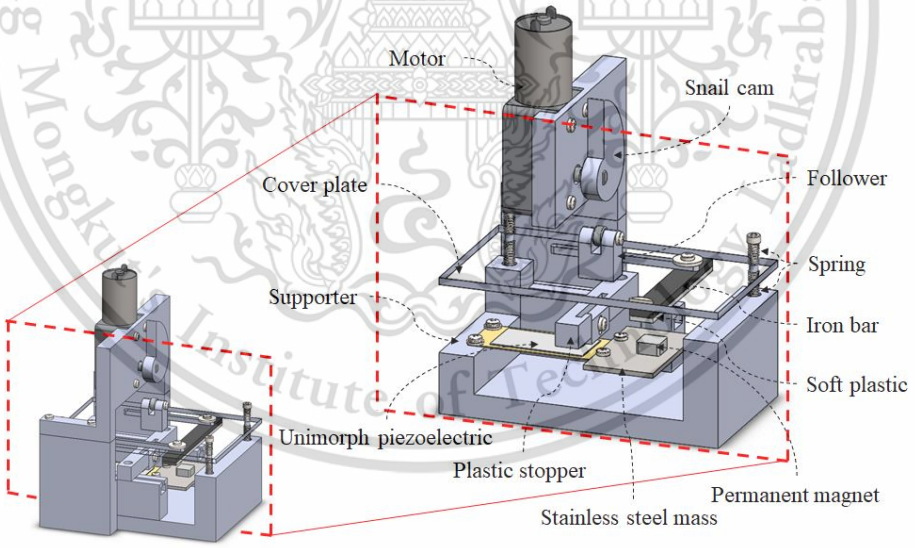

Figure 3.6 Schematic drawing of frequency up-converting mechanism

3.4 A setup for Performance Test of Piezoelectric Cantilever

A setup for performance test of piezoelectric cantilever is illustrates in figure 3.7, which was began with configuring the frequency up-converting mechanism in figure 3.7 (a). A 60 x 30 x 2 mm^3 stainless steel mass (416) was glued with a 10 x 10 x 5 mm^3

permanent magnet (NdFeB-N35), and then mounted on the free end of a unimorph PZT cantilever consisted of a 40 x 20 x 0.3 mm^3 PZT layer and a 60 x 25 x 0.2 mm^3 elastic layer. The main reason for selecting this commercial unimorph PZT cantilever was due to its economical price, which might be a reasonable option for experimentally proving the theory of designed floor tile mechanism. In general, the generated power is directly proportional to the displacement of the piezoelectric cantilever, the largest air gap between the plastic stopper and the PZT cantilever (d_1) is required. However, the PZT layer may crack from over-bending, thus a proper distance between the stopper and the cantilever needs to be set. For the implementation, one end of the PZT cantilever was clamped to the supporter and supplied with DC voltage while the other free end was pressed by a rack-and-pinion scale to vary the vertical displacement. Over-bending could be observed from the voltage at the free end. As shown in figure 3.8, as the PZT layer broke at a vertical displacement of approximately 7.1 mm, the voltage at the free end became zero. Therefore, a plastic stopper was used to fix the vertical displacement of the PZT cantilever to 4 mm (d_1 = 4 mm).

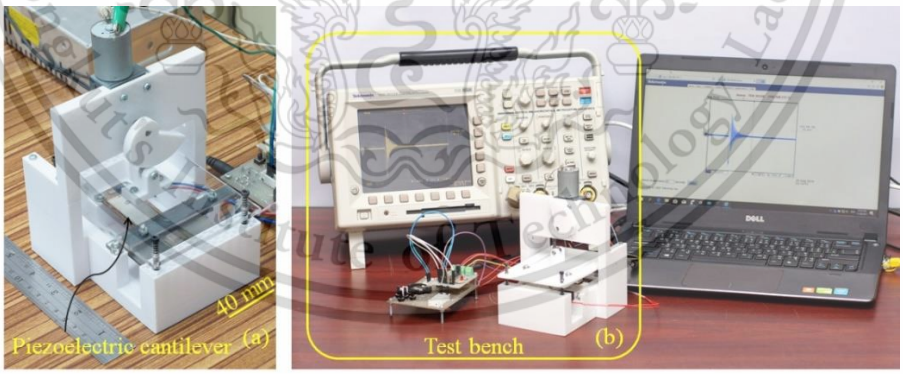

Figure 3.7 The setup used in the characterization of piezoelectric cantilever; (a) putting a piezoelectric cantilever in frequency up-converter; and (b) a test bench.

In addition to that optimization step, an optimal air gap between the permanent magnet and the iron bar (d_2) was determined by finite element analysis (FEA) simulation with FEMM 4.2 software. The simulation was implemented in 2D with parameters

shown in table 3.1. Figure 3.9 illustrates the simulation results of magnetic flux density. As can be seen, the magnetic flux density was diminished to approximately zero at 18 mm far from the permanent magnet. At this distance, the attractive force from the magnet approached zero according to equation (3.6). Thus, d_2 was set to be 18 mm. After these configuration steps, a test bench shown in figure 3.7 (b) can be set up. Finally, the piezoelectric cantilever was terminated with load resistor for investigation of electrical energy conversion capability and robustness.

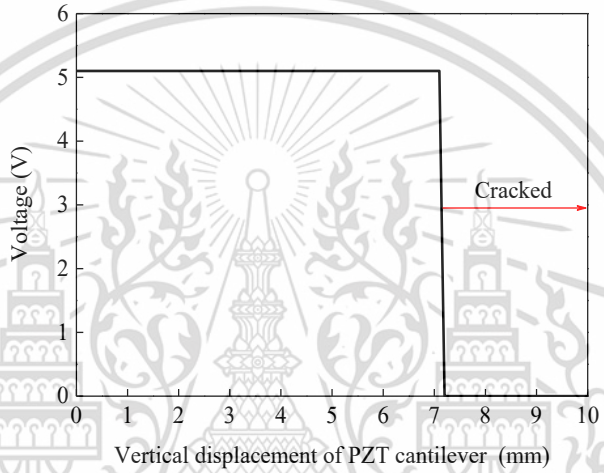

Figure 3.8 Voltage at the free end of the PZT cantilever as the vertical displacement was increased.

Table 3.1 Dimension and magnetic property of the materials used.

Parameters	Area (mm^2)	Length (mm)	Relative permittivity	Coercivity (A/m)	Electric conductivity (MS)
Iron bar	5 x 10	---	14872	---	---
Soft plastic	2 x 10	---	1	---	---
Air gap	---	10, 14, 18	1.0006	---	---
Permanent magnet	2 x 10	---	1.045	883310	0.667
Stainless-steel mass	2 x 30	---	440	---	---

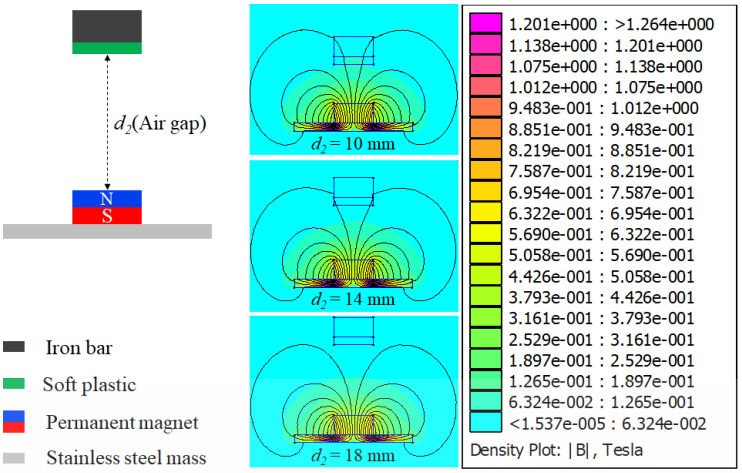

Figure 3.9 Magnetic flux density simulation.

3.5 Method to Compute Performance

As the voltage output of frequency up-converting energy harvester is a transient waveform [60], the instantaneous power $P(t_m)$ could be calculated by

$$P(\mathrm{t}_m) = \frac{V_L^2(t_m)}{R_L} \tag{3.16}$$

where $V_L(t_m)$ is the transient voltage across the resistive load at time t_m; m = 0, 1, 2, 3...identifies the voltage sample at a particular time; and R_L is the resistance of the resistive load. At time t_N where N is the number of voltage samples, the average power can be found as

$$P_{Avg}(\mathrm{t}_N) = \frac{1}{t_N}\int_0^{t_N} \frac{V_L^2(t)}{R_L} dt\,. \tag{3.17}$$

Thus, the energy produced from the prototype as a function of time was calculated by the following expression,

$$E(\mathrm{t}_N) = \sum_{m=0}^{N} P(\mathrm{t}_m)\Delta \mathrm{t}_m\,, \text{for } N\rangle 0\,, \tag{3.18}$$

where Δt_m is the measurement time interval of the voltage samples.

In addition, the energy conversion efficiency can be examined in the quantitative relation between the amount of the output electrical energy and the input mechanical

energy. The input mechanical energy was found from the potential energy stored in a PZT cantilever based on the displacement and effective spring constant by the following equations,

$$E_{Input} = \frac{1}{2} k_{eff} z_0^2 , \tag{3.19}$$

$$k_{eff} = \omega_n^2 M \tag{3.20}$$

where k_{eff} represents effective spring constant; z_0 is the tip displacement of a PZT cantilever; ω_n is the resonant frequency of a freely oscillating PZT cantilever; and M is the seismic mass attached to the tip of a freely oscillating PZT cantilever. The ω_n can be found from the time period of oscillation (T_P) appearing in transient waveform as shown in figure 3.11, which is given by $\omega_n = 1/T_P$.

3.6 Performance of a Tested Piezoelectric Cantilever

By running a frequency up-converter to excite a unimorph PZT cantilever singly, the electrical energy generation capability of such cantilever can be investigated. First, the open circuit test was implemented with a circuit shown in figure 3.10(a). The transient output voltage shown in figure 3.11 can be obtained, as can be seen, the peak-to-peak value of which during free oscillation is 68.4 V and the resonant frequency is found to be 10.54 Hz. This resonant frequency was confirmed by the impedance analyzer (Bode 100 - OMICRON Lab). The result showed a similar resonant frequency where 10. 63 Hz at a lowest impedance magnitude as illustrated in figure 3.12. Next, a PZT cantilever was mechanically connected to a load resistor as circuit given in figure 3.10 (b). The output voltage across load resistor was measured to consider the output power and energy. The average output power as a function of the resistive loads is given in figure 3.13. The maximum value of 0.075 mW is observed at optimal load resistance of approximately 740.74 kΩ. The load resistance shown in a such graph is the combined resistances of load resistor and oscilloscope probe in the form of parallel connection. With the entire time of free oscillation, the total output

energy dissipated at an optimal load resistor can be found as shown in figure 3.14, which is 0.39 mJ with conversion efficiency of 24.67 % as illustrated in figure 3.15.

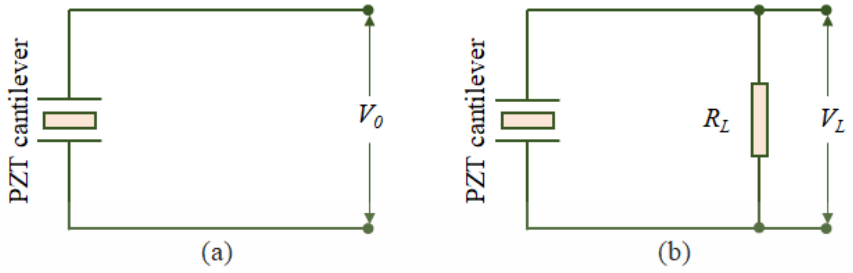

Figure 3.10 Circuits for the performance test of PZT cantilever; (a) open circuit and (b) circuit of connected PZT cantilever and load resistor.

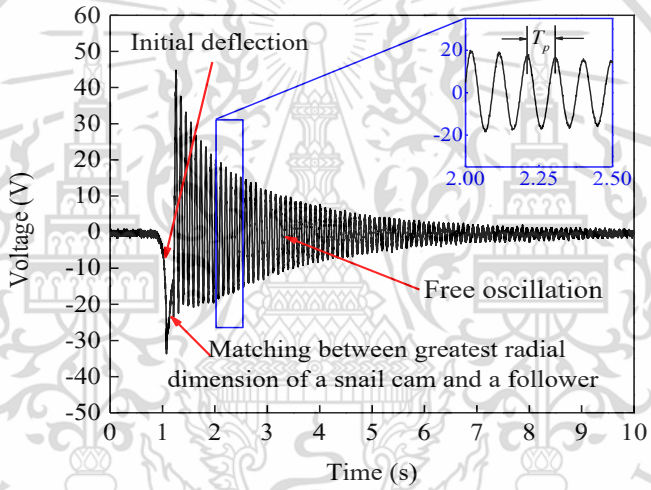

Figure 3.11 Generated open circuit voltage.

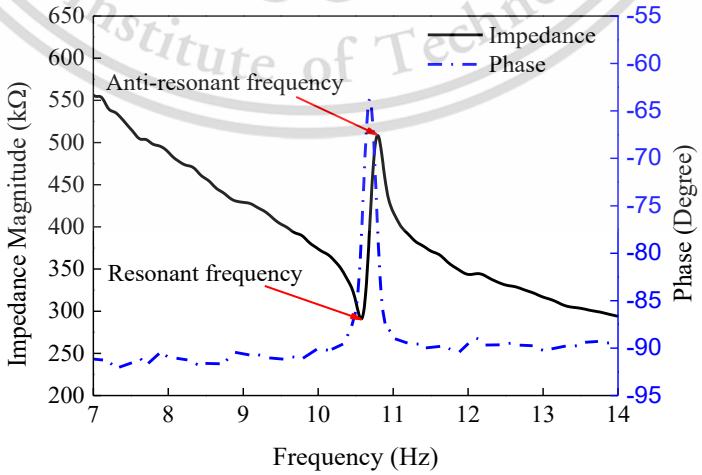

Figure 3.12 Impedance Vs phase measured by the impedance analyzer (Bode 100 - OMICRON Lab).

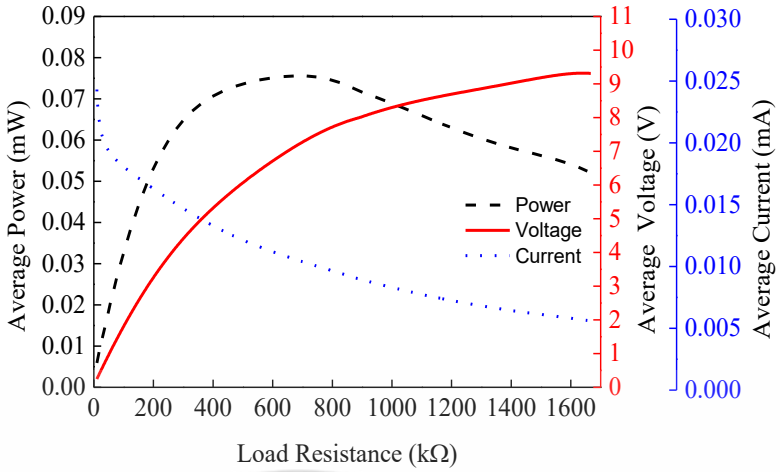

Figure 3.13 Average output power, voltage and current across resistive loads.

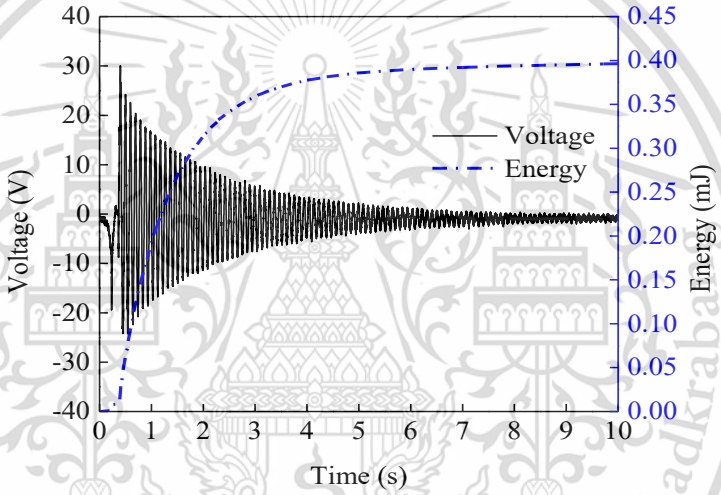

Figure 3.14 Output voltage and total energy across an optimal load resistor.

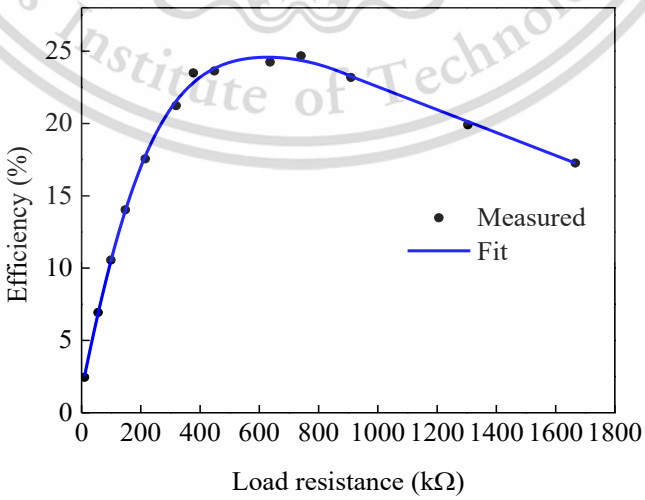

Figure 3.15 Measured energy conversion efficiency.

In addition to the electrical energy generation capability, the reliability test was carried out by running a frequency up-converter to continuously excite the unimorph PZT cantilever terminated with an optimal load resistor. It was found that the energy dissipated at an optimal load resistor steadily decreased from the first pluck up to the forty-thousandth pluck. This issue was not related to mechanical failure or regression of the PZT material. It occurred from progressive detachment of the PZT layer from the elastic layer that might come from insufficient adhesive function of the glue that bonded the two layers together under a large vertical displacement of the PZT cantilever. To remedy that situation, the PZT cantilever's vertical displacement was restricted to 2 mm (d_1 = 2 mm). However, the progressive detachment still happened as shown by the results in figure 3.16. A very short air gap d_1 might make the PZT cantilever last a longer time, but the output energy would be lower due to the low stress in the piezoelectric material.

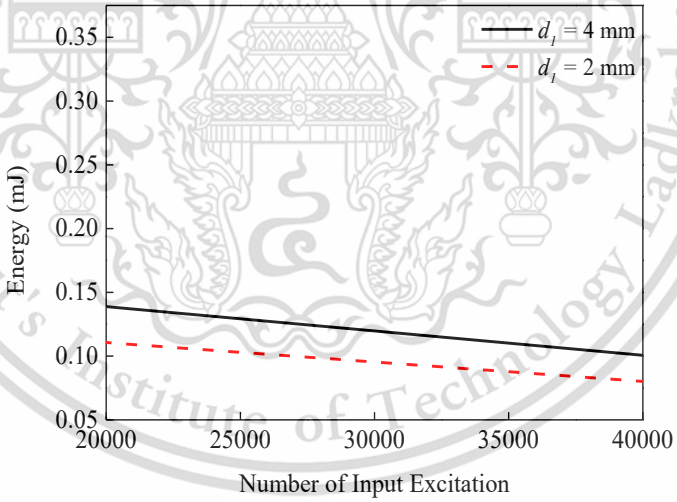

Figure 3.16 Output energy with increasing number of plucks.

3.7 Summary

This chapter introduced the performance test of piezoelectric cantilever which is targeted to employ in the energy harvesting floor tile. A test bench was designed by following a concept of the floor tile in which the magnetic plucking is utilized to up-covert the frequency of piezoelectric cantilever. The relevant parameters for

optimization of the system was defined from the theory of frequency up-converting energy harvesters. In the device setup, the finite element method (FEM) was used to analyze the magnetic field, then a distance between permanent and iron bar could be optimized. The maximum displacement of piezoelectric cantilever was considered by observing the over-bending with voltage transferred from end-to-end of it. After this step, the energy harvesting capability and robustness test of a unimorph PZT cantilever could be achieved. The results showed that a unimorph PZT cantilever gave a good energy conversion efficiency, but it has a problem on an aggressive detachment of the PZT layer from the elastic layer.

Chapter 4

Validation of Designed Mechanism and Evaluation of Energy Harvesting Floor Tile

The aim of this chapter is to propose an experimental validation of the design with human footstep simulated by a test bench and an experimentally evaluated the performance of the fabricated floor tile. An optimal setup for magnetic plucking mechanism will be verified before the energy harvesting behavior of the design is analyzed. After this step, the final tile will be introduced and then subjected to a series of experiments, both in a laboratory set-up and in the real scenario. The output energy obtained from actual pedestrian steps is assumed to power a few types of low-power wireless sensor node.

4.1 Validation of the Designed Mechanism

4.1.1 Validation Methods

Before configurating the energy harvesting floor tile, the concept designed need to be validated first. A gap between permanent magnet and iron bar (d_2) directly influencing on the output energy and the energy harvesting behavior indicating the feasibility of the design has to be verified. In the implementation, a test bench proposed in the chapter 3 was used for simulating the human footstep and an optimal load resistor was connected to the unimorph PZT cantilever on the observation of harvestable energy. Generally, walking velocity and frequency of pedestrian steps on the floor either in a crowded or uncrowded area are inconstant, depending on number of people and individual stride. These parameters could not be simulated exactly. One thing for certain is that the time interval that the foot of a pedestrian makes contact with the floor is longer for a slow walker and shorter for a fast walker. A high density of pedestrians may cause them to walk slower hence this time interval may be longer [71]. Accordingly, this simulation of energy harvesting behavior was based on

the step time interval (T_d) between the cover plate moving up and down, i.e., the cycle time of the greatest radial dimension of the snail cam pressing on the follower.

4.1.2 Validation Results

The first step was to verify the optimal air gap d_2. Figure 4.1 shows a comparison of the performances of the prototype installed with different air gaps d_2. The ratio of the total output energy generated when the air gap d_2 were 18 and 14 mm to the total output energy generated when d_2 was 10 mm were 3.35 and 2.73 to 1, respectively. Decreasing the amount of the air gap d_2 led to a significant drop in output energy because the vertical displacement of the oscillating PZT cantilever was diminished by the stronger attractive force between the permanent magnet and the iron bar as mentioned in chapter 3. Free oscillation would be stopped with the shortest air gap d_2, producing the minimum output energy. Therefore, the prototype was configured with d_2 = 18 mm.

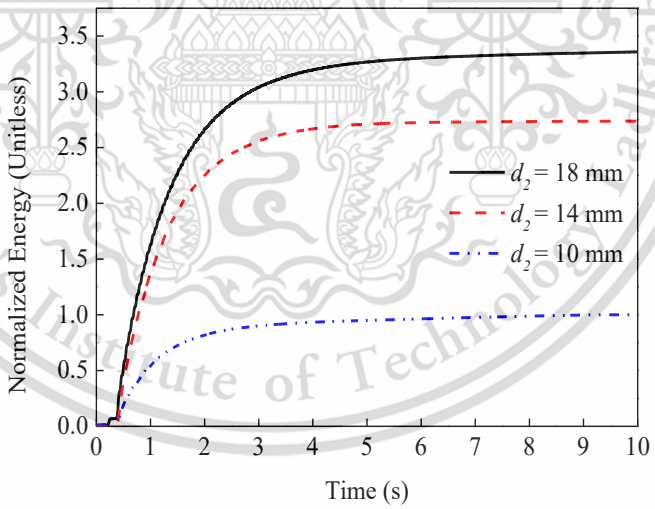

Figure 4.1 Normalized energy from using different airgaps (d_2).

The energy harvesting behavior was determined as follows. Following the experimental method in subsection 4.1.1, a snail cam was rotated at an angular velocity of 8 rad/s with various step time intervals (T_d) of 0.1, 0.5 and 1.0 s which were assumed to represent accurately the walking speeds of a pedestrian. Figure 4.2 (a), (b)

and (c) depict the output voltages from these walking speeds, respectively. The results show that the PZT cantilever plucking frequencies were 1.01Hz, 0.71 Hz and 0.52 Hz, respectively. Figure 4.2 (d) illustrates the energy harvested during 10 s with different step time intervals (T_d). The total output energies were 2.05, 1.42 and 1.00 mJ, respectively. Increasing the step time interval, i.e. slower walking speed, reduced the number of plucks on the PZT cantilever over time leading a decreasing in the total output energy.

Throughout these experimental results, it is safe to say that the designed mechanism is possible to convert the kinetic energy from human footstep into usable electrical energy.

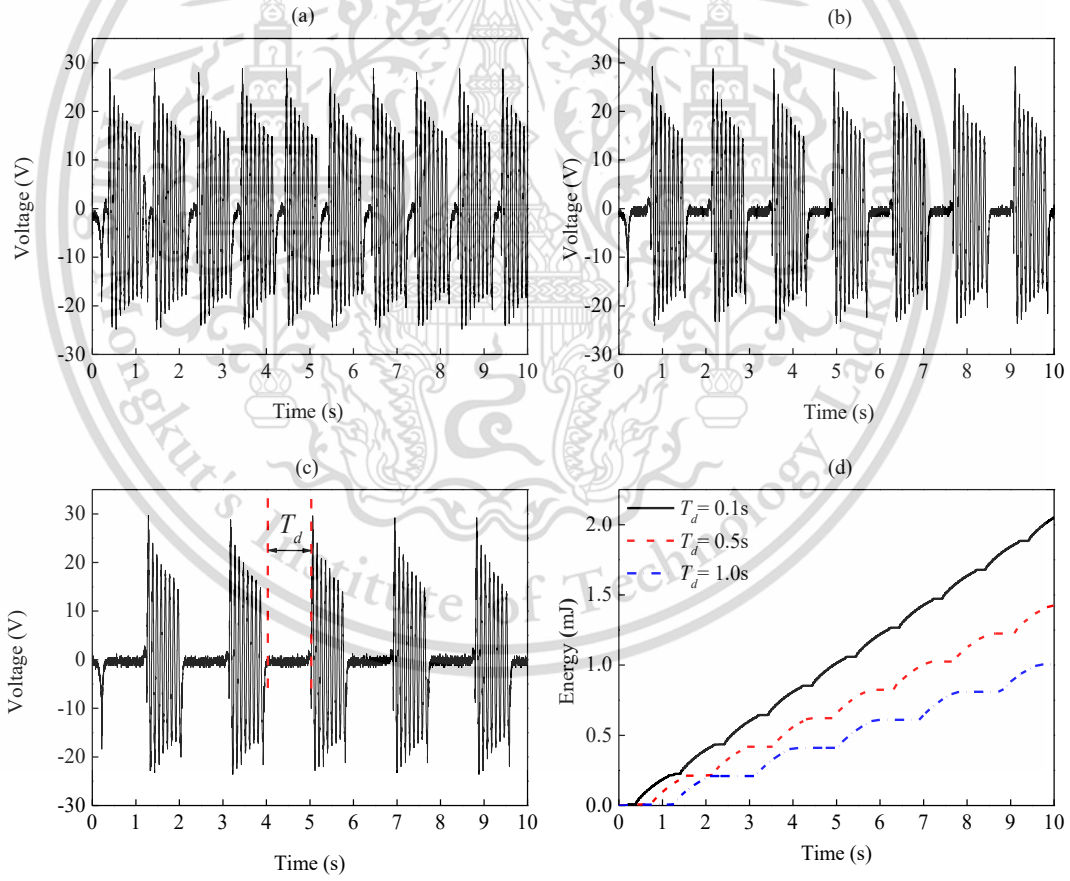

Figure 4.2 Voltages generated with step time intervals T_d of (a) 0.5, (b) 1 and (c) 1.5 s; (d) the trend of harvested energy that varied with step time interval.

4.2 Performance Evaluation of Energy Harvesting Floor Tile

4.2.1 Energy Harvesting Floor Tile

After the designed mechanism was validated as described in section 4.1, a 430 x 430 x 70.50 mm^3 energy harvesting floor was constructed. This size of tile was selected according to a simplification of the installation and easy movement during experiment, anyway, its appropriateness on energy harvesting must be considered. In addition, to achieve the high output energy, many unimorph PZT cantilevers should be mounted inside the tile, the maximum number of which can rely on the interaction among stainless-steel masses inducing the strong magnetic field as shown in figure 4.3. If the distances between stainless-steel masses along x-axis (d_3) and y-axis (d_4) are not large enough, the magnetic force will stop oscillating unimorph PZT cantilever, resulting in low energy conversion efficiency as discussed in section 3.2. The optimal distances d_3 and d_4 were considered by using the FEA simulation.

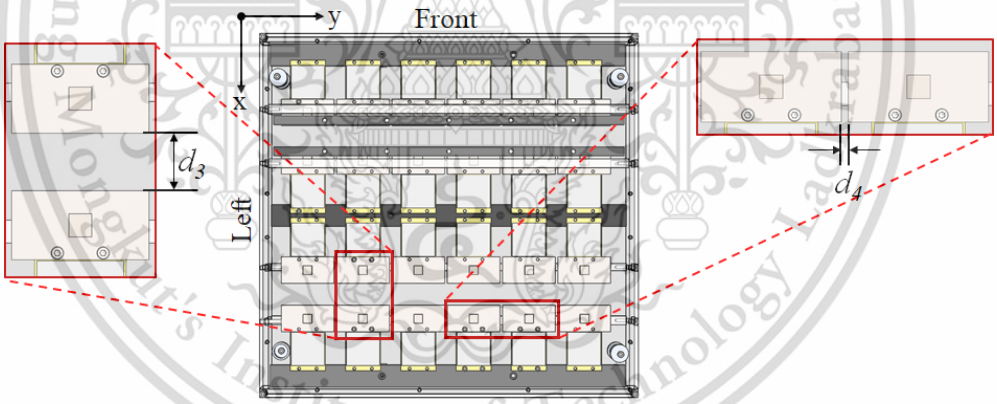

Figure 4.3 Schematic drawing showing the top view of energy harvesting floor tile.

In the simulation, the magnetic properties given in table 3.1 and dimension listed in table 4.1 of materials were used. The magnetic interaction between stainless steel masses was investigated in both repulsive and attractive interaction. As the results shown in figure 4.4 and 4.5, the repulsive interaction is weaker than attractive interaction, which was used in the tile. The repulsive force can diminish to zero with short distance d_3 of 7 mm and d_4 of 1 mm. For the configuration of the tile, to ensure

that there was no magnetic interaction among stainless steel masses, distance d_3 and d_4 were 15 mm and 5 mm, respectively. Thus, the tile with a given size fitted a maximum capacity of 24 unimorph PZT cantilevers as shown in figure 4.6 (a).

Table 4.1 Dimension of materials at different view orientations.

View orientation	Stainless steel mass area (mm^2)	Permanent magnet area (mm^2)	d_3 length (mm)	d_4 length (mm)
Left	2 x 30	5 x 10	3, 5, 7	---
Front	2 x 60	5 x 10	---	1, 2, 3

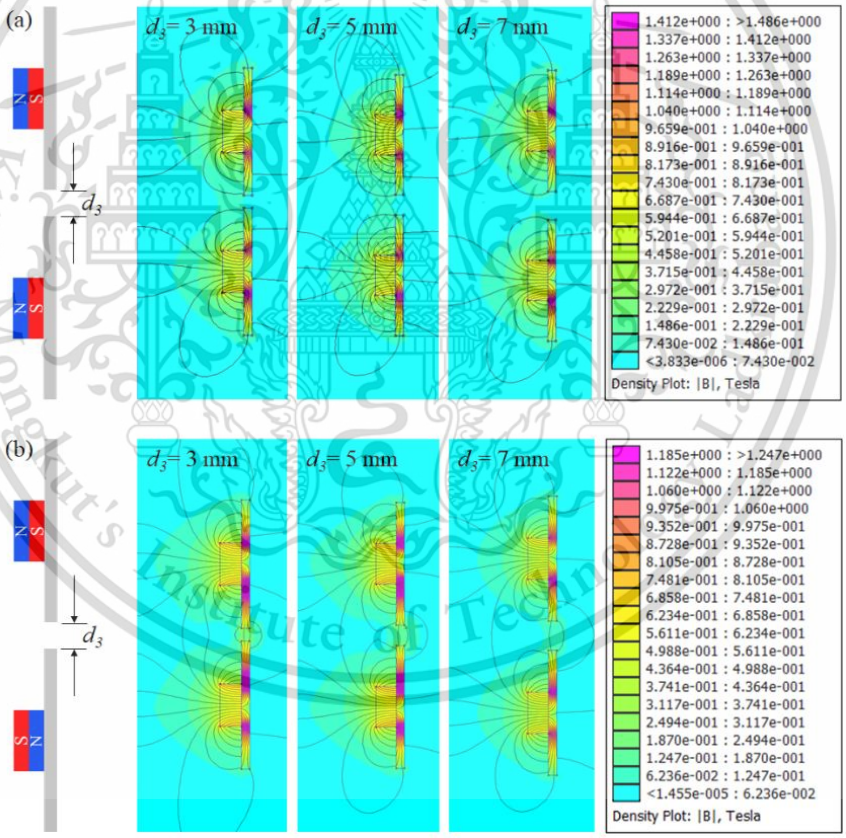

Figure 4.4 Magnetic interaction between stainless steel masses along x-axis; (a) repulsive and (b) attractive interactions.

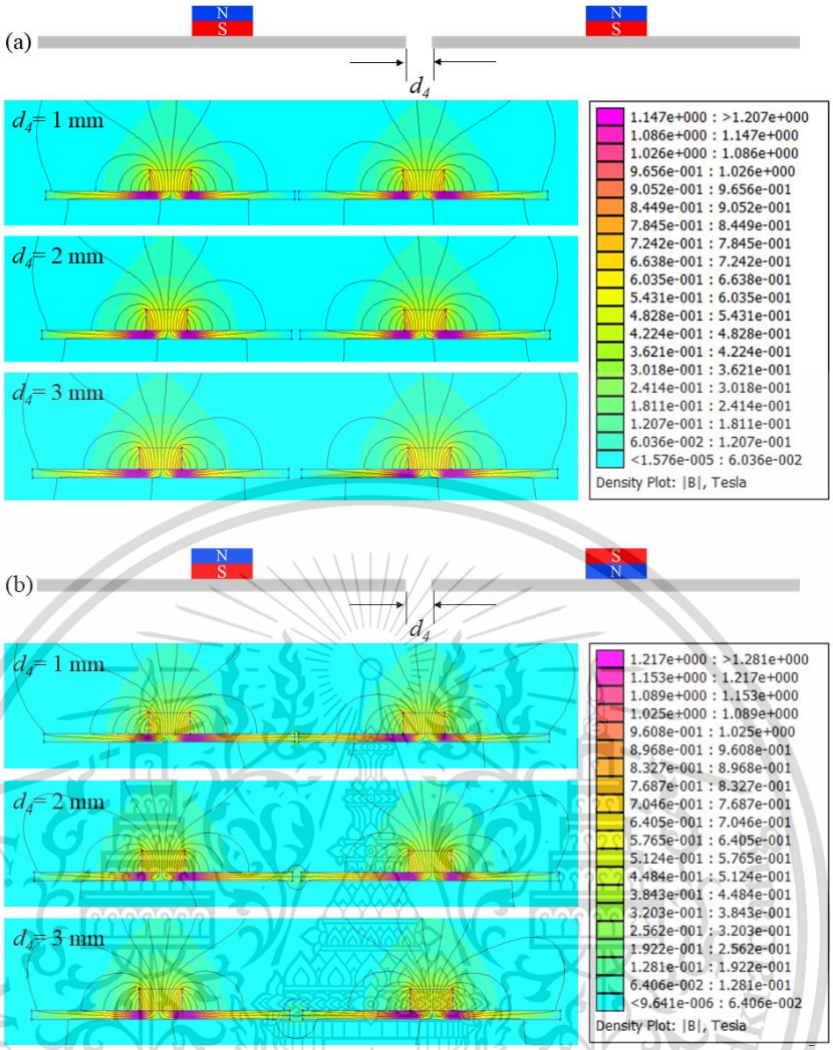

Figure 4.5 Magnetic interaction between stainless steel masses along y-axis; (a) repulsive and (b) attractive interactions.

Figure 4.6 A test setup showing (a) the energy harvesting floor tile and (b) the oscilloscope measuring the voltage (Tektronix TDS3032B).

The air gaps d_1 and d_2 (described in a concept of the floor tile, chapter 3) varied from 2 – 5 and 16 – 19 mm, respectively; they could not be set to one fixed distance

because of the slightly different curvature of the unimorph PZT cantilevers obtained from the manufacturer. A full wave bridge rectifier consisted of small signal Schottky diodes (BAT 46) was used with each of the PZT cantilevers and electrically parallelly connected to other rectifiers as shown in figure 4.7. A parallel circuit was used to sum the output currents from all PZT cantilevers. Its presence was due to each PZT producing only a low current even though it could generate a high voltage. The readiness for the further evaluation step of floor tile can be tested with the open-circuit voltages produced from each of 24 PZT cantilevers and 24 paralleled PZT cantilevers as shown in figure 4.8 and figure 4.9, respectively. The output voltage of each of 24 PZT cantilevers is varied with air gab d_1, anyway, they conform to the output voltage of 24 paralleled PZT cantilevers.

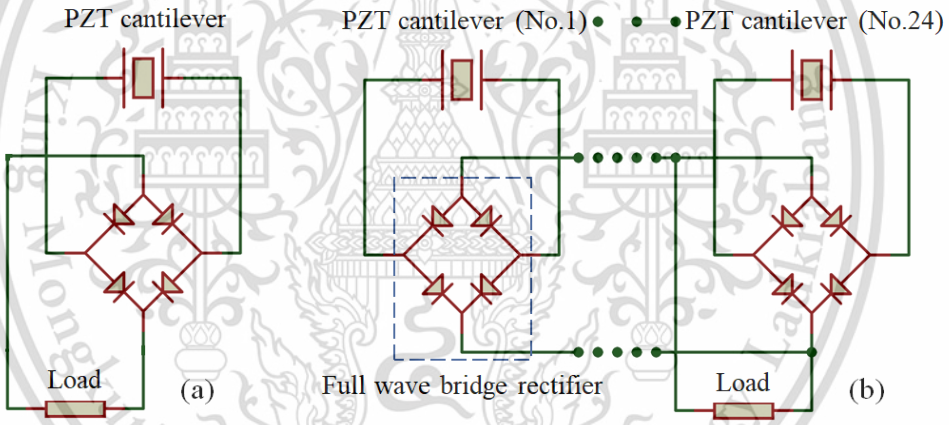

Figure 4.7 (a) Circuit of an individual PZT cantilever; (b) Circuit of electrically connected PZT cantilevers, rectifiers, and load resistors.

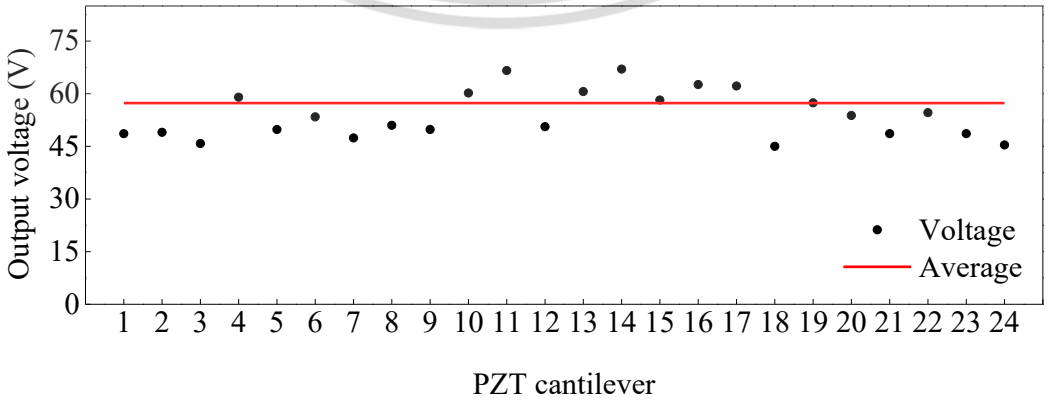

Figure 4.8 Peak open-circuit DC voltage generated by each PZT cantilever.

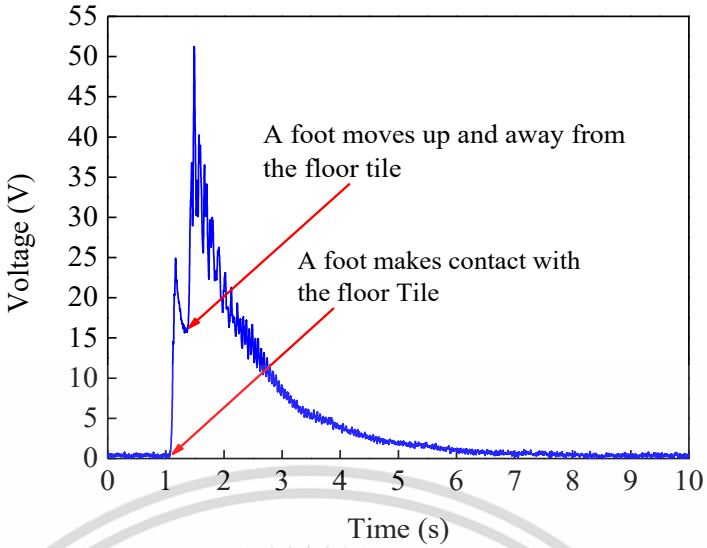

Figure 4.9 Open circuit voltage produced by 24 paralleled unimorph PZT cantilevers.

4.2.2 Performance Evaluation Method

Three kinds of evaluation were performed: evaluation of the energy harvesting performance of one then 24 PZT cantilevers; the effect on energy harvesting performance of the placement location of footsteps; and the energy harvesting performance of the tile in a real scenario. Firstly, the energy harvesting performances of one PZT cantilever and 24 PZT cantilevers were investigated with various load resistors as shown in the figure 4.7 (a) and (b). Each of three randomly selected PZT cantilevers was performance tested. The performance of all 24 connected PZT cantilevers was then evaluated. The load resistor that maximized the power transfer of all of these cantilevers was selected as the optimal load resistor for the other kinds of evaluation. Secondly, the output energy generated by stepping on each different location of the energy harvesting floor was measured and compared. The results would show whether the performance of the tile was consistent or not when it was stepped on its different areas hence they would indicate whether the tile was too big or not. And lastly, the tile's energy harvesting performance when it was mounted and actually stepped on by a pedestrian was determined. The result would indicate whether the amount of the harvested energy would be sufficient or not for supplying a typical wireless sensor node.

4.2.3 Performance Evaluation Results and Discussion

The experimental results of first test are shown in figure 4.10. By exciting the energy harvesting floor tile with a single footstep, the average output power per one PZT cantilever were 0.069, 0.054, and 0.068 mW at optimal load resistances of 377.21, 377.21, and 448.90 kΩ for cantilever #1, #2 and #3, respectively. Their different average output power varied with their vertical displacement (air gap d_1) as mentioned before. The #1 and #3 PZT cantilevers with an air gap d_1 of proximately 4 mm was able to generate a higher average power than #2 with an air gap d_1 of proximately 3 mm. Since the air gaps d_1 that fixed the vertical displacement of many PZT cantilevers were shorter than 4 mm, the average output power from paralleled 24 PZT cantilevers was only 1.24 mW at optimal load resistance of 74.44 kΩ, not the total sum of 1.65 mW as expected. This demonstrates that it is possible to obtain the highest conversion efficiency by fine-tuning the air gap distance of every piezoelectric cantilevers properly or, simpler, if we can obtain cantilevers from a manufacturer with very tight tolerance of their curvature so that no air-gap tuning is needed, we will be able to achieve the highest conversion efficiency.

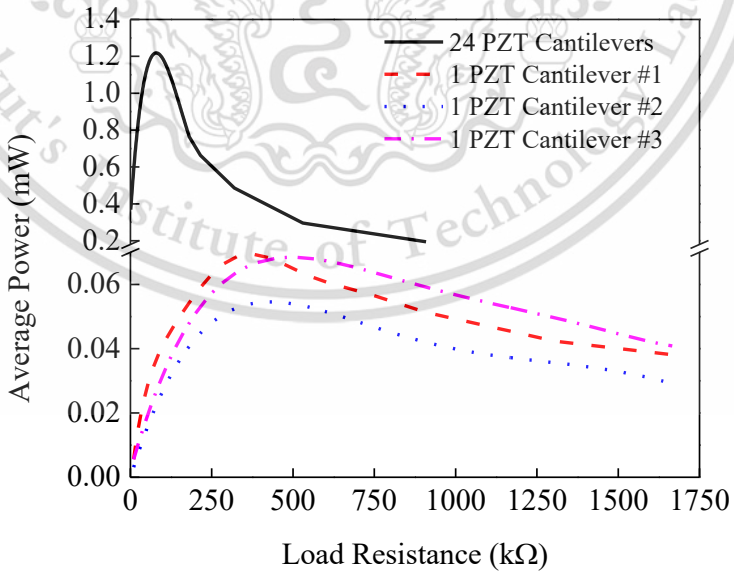

Figure 4.10 The average power of one unimorph PZT cantilever and 24 paralleled unimorph PZT cantilevers.

For the second test, the energy harvesting floor was stepped on at five numbered locations shown in figure 4.11. The total output energy of 2.80, 2.87, 3.49, 2.78, and 2.61 mJ were respectively obtained as exhibited in figure 4.12. The experimental results show that stepping on the location #3 was better than any other locations, since the force could distribute evenly throughout the cover plate, resulting in even movement of the iron bars mounted under the plate relative to the permanent magnet mounted on the PZT cantilevers, thus inducing all cantilevers evenly and consistently. On the other hand, stepping on the cover plate at a corner (First, Second, Fourth or Fifth location) could compress the assembly only locally around that corner because the distributed force to the other corners was low and could not compress down the supporting springs at those corners sufficiently. Thus, only some of the 24 PZT cantilevers were excited. This result suggested to us that the production floor tile should be of a smaller size such that the cover plate will be evenly pressed down by a footstep no matter what location on the plate it lands on.

With step landing on the optimal location #3, the energy conversion efficiency can be examined in the quantitative relation between the amount of the output electrical energy and the input mechanical energy. Figure 4.13 demonstrates the measured conversion efficiency with various load resistors; as can be seen, the greatest conversion efficiency was 17.12 % at the optimal load resistor of 74.44 kΩ.

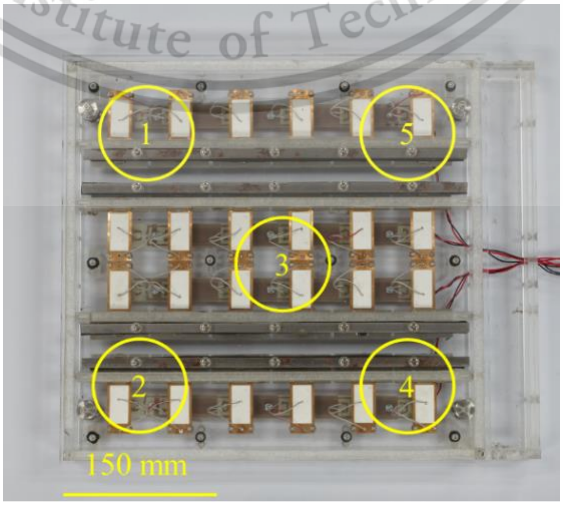

Figure 4.11 Numbered locations on the cover plate.

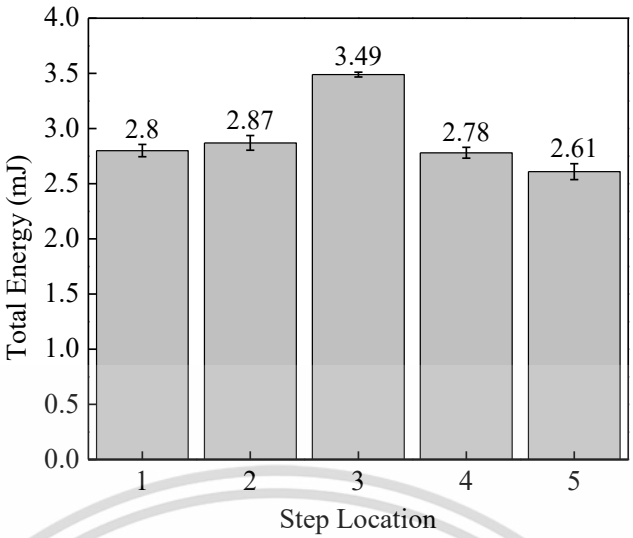

Figure 4.12 Output energy generated by a step that landed on different locations of the energy harvesting floor tile.

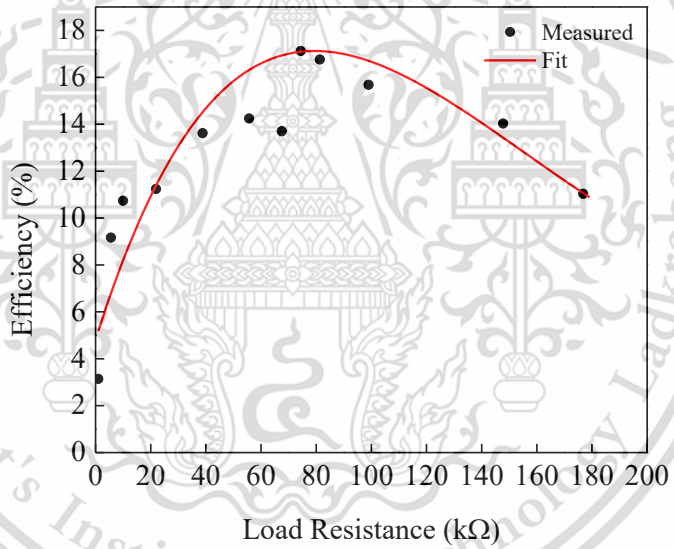

Figure 4.13 Energy conversion efficiency versus load resistor values.

In the final test, the energy harvesting floor tile was placed on a passageway in front of a classroom where 45 students had to walk by and step on it. In this scenario, the output voltage and trend of harvestable energy over time were recorded and calculated and are shown in figure 4.14. The amplitudes of the output DC voltage were in the range of 10.15 - 21.41V. The different voltage values were not due to the weight of each pedestrian, rather it was due to the pedestrians not stepping on the same

location on the cover plate every time as discussed above. The total output energy derived from this experiment was 42.09 mJ. The average energy per one step was approximately 0.93 mJ.

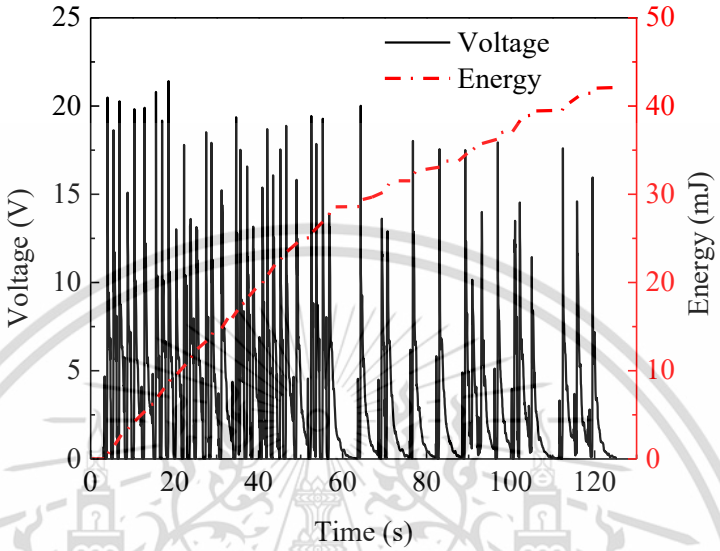

Figure 4.14 Output voltage and energy generated by many pedestrians stepping on the energy harvesting floor tile.

4.3 Wireless Sensor Node Powering Simulation

As the concept of this work is to employ the energy harvesting floor tile in the field of smart city, for providing a sustainable power source to low-power electronic devices, its total output energy of 42.09 mJ was assumed to supply low-power wireless sensor nodes presented in [72]–[74] and shown in table 4.12. The supplied energy can power an accelerometer, a capacitive strain gauge, and smoke detecting wireless sensor nodes to operate for approximately 1.60, 70.15, and 8,503.03 s, respectively. These wireless sensor nodes usually operate in both hibernated and active states in order to reduce power consumption; therefore, it is feasible to store the harvested energy in a capacitor during the node's hibernated state for sufficient use in the further duty cycle of data tracking and transmission. It should be noted that the relatively high amount of energy found in this study was from using an optimal resistor as a load. In real applications, some amount of the energy achieved in this experiment will be lost

when it is stored in a capacitor as a power source for a wireless device due to self-discharge of the capacitor and leakage current in the electronic components when nobody is stepping on the floor tile. The leakage current can be minimized by optimizing the energy magnet circuit and using low-power electronic components [75], [76].

Table 4.2 Estimation of operational time of a low-power wireless sensor node assumed powered by output energy from actual pedestrian steps.

Wireless sensor node	Power consumption (mW)	Operational time (s)
Accelerometer [72]	26.31	1.60
Capacitive strain gauge [73]	0.6	70.15
Smoke detecting [74]	4.95×10^{-3}	8,503.03

4.4 Summary

The energy harvesting floor tile aimed to convert the kinetic energy from human footstep into usable electrical energy was realized and evaluated in this chapter. An optimal setup for magnetic plucking of a PZT cantilever and the feasibility of a designed mechanism were verified through a test bench first. The energy harvesting behavior was analyzed with the simulated human footstep. Then, the prototype was configured, the tile fitted with maximum capacity of 24 PZT cantilevers and the readiness of which for the evaluation step was confirmed by the DC output voltages of each PZT cantilevers and 24 paralleled PZT cantilevers. After that, the three kind of experiments were carried out to evaluate the energy harvesting performance of the tile when operated with one PZT cantilever and 24 paralleled PZT cantilevers and when excited by a step that landed on different locations as well as the actual pedestrian steps. Finally, the wireless sensor powering simulation is given.

Chapter 5
Conclusions

5.1 Research Summary

The starting point of this research is the general introduction of piezoelectric energy harvesting, giving the understanding on piezoelectricity, figure of merit for choosing the bulk piezoelectric material and literature review of different strategies to deal with low frequency and random vibrations. The technique of frequency self-tuning or non-linear vibration is possible for broadband harvesting. The frequency up-conversion technique is optimal for the operation of the energy harvesting floor tile. Regardless of the input excitation, energy can be converted more efficiently.

After that, the relevant parameters were analyzed and an energy harvesting floor tile with frequency up-conversion mechanism was designed. The frequency up-conversion was achieved by using restoring forces from springs to rapidly separate an iron bar away from a permanent magnet where they were attracted to each other via magmatic force. The airgap between the permanent magnet and the iron bar strongly influenced the energy generation; the relationship was analyzed by a Finite Element Method (FEM). When the airgap was large enough to diminish the magnetic force attracting the iron bar to zero, an oscillating piezoelectric cantilever gave the maximum output energy. Too large a displacement of the unimorph cantilever could cause a crack in the piezoelectric layer; this situation was examined then prevented from happening further by using a stopper.

Then, a configuration to test the performance of a sample unimorph PZT cantilever used in this research was performed. The testing results suggested that the unimorph PZT cantilever presents a good energy conversion efficiency, but it has a problem of laminated layers between piezoelectric layer and elastic layer peeling off from each other.

Finally, the validation of the designed mechanism was made with a human footstep simulated by a test bench. The results presented the success of the design,

thus the energy harvesting floor tile was scaled up to consist of 24 PZT cantilevers and used in a performance evaluation experiment. It was observed that the differences in the curvature of the PZT cantilevers and the large size of energy harvesting floor could reduce the total output energy. The former issue was dealt with by fine-tuning individually the amount of displacement that each cantilever could travel, while the latter issue would be dealt with in a future work by making the floor tile smaller. In an actual test having people walking and stepping on the floor tile for 45 steps, it was found that this number of steps could provide high enough harvested energy to activate a few low-power wireless sensor nodes.

5.2 Future Work

In the present work, the principle of energy harvesting floor tile mechanism has been successfully proven and comprehensive modeling has been proposed. In term of the prototype, an energy conversion efficiency can be increased by using a higher-energy-output and more robust piezoelectric cantilever with no lamination between piezoelectric layer and elastic layer so that no fine-tuning of cantilever displacement. Two interesting piezoelectric cantilevers (S230-J1FR-1808XB and T220-H4BR-2513XB bimorphs, Mide Technology) are listed in table 5.1, which exhibit good performance in energy harvesting application [77], [78]. These bimorphs and a PZT cantilever used in the present work are not much different in size, simplifying the installation. Being tested with the same parameter setup and input excitation, a T220-H4BR-2513XB bimorph can generate power of roughly 42 % higher than a S230-J1FR-1808XB bimorph as illustrated in figure 5.1. In addition to the power generation capability, in the structure side, a S230-J1FR-1808XB bimorph having three FR4 layers might be more durable and long-lasting than a T220-H4BR-2513XB bimorph made of one brass layer; where FR4 and brass layers are elastic layer. The performance of both bimorphs can be more investigated by a test bench given in chapter 3 to select the optimal one.

Table 5.1 Specification of bimorph cantilevers.

Specification	S230-J1FR-1808XB	T220-H4BR-2513XB
	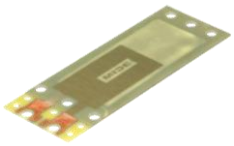	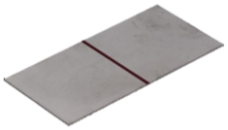
Price	$274.00	$152.00
Total size	71 x 25.4 x 0.76 mm^3	63.5 x 31.8 x 0.51 mm^3
Piezoelectric layer	Two PZT-5J layers	Two PZT-5H layers
Elastic layer	Three FR4 layers	One brass layer

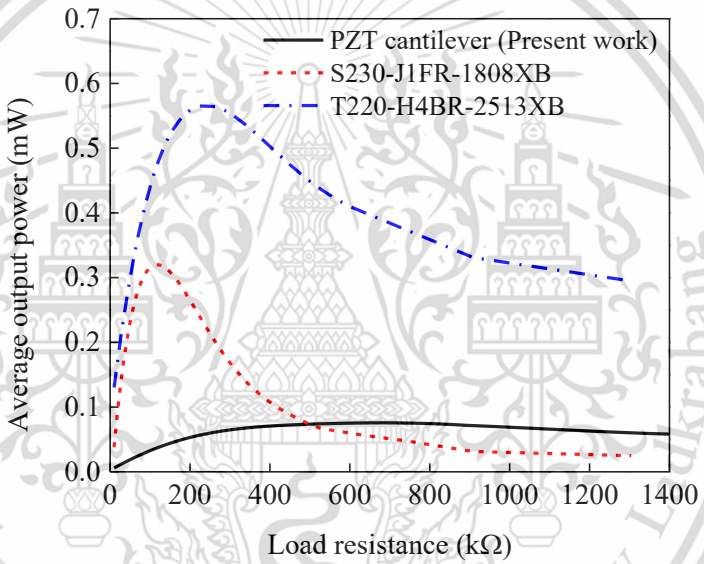

Figure 5.1 Average output power of a PZT cantilever used in the present work and two interesting bimorphs.

Another area of high interest is the optimization of the size and configuration of the tile to overcome the challenge found in the present work that large size of tile results in low energy conversion efficiency, e.g., the force exerted by a foot steeping on a corner of cover plate of the tile was not sufficient for compressing the cover plate down evenly. For an interesting concept, a smaller tile would be fabricated as a generator and then assembled to the tile surface by using a connecter as shown in figure 5.2. The tile surface might be fitted to adult foot with an area of 300 x 300 mm^2 to evenly excite four generators through a connector mounted on the center of their

cover plate. Exciting on the center of cover plate can activate all piezoelectric cantilevers inside each generator, achieving the maximum energy conversion efficiency as discussed in the section 4.2. Therefore, this configuration might be a good option.

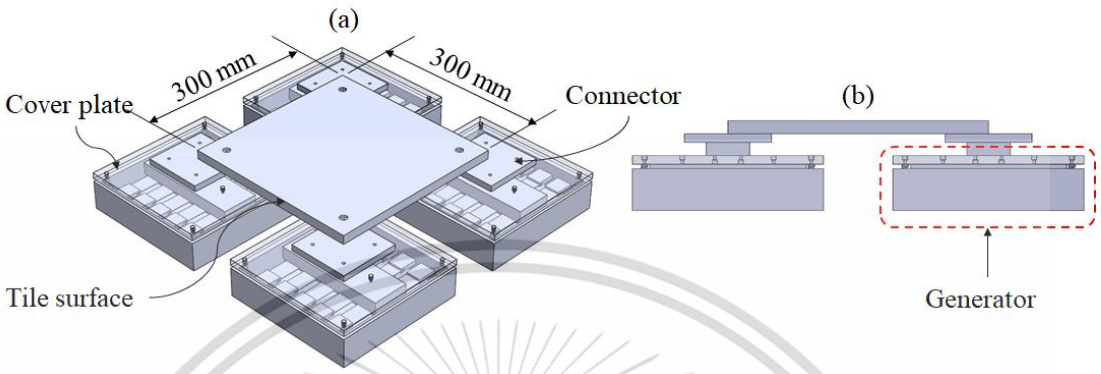

Figure 5.2 Schematic drawing of the tile with the interesting size and configuration; (a) the isometric and (b) side view orientations.

In a grander scheme, a combination of the energy harvesting floor tile with wireless sensor nodes or low-power electronic devices is important. The energy storage and management circuits are what finally make it viable for real applications.

Bibliography

[1] S. Roundy, P. K. Wright, and J. Rabaey, "A study of low level vibrations as a power source for wireless sensor nodes," *Comput. Commun.*, vol. 26, no. 11, pp. 1131–1144, Jul. 2003.

[2] F. Peano and T. Tambosso, "Design and optimization of a MEMS electret-based capacitive energy scavenger," *J. Microelectromechanical Syst.*, vol. 14, no. 3, pp. 429–435, Jun. 2005.

[3] T. Sterken, P. Fiorini, G. Altena, C. V. Hoof, and R. Puers, "Harvesting Energy from Vibrations by a Micromachined Electret Generator," in *TRANSDUCERS 2007 - 2007 International Solid-State Sensors, Actuators and Microsystems Conference*, 2007, pp. 129–132.

[4] Y. Suzuki, "Energy Harvesting from Vibration Using Polymer Electret," in *2008 International Symposium on Micro-NanoMechatronics and Human Science*, 2008, pp. 180–183.

[5] S. Roundy and P. K. Wright, "A piezoelectric vibration based generator for wireless electronics," *Smart Mater. Struct.*, vol. 13, no. 5, pp. 1131–1142, Aug. 2004.

[6] D. Paci, M. Schipani, V. Bottarel, and D. Miatton, "Optimization of a piezoelectric energy harvester for environmental broadband vibrations," in *2008 15th IEEE International Conference on Electronics, Circuits and Systems*, 2008, pp. 177–181.

[7] E. K Reilly, L. Miller, R. Fain, and P. Wright, "A study of ambient vibrations for piezoelectric energy conversion," *Proc PowerMEMS*, pp. 312–315, 2009.

[8] T. von Buren, P. Lukowicz, and G. Troster, "Kinetic energy powered computing - an experimental feasibility study," in *Seventh IEEE International Symposium on Wearable Computers, 2003. Proceedings.*, 2003, pp. 22–24.

[9] "Tourist numbers soaring at Siam Piwat malls," *The Nation*. [Online]. Available: http://www.nationmultimedia.com/detail/Corporate/30334819. [Accessed: 03-May-2019].

[10] Thailand Business News, "Bangkok Suvarnabhumi Airport passengers to jumps to 59 millions in 2017 – Travel." [Online]. Available: https://www.thailand-business-news.com/travel/57886-bangkok-suvarnabhumi-airport-passengers-jumps-59-millions-2017.html. [Accessed: 06-May-2019].

[11] BTS Group Holdings Public Company Limited, “Annual Report 2017/18.” [Online]. Available: http://bts.listedcompany.com/misc/ar/bts-ar201718-en.html. [Accessed: 06-May-2019].

[12] R. Xu and S. G. Kim, “Figures of Merits of Piezoelectric Materials in Energy Harvesters,” *Proc. PowerMEMS*, pp. 464–467, 2012.

[13] R. A. Islam and S. Priya, “Realization of high-energy density polycrystalline piezoelectric ceramics,” *Appl. Phys. Lett.*, vol. 88, no. 3, pp. 1–3, 2006.

[14] MEMS & Nanotechnology Exchange, “Material.” [Online]. Available: http://www.memsnet.org/material/. [Accessed: 03-May-2019].

[15] J. Yin, B. Jiang, and W. Cao, “Elastic, piezoelectric, and dielectric properties of 0.955Pb(Zn/sub 1/3/Nb/sub 2/3/)O/sub 3/-0.45PbTiO/sub 3/ single crystal with designed multidomains,” *IEEE Trans. Ultrason. Ferroelectr. Freq. Control*, vol. 47, no. 1, pp. 285–291, Jan. 2000.

[16] R. Zhang, B. Jiang, and W. Cao, “Elastic, piezoelectric, and dielectric properties of multidomain 0.67Pb(Mg1/3Nb2/3)O3-0.33PbTiO3 single crystals,” *J. Appl. Phys.*, vol. 90, no. 7, pp. 3471–3475, 2001.

[17] D. G. Zong *et al.*, “Tensile strength of aluminium nitride films,” *Philos. Mag.*, vol. 84, no. 31, pp. 3353–3373, 2004.

[18] TRS Ceramics, Inc., “PMN-PT - Single Crystal.” [Online]. Available: http://www.trstechnologies.com/Materials/High-Performance-PMN-PT-Piezoelectric-Single-Crystal. [Accessed: 03-May-2019].

[19] L. M. Miller, P. K. Wright, C. C. Ho, J. W. Evans, P. C. Shafer, and R. Ramesh, “Integration of a low frequency, tunable MEMS piezoelectric energy harvester and a thick film micro capacitor as a power supply system for wireless sensor nodes,” in *2009 IEEE Energy Conversion Congress and Exposition*, 2009, pp. 2627–2634.

[20] L. M. Miller, E. Halvorsen, T. Dong, and P. K. Wright, “Modeling and experimental verification of low-frequency MEMS energy harvesting from ambient vibrations,” *J. Micromechanics Microengineering*, vol. 21, no. 4, p. 045029, Mar. 2011.

[21] L. M. Miller, “Micro-scale piezoelectric vibration energy harvesting: from fixed-frequency to adaptable-frequency devices,” UC Berkeley, 2012.

[22] D. Zhu, M. J. Tudor, and S. P. Beeby, “Strategies for increasing the operating frequency range of vibration energy harvesters: a review,” 2010.

[23] A. G. Mukherjee, P. Mitcheson, S. Wright, E. Yeatman, D. Zhu, and S. Beeby, “Magnetic potential well tuning of resonant cantilever energy harvester,” presented at the Power MEMS, 2012, pp. 480–483.

[24] S. Roundy and Y. Zhang, “Toward self-tuning adaptive vibration-based microgenerators,” in *Smart Structures, Devices, and Systems II*, 2005, vol. 5649, pp. 373–385.

[25] M. Marzencki, M. Defosseux, and S. Basrour, “MEMS Vibration Energy Harvesting Devices With Passive Resonance Frequency Adaptation Capability,” *J. Microelectromechanical Syst.*, vol. 18, no. 6, pp. 1444–1453, Dec. 2009.

[26] L. M. Miller, P. Pillatsch, E. Halvorsen, P. K. Wright, E. M. Yeatman, and A. S. Holmes, “d” *J. Sound Vib.*, vol. 332, no. 26, pp. 7142–7152, Dec. 2013.

[27] A. Boudaoud, Y. Couder, and M. Ben Amar, “A self-adaptative oscillator,” *Eur. Phys. J. B - Condens. Matter Complex Syst.*, vol. 9, no. 1, pp. 159–165, May 1999.

[28] E. C. Miranda and J. J. Thomsen, “Vibration Induced Sliding: Theory and Experiment for a Beam with a Spring-Loaded Mass,” *Nonlinear Dyn.*, vol. 16, no. 2, pp. 167–186, Jun. 1998.

[29] I. Kozinsky, “Study of Passive Self-Tuning Resonator for Broadband Power Harvesting,” 2019.

[30] L. Gu and C. Livermore, “Passive self-tuning energy harvester for extracting energy from rotational motion,” *Appl. Phys. Lett.*, vol. 97, pp. 081904–081904, 2010.

[31] L. Gu and C. Livermore, “Compact passively self-tuning energy harvesting for rotating applications,” *Smart Mater. Struct.*, vol. 21, no. 1, p. 015002, Dec. 2011.

[32] M. Ferrari, V. Ferrari, M. Guizzetti, D. Marioli, and A. Taroni, “Piezoelectric multifrequency energy converter for power harvesting in autonomous microsystems,” *Sens. Actuators Phys.*, vol. 142, pp. 329–335, 2008.

[33] D. Castagnetti, “Experimental modal analysis of fractal-inspired multi-frequency structures for piezoelectric energy converters,” *Smart Mater. Struct.*, vol. 21, no. 9, p. 094009, Aug. 2012.

[34] S. P. Beeby *et al.*, “A comparison of power output from linear and non-linear kinetic energy harvesters using real vibration data,” *Smart Mater. Struct.*, vol. 22, p. 75022, Jul. 2013.

[35] A. Abdelkefi, F. Najar, A. H. Nayfeh, and S. B. Ayed, “An energy harvester using piezoelectric cantilever beams undergoing coupled bending–torsion vibrations,” *Smart Mater. Struct.*, vol. 20, no. 11, p. 115007, Oct. 2011.

[36] Y. Zhu, J. Zu, and W. Su, “Broadband energy harvesting through a piezoelectric beam subjected to dynamic compressive loading,” *Smart Mater. Struct.*, vol. 22, no. 4, p. 045007, Mar. 2013.

[37] Ji-Tzuoh Lin, W. Jones, B. Alphenaar, Yang Xu, and D. Alphenaar, “Passive magnetic coupling to enhance piezoelectric cantilever response in energy scavenging applications,” in *2008 17th IEEE International Symposium on the Applications of Ferroelectrics*, Santa Re, NM, USA, 2008, pp. 1–2.

[38] M. Ferrari, V. Ferrari, M. Guizzetti, B. Andò, S. Baglio, and C. Trigona, “Improved energy harvesting from wideband vibrations by nonlinear piezoelectric converters,” *Sens. Actuators Phys.*, vol. 162, no. 2, pp. 425–431, Aug. 2010.

[39] M. Ferrari, M. Baù, M. Guizzetti, and V. Ferrari, “A single-magnet nonlinear piezoelectric converter for enhanced energy harvesting from random vibrations,” *Sens. Actuators Phys.*, vol. 1, no. 172, pp. 287–292, 2011.

[40] B. Marinkovic and H. Koser, “Demonstration of wide bandwidth energy harvesting from vibrations,” *Smart Mater. Struct.*, vol. 21, no. 6, p. 065006, May 2012.

[41] A. Hajati, S. P. Bathurst, H. J. Lee, and S. G. Kim, “Design and fabrication of a nonlinear resonator for ultra wide-bandwidth energy harvesting applications,” in *2011 IEEE 24th International Conference on Micro Electro Mechanical Systems*, 2011, pp. 1301–1304.

[42] A. Hajati, “Wide-Bandwidth MEMS-Scale Piezoelectric Energy Harvester,” 2009.

[43] A. Hajati and S.-G. Kim, “Ultra-wide bandwidth piezoelectric energy harvesting,” *Appl. Phys. Lett.*, vol. 99, no. 8, p. 083105, Aug. 2011.

[44] F. Cottone, L. Gammaitoni, H. Vocca, M. Ferrari, and V. Ferrari, “Piezoelectric buckled beams for random vibration energy harvesting,” *Smart Mater. Struct.*, vol. 21, no. 3, p. 035021, Feb. 2012.

[45] S. A. Emam and A. H. Nayfeh, “On the Nonlinear Dynamics of a Buckled Beam Subjected to a Primary-Resonance Excitation,” *Nonlinear Dyn.*, vol. 35, no. 1, pp. 1–17, Jan. 2004.

[46] J. F. Blackburn and M. G. Cain, “Nonlinear piezoelectric resonance: A theoretically rigorous approach to constant I–V measurements,” *J. Appl. Phys.*, vol. 100, no. 11, p. 114101, Dec. 2006.

[47] T. Galchev, E. E. Aktakka, H. Kim, and K. Najafi, “A piezoelectric frequency-increased power generator for scavenging low-frequency ambient vibration,” in *2010 IEEE 23rd International Conference on Micro Electro Mechanical Systems (MEMS)*, 2010, pp. 1203–1206.

[48] M. Umeda, K. Nakamura, and S. Ueha, “Analysis of the Transformation of Mechanical Impact Energy to Electric Energy Using Piezoelectric Vibrator,” *Jpn. J. Appl. Phys.*, vol. 35, no. 5S, p. 3267, May 1996.

[49] M. Umeda, K. Nakamura, and S. Ueha, “Energy Storage Characteristics of a Piezo-Generator using Impact Induced Vibration,” *Jpn. J. Appl. Phys.*, vol. 36, no. 5S, p. 3146, May 1997.

[50] Y. Zhang and C. S. Cai, “A retrofitted energy harvester for low frequency vibrations,” *Smart Mater. Struct.*, vol. 21, no. 7, p. 075007, Jun. 2012.

[51] M. Renaud, P. Fiorini, R. van Schaijk, and C. van Hoof, “An impact based piezoelectric harvester adapted to low frequency environmental vibrations,” in *TRANSDUCERS 2009 - 2009 International Solid-State Sensors, Actuators and Microsystems Conference*, 2009, pp. 2094–2097.

[52] M. Renaud, P. Fiorini, and C. van Hoof, “Optimization of a piezoelectric unimorph for shock and impact energy harvesting,” *Smart Mater. Struct.*, vol. 16, no. 4, pp. 1125–1135, Jun. 2007.

[53] L. Gu and C. Livermore, “Impact-driven, frequency up-converting coupled vibration energy harvesting device for low frequency operation,” *Smart Mater. Struct.*, vol. 20, no. 4, p. 045004, Mar. 2011.

[54] L. Gu, “Low-frequency piezoelectric energy harvesting prototype suitable for the MEMS implementation,” *Microelectron. J.*, vol. 42, no. 2, pp. 277–282, Feb. 2011.

[55] E. Jacquelin, S. Adhikari, and M. I. Friswell, “A piezoelectric device for impact energy harvesting,” *Smart Mater. Struct.*, vol. 20, no. 10, p. 105008, Aug. 2011.

[56] M. Pozzi, M. S. H. Aung, M. Zhu, R. K. Jones, and J. Y. Goulermas, “The pizzicato knee-joint energy harvester: characterization with biomechanical data and the effect of backpack load,” *Smart Mater. Struct.*, vol. 21, no. 7, p. 075023, Jun. 2012.

[57] M. Pozzi and M. Zhu, “Pizzicato excitation for wearable energy harvesters,” *SPIE Newsroom*, Jul. 2012.

[58] M. Pozzi and M. Zhu, “Plucked piezoelectric bimorphs for knee-joint energy harvesting: modelling and experimental validation,” *Smart Mater. Struct.*, vol. 20, no. 5, p. 055007, Apr. 2011.

[59] M. Pozzi and M. Zhu, “Characterization of a rotary piezoelectric energy harvester based on plucking excitation for knee-joint wearable applications,” *Smart Mater. Struct.*, vol. 21, no. 5, p. 055004, Apr. 2012.

[60] P. Janphuang, R. A. Lockhart, D. Isarakorn, S. Henein, D. Briand, and N. F. de Rooij, “Harvesting Energy From a Rotating Gear Using an AFM-Like MEMS Piezoelectric Frequency Up-Converting Energy Harvester,” *J. Microelectromechanical Syst.*, vol. 24, no. 3, pp. 742–754, Jun. 2015.

[61] Y. Kuang, Z. Yang, and M. Zhu, “Design and characterisation of a piezoelectric knee-joint energy harvester with frequency up-conversion through magnetic plucking,” *Smart Mater. Struct.*, vol. 25, no. 8, p. 085029, Jul. 2016.

[62] P. Pillatsch, E. M. Yeatman, and A. S. Holmes, “A piezoelectric frequency up-converting energy harvester with rotating proof mass for human body applications,” *Sens. Actuators Phys.*, vol. 206, pp. 178–185, 2014.

[63] H. T. Luong and N. S. Goo, “Use of a magnetic force exciter to vibrate a piezocomposite generating element in a small-scale windmill,” *Smart Mater. Struct.*, vol. 21, no. 2, p. 025017, Jan. 2012.

[64] Q. C. Tang, X. Y. Xia, and X. X. Li, “Non-contact frequency-up-conversion energy harvester for durable broad-band automotive TPMS application,” in *2012 IEEE 25th International Conference on Micro Electro Mechanical Systems (MEMS)*, 2012, pp. 1273–1276.

[65] Q. C. Tang, Y. L. Yang, and X. Li, “Bi-stable frequency up-conversion piezoelectric energy harvester driven by non-contact magnetic repulsion,” *Smart Mater. Struct.*, vol. 20, no. 12, p. 125011, Nov. 2011.

[66] Y. Yang, Q. Tang, and X. Li, “Non-contact repulsive-force excitation for highly endurable wide frequency-range energy-harvesting,” in *2011 16th International Solid-State Sensors, Actuators and Microsystems Conference*, 2011, pp. 687–690.

[67] A. M. Wickenheiser and E. Garcia, “Broadband vibration-based energy harvesting improvement through frequency up-conversion by magnetic excitation,” *Smart Mater. Struct.*, vol. 19, no. 6, p. 065020, May 2010.

[68] A. M. Wickenheiser, “Analysis of Energy Harvesting Using Frequency Up-Conversion by Analytic Approximations,” 2012.

[69] T. Galchev, H. Kim, and K. Najafi, “Micro Power Generator for Harvesting Low-Frequency and Nonperiodic Vibrations,” *J. Microelectromechanical Syst.*, vol. 20, no. 4, pp. 852–866, Aug. 2011.

[70] X. Gao, W.-H. Shih, and W. Y. Shih, “Induced voltage of piezoelectric unimorph cantilevers of different nonpiezoelectric/piezoelectric length ratios,” *Smart Mater. Struct.*, vol. 18, no. 12, p. 125018, Oct. 2009.

[71] V. M. Tom, “Pedestrian crossing - Traffic Engineering and Management - Lecture Notes - Docsity.” [Online]. Available: https://www.docsity.com/en/pedestrian-crossing-traffic-engineering-and-management-lecture-notes/317343/. [Accessed: 03-May-2019].

[72] T. Sudhawiyangkul and D. Isarakorn, “Design and realization of an energy autonomous wireless sensor system for ball screw fault diagnosis,” *Sens. Actuators Phys.*, vol. 258, pp. 49–58, 2017.

[73] R. Zeiser, T. Fellner, and J. Wilde, “Capacitive strain gauges on flexible polymer substrates for wireless, intelligent systems,” *J. Sens. Sens. Syst.*, vol. 3, no. 1, pp. 77–86, Apr. 2014.

[74] J. A. Luis, J. A. G. Galán, and J. A. Espigado, “Low Power Wireless Smoke Alarm System in Home Fires,” *Sensors*, vol. 15, no. 8, pp. 20717–20729, Aug. 2015.

[75] M. A. Halim and J. Y. Park, “Theoretical modeling and analysis of mechanical impact driven and frequency up-converted piezoelectric energy harvester for low-frequency and wide-bandwidth operation,” *Sens. Actuators Phys.*, vol. 208, pp. 56–65, Feb. 2014.

[76] D. Alghisi, S. Dalola, M. Ferrari, and V. Ferrari, “Triaxial ball-impact piezoelectric converter for autonomous sensors exploiting energy harvesting from vibrations and human motion,” *Sens. Actuators Phys.*, vol. 233, pp. 569–581, Sep. 2015.

[77] Mide Technology, “Piezoelectric Bending Transducer (S230-J1FR-1808XB),” *PIEZO.COM*. [Online]. Available: https://piezo.com/products/piezoelectric-bending-transducer-s230-j1fr-1808xb. [Accessed: 16-Jul-2019].

[78] Mide Technology, “Piezoelectric Bending Transducer (T220-H4BR-2513XB),” *PIEZO.COM*. [Online]. Available: https://piezo.com/products/piezoelectric-bending-transducer-t220-h4br-2513xb. [Accessed: 16-Jul-2019].

Publications

Journal:

P. Panthongsy, D. Isarakorn, P. Janphuang, and K. Hamamoto, "Fabrication and evaluation of energy harvesting floor using piezoelectric frequency up-converting mechanism," *Sens. Actuators A Phys.*, vol. 279, pp. 321–330, Aug. 2018.

Conferences:

P. Panthongsy, D. Isarakorn, and K. Hamamoto, "A Test Bench for Characterization of Piezoelectric Frequency Up-Converting Energy Harvesters," in *the 15th International Conference on Electrical Engineering/Electronics, Computer, Telecommunications and Information Technology (ECTI-CON),* 2018, pp. 134–137.

P. Panthongsy, D. Isarakorn, K. Hamamoto and P. Janphuang, "Performance and Behavior Analysis of Piezoelectric Energy Harvesting Floor Tiles," in *the 5th International Conference on Engineering, Applied Sciences and Technology (ICEAST)*, 2019, pp. 446–449.

Petty Patent:

ดอน อิศรากร, **โพสี ปานทองสี**, "อุปกรณ์ทดสอบคุณสมบัติของเพียโซอิเล็กทริกโดยใช้วิธีการแบบสั่นต่อเนื่อง." Thailand, no. 14609, November 2018.

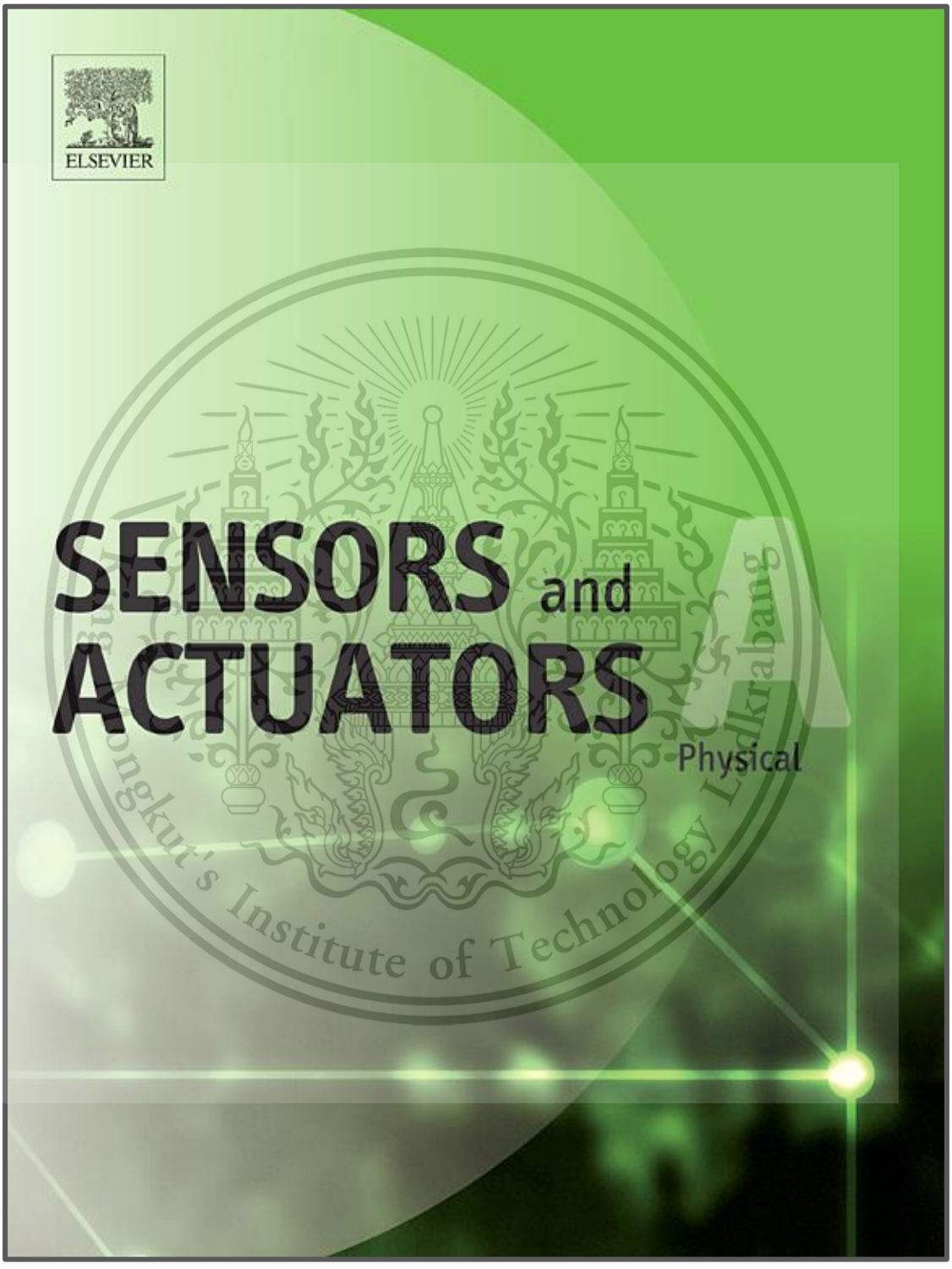

Sensors and Actuators A 279 (2018) 321–330

Contents lists available at ScienceDirect

Sensors and Actuators A: Physical

journal homepage: www.elsevier.com/locate/sna

Fabrication and evaluation of energy harvesting floor using piezoelectric frequency up-converting mechanism

Phosy Panthongsy[a], Don Isarakorn[b,*], Pattanaphong Janphuang[c], Kazuhiko Hamamoto[d]

[a] Department of Instrumentation and Control Engineering, Faculty of Engineering, King Mongkut's Institute of Technology Ladkrabang, Bangkok, 10520, Thailand
[b] Department of Instrumentation and Control Engineering, Faculty of Engineering, King Mongkut's Institute of Technology Ladkrabang, Bangkok, 10520, Thailand
[c] Synchrotron Light Research Institute, 111 University Avenue, Muang District, Nakhon Ratchasima, 30000, Thailand
[d] Department of Information Media Technology, School of Information and Telecommunication Engineering, Tokai University, 2-3-23 Takanawa Minato-ku, Tokyo, 108-8619, Japan

ARTICLE INFO

Article history:
Received 11 November 2017
Received in revised form 22 May 2018
Accepted 17 June 2018
Available online 20 June 2018

Keywords:
Energy harvesting floor
Frequency up-converting strategy
Low-Frequency energy harvesting
Piezoelectric harvester

ABSTRACT

This paper reports on the fabrication and evaluation of an energy harvesting floor tile using unimorph PZT piezoelectric cantilevers to convert kinetic energy from human footsteps into usable electricity. The operation of the tile is based on frequency up-converting mechanism in which low frequency input vibrations are converted into high frequency vibrations of an electromechanical transduction. The operational frequency of the PZT unimorph cantilever was converted up by an interaction between a permanent magnet and an iron bar. Vertical displacement of the oscillating cantilever was localized with a stopper preventing damage to the piezoelectric layer from shock or over-displacement excitation. The magnetic field density between the magnet and the iron bar was investigated through finite element analysis simulation in order to define an optimal air gap. Experimentally, a unimorph PZT cantilever was initially prototyped to validate the design. The results showed a successful frequency up-conversion with a resonant frequency of 10.54 Hz. Then, it was scaled up by accommodating 24 unimorph PZT cantilevers followed by experimental validation to evaluate its energy harvesting performance. Each cantilever was connected to a full wave bridge rectifier then connected in parallel with the other cantilevers. The generated electrical power and energy were investigated through various resistive loads. The average power and total output energy produced by one foot step on the tile were found to be 1.24 mW and 3.49 mJ, respectively at an optimal load resistance of 74.44 kΩ. The energy conversion efficiency reached 17.12% demonstrating the potential of harvesting energy from human motion.

1. Introduction

Wireless sensor node emerged decades ago has been continuously important in a variety of fields including industry, agriculture, infrastructure, disaster prediction and environment monitoring due to its ability to track information in a hard-to-reach location at a lower cost than wire solution. Following the feature of communication without wiring and recent trend of electronics technology that electronic components are reduced in size and power consumption, many existed wireless sensor nodes are powered by battery. However, there are several issues on battery use such as limited energy storage capacity, battery lifespan, and inconvenient maintenance of depleted batteries in unreachable location especially implanted sensors. Therefore, harvesting ambient environment energy to supply sustainable electrical power to devices such as an energy autonomous system is highly desirable. Energy powering small embedded device is typically harvested from light, thermal or vibration sources. Environmental vibration has particularly attracted many researchers because of its ubiquity. In this respect, electrical energy can be obtained by electrostatic [1], electromagnetic [2] or piezoelectric [3] conversion. Piezoelectric generator has received great interest due to its simple, low structure profile, ease of integration, high power density and high energy conversion efficiency [4,5].

At present, piezoelectric energy harvesters are usually resonant-type device. Its resonant frequency is closely matched to the frequency of the surrounding vibration sources in order to achieve maximum power generation. However, resonant-type device is not a good option for conversion of human movement or variable vibration over time. Its generated electrical energy drops significantly at

* Corresponding author.
E-mail address: don.is@kmitl.ac.th (D. Isarakorn).

https://doi.org/10.1016/j.sna.2018.06.035
0924-4247/

low frequency when the resonant frequency of the harvester deviates far from the frequency of the vibration source [6,7]. To achieve a high harvesting efficiency, several frequency up-conversion mechanisms that excite a harvester from low-frequency input vibration have been investigated recently. A commonly used strategy is to make the cantilever or buzzer disk of a piezoelectric harvester deflect initially and then leave it to oscillate freely. An initial deflection can be implemented by mechanical contact or by non-contact magnetic interaction.

A contact frequency up-conversion mechanism was firstly presented by Umeda et al [8,9]; they investigated the generated energy from a piezoelectric beam impacted by a steel ball. After this pioneering paper, many researchers have begun further investigations. For example, Ranaud et al. [10] used a moving mass to strike one of two piezoelectric cantilevers located at each end of a harvester container while the harvester was being shaken from side to side. The impact from the moving mass increased the operational frequency of the piezoelectric enabling it to harvest energy from low-frequency and high-amplitude input and provide power to wearable gait monitoring device. Pozzi et al. [11] applied a plucking-based frequency up-conversion strategy to a piezoelectric wearable energy harvester in order to convert energy from knee-joint motion. This mechanical plucking deflected the piezoelectric beams through a plectrum and then rapidly left them free to vibrate. The core challenge in integration of a contact frequency up-conversion mechanism to a harvester is the decrease in life span of the piezoelectric cantilever [12].

On the non-contact up-conversion mechanism side, Kulah et al. [13] reported one that employed the attractive force between permanent magnet and metal to increase the vibrational frequency of cantilever coils in an electromagnetic energy harvester. In addition, Pillatsch et al. [14] demonstrated a body-movement-energy harvesting device that used a rotational system. In this device, magnetic coupling with a rotating proof mass was used to pluck the piezoelectric cantilever. In another study, Luong et al. [15] used magnetic force interaction between permanent magnets to excite a piezocomposite generating element (PCGE) in a small-scale windmill. The primary magnet was attached to the input rotor, and the secondary magnet was attached to the free end of the PCGE. The main advantage of non-contact frequency up-conversation mechanism is that the piezoelectric or coil cantilevers do not have to suffer repeated damaging physical contact with anything which makes their operation more reliable than that of the contact frequency up-conversation mechanism. However, the energy by generated a non-contact generator drops significantly at high speed of magnetic plucking [16]. Therefore, an efficient energy harvester with frequency up-conversion mechanism that has a long operational life time and suffers no effect of high plucking speed is of much interest.

This paper proposes an energy harvesting floor tile based on frequency up-conversion principle for converting low-frequency vibration especially pedestrian's step into usable electrical energy. Its conceptual model and the frequency up-conversion mechanism are introduced first. Then, the validation of the design is presented. Next, the fabrication and evaluation of the energy harvesting floor tile are described. Lastly, a conclusion is given.

2. Concepts of energy harvesting floor tile and frequency up-conversion strategy

The schematic diagram of the energy harvesting floor tile with the frequency up-conversion mechanism is illustrated in Fig. 1. Twenty-four unimorph piezoelectric cantilevers are mounted on a supporter, the free ends of which are attached to a stainless-steel mass to increase the strain in the piezoelectric substance causing the increase of electrical output power during oscillation. The permanent magnets are glued to the top surface of the mass for attracting the iron bar underneath the cover plate when the floor tile is stepped on. The soft plastic is used to absorb the impact force between the iron bar and the permanent magnet. Four springs are installed at each corner pulling up the cover plate. A stopper is used to protect the piezoelectric layer from damage from over-displacement excitation.

Fig. 2 illustrates the frequency up-converting sequences of energy harvesting floor tile. In the waiting for load state (Fig. 2(a)), the air gap between the permanent magnet and the iron bar (d_2) should be optimized to ensure that the attracting force from the permanent magnet (F_{iM}) to the iron bar is not going to stop vibrating cantilever; therefore, the iron bar should be located where $F_{iM} = 0$. The attractive force exerted by the permanent magnet at the air gap is given by the following Maxwell's equation:

$$F_{iM} = \frac{B^2 A_i}{2\mu_0}, \tag{1}$$

where the subscript $i = 1, 2, 3\ldots$ and 24 identifies a particular permanent magnet and unimorph cantilever. B represents the magnetic flux density, A_i is the cross section of the area of the pole, and μ_0 is the permeability of the air.

For the loaded state shown in Fig. 2(b), when the energy harvesting floor tile is stepped on, springs are compressed by a compressive force (F_L) from the weight of the pedestrian. The compressive force F_L should be larger than the restoring force of the spring (F_{jS}); $F_L \rangle \sum_{j=1}^{a} F_{jS}$ where a is the total number of the springs used. From Newton's second law and Hooke's law, F_L and F_{jS} can be calculated by the equations below,

$$F_L = m_L g, \tag{2}$$

$$F_{jS} = -k_{jS} h, \tag{3}$$

where the subscript $j = 1, 2, 3$ and 4 identifies a particular spring; m_L is the mass of the pedestrian; g is the gravitational acceleration; k_{jS} is the spring constant; and h represents the displacement from the equilibrium position of the spring. The loaded state is also a state that the iron bar comes close to a location where the magnetic field density is high so that the bar will be attracted by the permanent magnet. Thus, the permanent magnet deflects the piezoelectric cantilever underneath the iron bar. The resultant force in the z-axis (F_{iZ}) deflecting the unimorph piezoelectric cantilever is equal to

$$F_{iz} = F_{iM}\cos\theta - (F_{iC}\cos\theta + m_{iT} g), \tag{4}$$

where F_{iC} is the restoring force of the unimorph piezoelectric cantilever; θ is the top surface angle of permanent magnet, and m_{iT} represents the total mass of the magnet and the stainless-steel mass at tip of piezoelectric unimorph cantilever. The restoring force F_{iC} can be calculated from the equation below: [17]

$$F_{iC} = k_{iC} d_1, \tag{5}$$

where k_{iC} is the effective spring constant of the unimorph piezoelectric cantilever; d_1 is the displacement of the unimorph piezoelectric cantilever from its rest position; and k_{iC} is calculated by the following equation,

$$k_{iC} = \frac{3(EI)_{Cantilever}}{l^3} = \frac{3(E_p I_p + E_e I_e)}{l^3}, \tag{6}$$

where $(EI)_{Cantilever}$ is the effective bending modulus of the unimorph piezoelectric cantilever; l is the length of the piezoelectric and elastic layers; E_p and E_e are the Young's modulus of the piezoelectric and elastic layers; and I_p and I_e are the moments of inertia

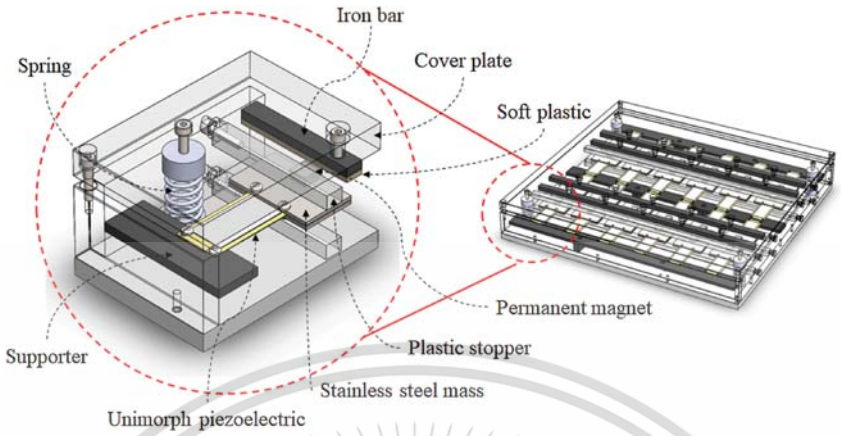

Fig. 1. Schematic drawing of energy harvesting floor tile.

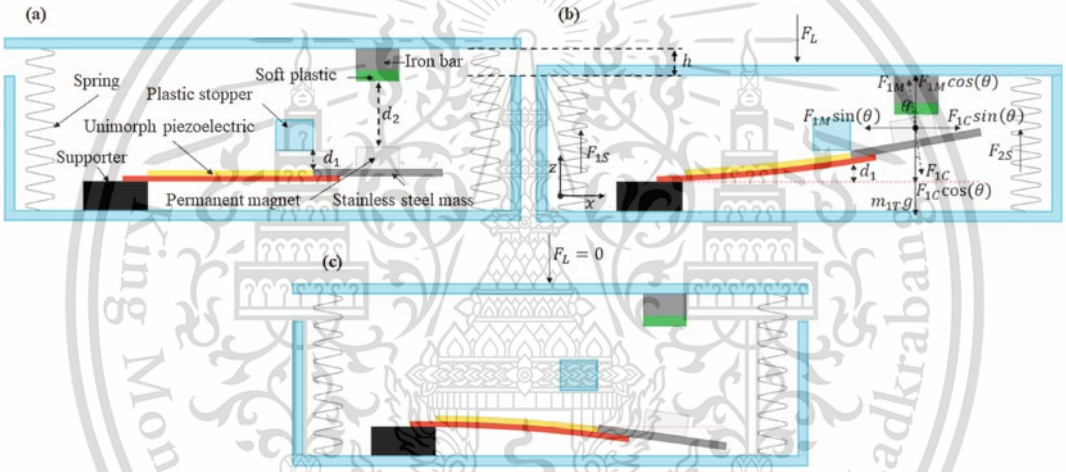

Fig. 2. (a) Waiting for load; (b) and (c) Loaded and unloaded states of energy harvesting floor tile.

of the piezoelectric and elastic layers. The moments of inertia of the piezoelectric and elastic layers can be determined by the following equations [18],

$$I_p = \frac{w_p t_p^3}{l^3} + w_p t_p \left(\frac{t_p}{2} - t_n\right)^2, \tag{7}$$

$$I_e = \frac{w_e t_e^3}{l^3} + w_e t_e \left(\frac{t_e}{2} - t_n\right)^2, \tag{8}$$

where w_p and w_e are the widths of the piezoelectric and elastic layers; t_p and t_e are the thicknesses of the piezoelectric and elastic layers; and t_n is the distance of the neutral plane in the piezoelectric layer, shown in Fig. 3, which can be calculated by the equation below,

$$t_n = \frac{E_p t_p^2 - E_e t_e^2}{2(E_p t_p + E_e t_e)}. \tag{9}$$

Furthermore, the compressive stress in the unimorph piezoelectric cantilever is induced by the resultant force in the x-axis,

$$F_{ix} = F_{iM} \sin\theta - F_{iC} \sin\theta. \tag{10}$$

In the unloaded state, when the foot moves up and away from the energy harvesting floor tile; $F_L = 0$ as shown in Fig. 2(c) and the total restoring force of the spring is higher than the total force in the z-axis; $\sum_{j=1}^{a} F_{jS} \rangle \sum_{i=1}^{b} F_{iz}$ where b is the number of the cantilevers with an attached permanent magnet; the springs will push the cover plate and the iron bar up and away from the permanent magnet. This step will rapidly separate the permanent magnet from the iron bar allowing the unimorph piezoelectric cantilever to freely oscillate at a high frequency.

3. Verification of the feasibility of the designed mechanism

3.1. Prototype of the proposed tile

A unimorph piezoelectric cantilever as shown in Fig. 4 was firstly prototyped and properly characterized before the system was scaled up to be composed of 24 unimorph PZT cantilevers. To optimize and verify the design of the energy harvesting floor tile, the following structure was configured. A $60 \times 30 \times 2\,mm^3$ stainless steel mass was glued with a $10 \times 10 \times 5$ mm^3 permanent magnet (NdFeB), and then mounted on the free end of a unimorph PZT cantilever consisted of a $40 \times 20 \times 0.3\,mm^3$ PZT layer and a $60 \times 25 \times 0.2\,mm^3$ elastic layer. The configuration was as that

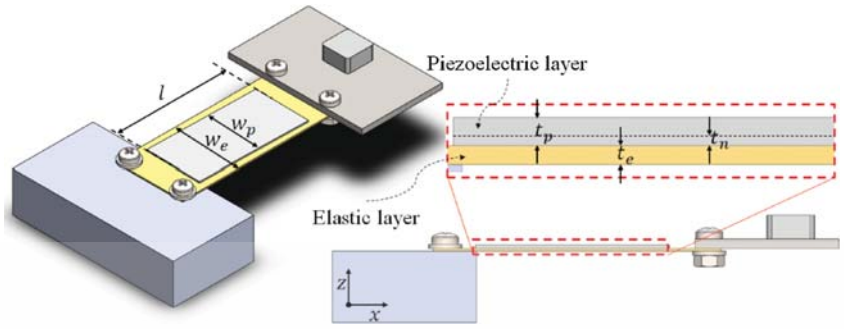

Fig. 3. Schematic of a unimorph piezoelectric cantilever with a proof mass.

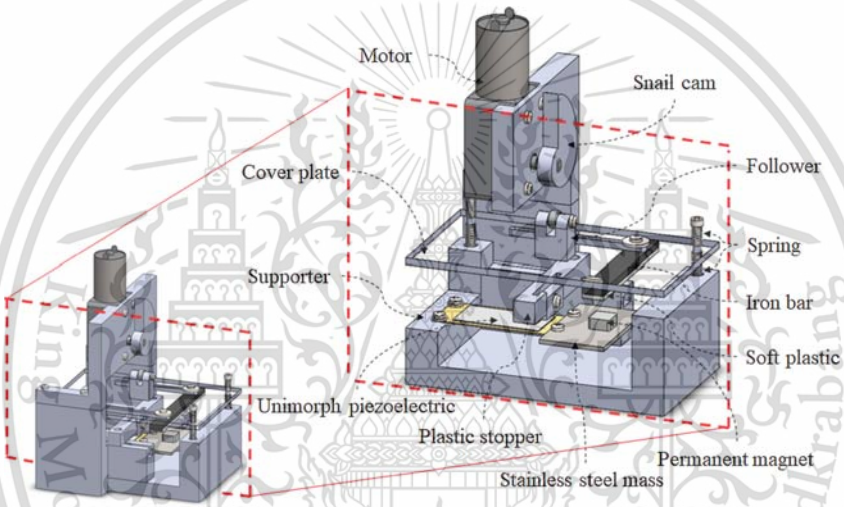

Fig. 4. Validation of the designed mechanism.

Table 1
Dimension and magnetic property of the materials used.

Parameters	Dimension	Relative permittivity	Coercivity (A/m)	Electric conductivity (MS)
Iron bar	5 mm × 10 mm	14872	–	–
Soft plastic	2 mm × 10 mm	1	–	–
Air gap	10, 14, and 18 mm	1.0006	–	–
Permanent magnet (NeFeB)	10 mm × 5 mm	1.045	883310	0.667
416 stainless-steel mass	30 mm × 2 mm	440	–	–

shown in Fig. 2(a) of the schematic of the waiting for load state (equilibrium state). Since the generated power is proportional to the displacement of the piezoelectric cantilever, the largest air gap between the plastic stopper and the PZT cantilever (d_1) is required. However, the PZT layer may crack from over-bending, thus we needed to set a proper distance between the stopper and the cantilever. In our implementation, one end of the PZT cantilever was clamped to the supporter and supplied with DC voltage while the other free end was pressed by a rack-and-pinion scale to vary the vertical displacement. Over-bending could be observed from the voltage at the free end. As shown in Fig. 5, as the PZT layer broke at a vertical displacement of approximately 7.1 mm, the voltage at the free end became zero. Therefore, a plastic stopper was used to fix the vertical displacement of the PZT cantilever to 4 mm (d_1 = 4 mm). In addition to that optimization step, an optimal air gap between the permanent magnet and the iron bar (d_2) was determined by finite element analysis simulation with FEMM 4.2 software. The simulation was implemented in 2D with parameters shown in Table 1. Fig. 6 illustrates the simulation results of magnetic flux density. As can be seen, the magnetic flux density was diminished to approximately zero at 18 mm far from the permanent magnet. At this distance, the attractive force from the magnet approached zero according to Eq. (1). Thus, d_2 was set to be 18 mm for the prototype. This value of d_2 from simulation was verified in an actual experiment that it was truly optimal.

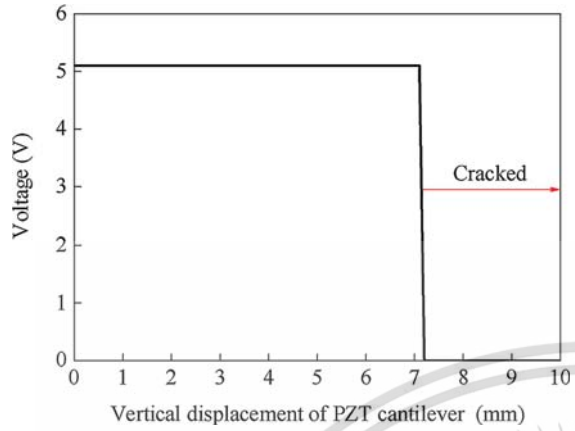

Fig. 5. Voltage at the free end of the PZT cantilever as the vertical displacement was increased.

TD 3032B). As the measured voltage was a transient waveform [20], the instantaneous power $P(t_m)$ could be calculated by

$$P(t_m) = \frac{V_L^2(t_m)}{R_L}, \tag{11}$$

where $V_L(t_m)$ is the transient voltage across the resistive load at time t_m; $m = 0,1,2,3\ldots$ identifies the voltage sample at a particular time; and R_L is the resistance of the resistive load. At time t_N where N is the number of voltage samples, the average power can be found as

$$P_{Avg}(t_N) = \frac{1}{t_N}\int_0^{t_N} \frac{V_L^2(t)}{R_L} dt \tag{12}$$

Thus, the energy produced from the prototype as a function of time was calculated by the following expression,

$$E(t_N) = \sum_{m=0}^{N} P(t_m)\Delta t_m, \quad for\ N \rangle 0, \tag{13}$$

where Δt_m is the measurement time interval of the voltage samples.

3.2. Verification method

A motor and a snail cam for simulating force of human steps were mounted on the prototype as shown in Fig. 4. The snail cam attached to the shaft of the motor was used to transform the motor's rotary motion into linear motion. The follower of the snail cam made the cover plate move up and down, simulating movement caused by pedestrian step. Generally, walking velocity and frequency of pedestrian steps on the floor either in a crowded or uncrowded area are inconstant, depending on number of people and individual stride. These parameters could not be simulated exactly. One thing for certain is that the time interval that the foot of a pedestrian makes contact with the floor is longer for a slow walker and shorter for a fast walker. A high density of pedestrians may cause them to walk slower hence this time interval may be longer [19]. Accordingly, this simulation of energy harvesting behavior was based on the step time interval (T_d) between the cover plate moving up and down, i.e., the cycle time of the greatest radial dimension of the snail cam pressing on the follower. The generated energy was investigated with various resistive loads. The voltage across resistive load was measured with an oscilloscope (Tektronix

3.3. Verification results

Before experimentally investigating the energy harvesting performance, an optimal load resistor was found by connecting various resistive loads to the prototype directly and rotating the snail cam with an angular velocity of 8 rad/s and step time interval T_d of 0.1 s. The capacitance and resistance of the PZT cantilever in the prototype were 46.84 nF and 320.13 kΩ, respectively, measured by an impedance analyzer (Bode 100 - OMICRON Lab). The maximum average power was observed with a load resistor of 800 kΩ; this resistor was thus chosen as the optimal one. The next step was to find the optimal air gap. Fig. 7 shows a comparison of the performances of the prototype installed with different air gaps d_2. The ratio of the total output energy generated when the air gap d_2 were 18 and 14 mm to the total output energy generated when d_2 was 10 mm were 3.35 and 2.73 to 1, respectively. Decreasing the amount of the air gap d_2 led to a significant drop in output energy because the vertical displacement of the oscillating PZT cantilever was diminished by the stronger attractive force between the permanent magnet and the iron bar as mentioned in section II. Free oscillation would be stopped with the shortest air gap d_2, producing

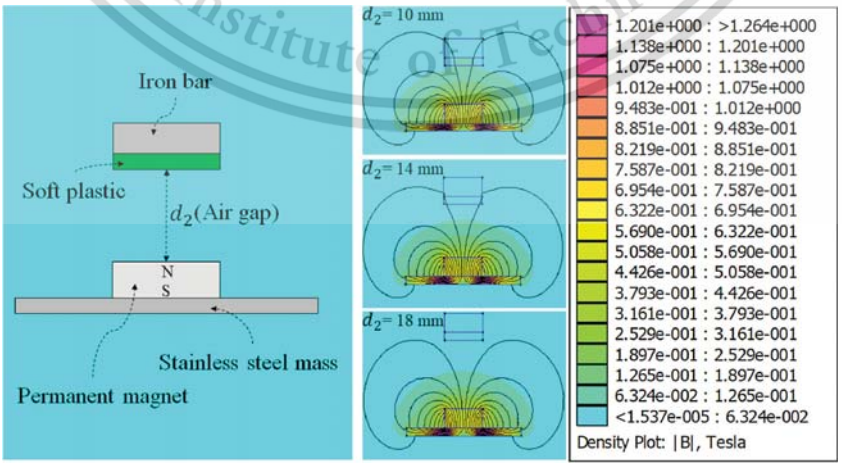

Fig. 6. Magnetic flux density simulation.

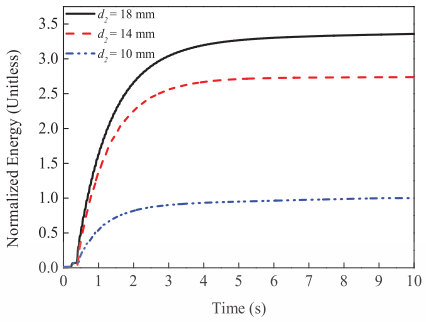

Fig. 7. Normalized energy from using different airgaps (d_2).

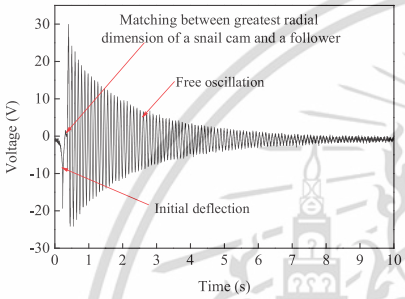

Fig. 8. Oscillating voltage across the optimal load resistor.

the minimum output energy. Therefore, the prototype was configured with d_2 = 18 mm that could generate an average power of 0.075 mW with a peak-to-peak voltage of 54.20 V as shown in Fig. 8.

The energy harvesting performance was determined as follows. Following the experimental method in subsection B, a snail cam was rotated at an angular velocity of 8 rad/s with various step time intervals (T_d) of 0.1, 0.5 and 1.0 s which were assumed to represent accurately the walking speeds of a pedestrian. Fig. 9(a), (b) and (c) depict the output voltages from these walking speeds, respectively. The results show that the PZT cantilever plucking frequencies were 1.01 Hz, 0.71 Hz and 0.52 Hz, respectively. Fig. 9(d) illustrates the energy harvested during 10 s with different step time intervals (T_d). The total output energies were 2.05, 1.42 and 1.00 mJ, respectively. Increasing the step time interval, i.e. slower walking speed, reduced the number of plucks on the PZT cantilever over time leading a decreasing in the total output energy.

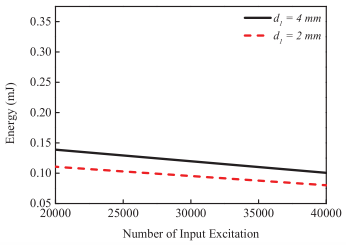

Fig. 10. Output energy with increasing number of plucks.

Next, the reliability of the prototype was examined. For the reliability test, the snail cam was continuously rotated with a step time interval T_d of 0.1 s to excite the prototype. It was found that the harvestable energy steadily decreased from the first pluck up to the forty-thousandth pluck. This issue was not related to mechanical failure or regression of the PZT cantilever. It occurred from progressive detachment of the piezoelectric layer from the elastic layer that might come from insufficient adhesive function of the glue that bonded the two layers together under a large vertical displacement of the PZT cantilever. To remedy that situation, the PZT cantilever's vertical displacement was restricted to 2 mm

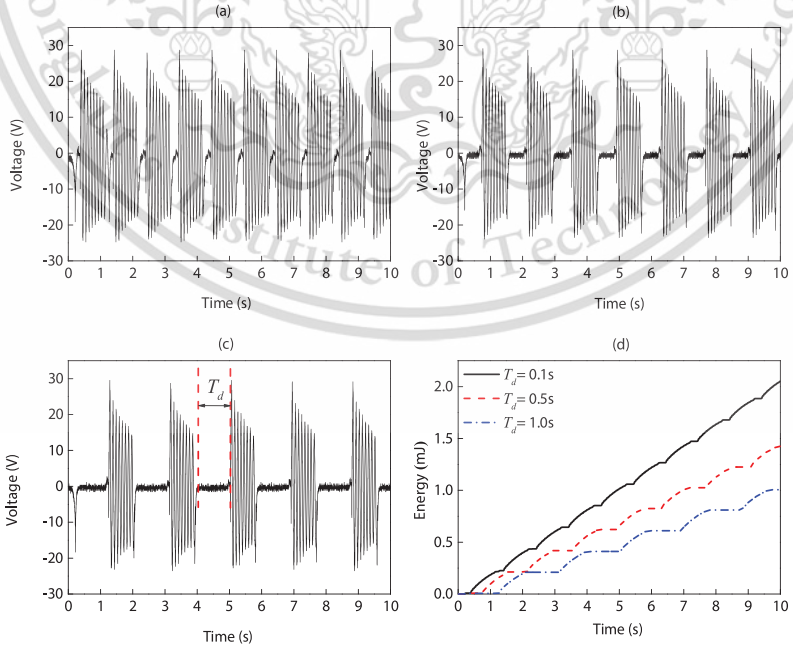

Fig. 9. Voltages generated with step time intervals T_d of (a) 0.5, (b) 1 and (c) 1.5 s; (d) the trend of harvested energy that varied with step time interval.

Fig. 11. A test setup showing (a) the energy harvesting floor tile and (b) the oscilloscope measuring the voltage (Tektronix TDS3032B).

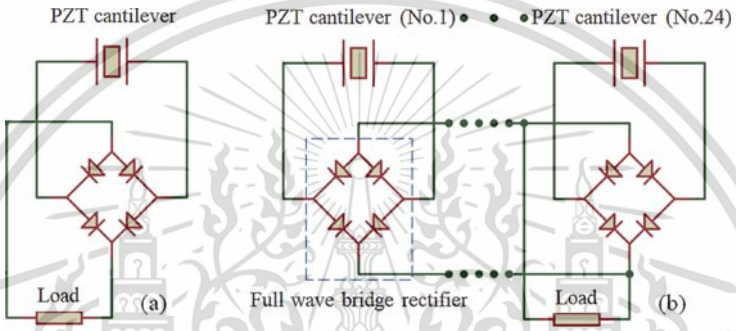

Fig. 12. (a) Circuit of an individual PZT cantilever; (b) Circuit of electrically connected PZT cantilevers, rectifiers, and load resistors.

(d_1 = 2 mm). However, the progressive detachment still happened as shown by the results in Fig. 10. A very short air gap d_1 might make the PZT cantilever last a longer time, but the output energy would be lower due to the low stress in the piezoelectric material.

4. Evaluation of the performance of the energy harvesting floor tile

4.1. Energy harvesting floor tile and performance evaluation method

The prototype validated as described in Section III, a $430 \times 430 \times 70.50\,mm^3$ energy harvesting floor tile was constructed of 24 unimorph PZT cantilevers as shown in Fig. 11. The air gaps d_1 and d_2 varied from 2–5 and 16–19 mm, respectively; they could not be set to one fixed distance because of the slightly different curvature of the unimorph PZT cantilevers obtained from the manufacturer. A full wave bridge rectifier consisted of small signal Schottky diodes (BAT 46) was used with each PZT cantilever and electrically parallelly connected to other rectifiers as shown in Fig. 12(b). A parallel circuit was used to sum the output currents from all PZT cantilevers. Its presence was due to each PZT producing only a low current even though it could generate a high voltage.

Three kinds of evaluation were performed: evaluation of the energy harvesting performance of one then 24 PZT cantilevers; the effect on energy harvesting performance of the placement location of footsteps; and the energy harvesting performance of the tile in a real scenario. Firstly, the energy harvesting performances of one PZT cantilever and 24 PZT cantilevers were investigated with various load resistors as shown in the Fig. 12(a) and (b). Each of three randomly selected PZT cantilevers was performance tested. The performance of all 24 connected PZT cantilevers was then evaluated. The load resistor that maximized the power transfer of all of these cantilevers was selected as the optimal load resistor for the other kinds of evaluation. Secondly, the output energy generated by stepping on each different location of the energy harvesting floor was measured and compared. The results would show whether the performance of the tile was consistent or not when it was stepped on its different areas hence they would indicate whether the tile was too big or not. And lastly, the tile's energy harvesting performance when it was mounted and actually stepped on by a pedestrian was determined. The result would indicate whether the amount of the harvested energy would be sufficient or not for supplying a typical wireless sensor node.

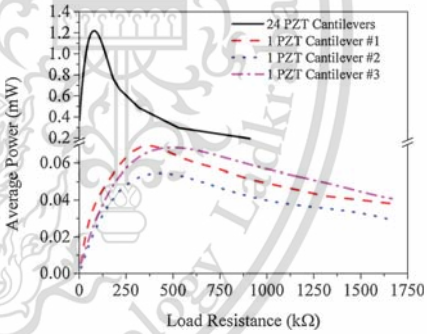

Fig. 13. The average power of one unimorph PZT cantilever and 24 paralleled unimorph PZT cantilevers.

5. Results and discussion

The experimental results of first test are shown in Fig. 13. By exciting the energy harvesting floor with a single foot step, the average output power per one PZT cantilever were 0.069, 0.054,

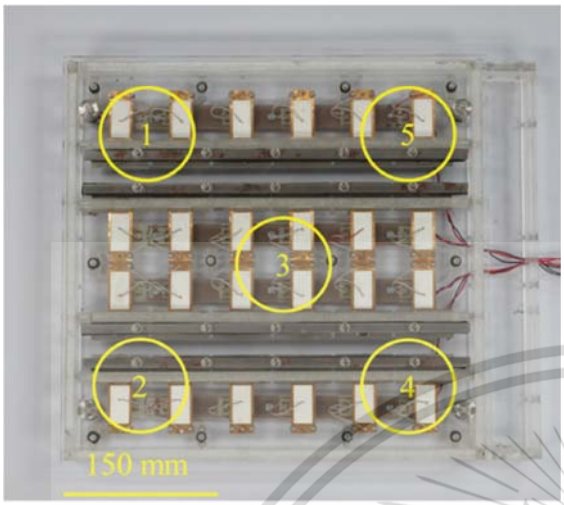

Fig. 14. Numbered locations on the cover plate.

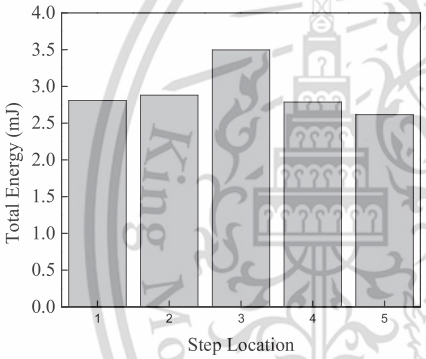

Fig. 15. Output energy generated by a step that landed on different locations of the energy harvesting floor tile.

and 0.068 mW at optimal load resistances of 377.21, 377.21, and 448.90 kΩ for cantilever #1, #2 and #3, respectively. Their different average output power varied with their vertical displacement (air gap d_1). The #1 and #3 PZT cantilevers with an air gap d_1 of proximately 4 mm were able to generate a higher average power than #2 with an air gap d_1 of proximately 3 mm. Since the air gaps d_1 that fixed the vertical displacement of many PZT cantilevers were shorter than 4 mm, the average output power from paralleled 24 PZT cantilevers was only 1.24 mW at optimal load resistance of 74.44 Ωk, not the total sum of 1.65 mW as expected. This demonstrates that it is possible to obtain the highest conversion efficiency by fine-tuning the air gap distance of every piezoelectric cantilevers properly or, simpler, if we can obtain cantilevers from a manufacturer with very tight tolerance of their curvature so that no air-gap tuning is needed, we will be able to achieve the highest conversion efficiency.

For the second test, the energy harvesting floor was stepped on at five numbered locations shown in Fig. 14. The total output energy of 2.80, 2.87, 3.49, 2.78, and 2.61 mJ were respectively obtained as exhibited in Fig. 15. The experimental results show that stepping on the location #3 was better than any other locations, since the force could distribute evenly throughout the cover plate, resulting in even movement of the iron bars mounted under the plate relative to the permanent magnet mounted on the PZT cantilevers, thus

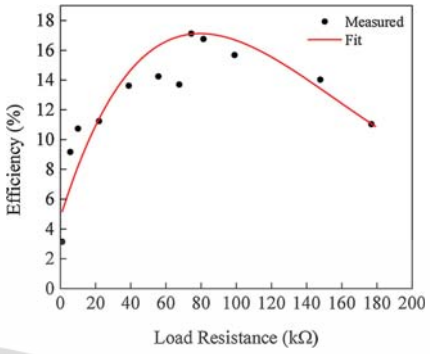

Fig. 16. Energy conversion efficiency versus load resistor values.

inducing all cantilevers evenly and consistently. On the other hand, stepping on the cover plate at a corner (First, Second, Fourth or Fifth location) could compress the assembly only locally around that corner because the distributed force to the other corners was low and could not compress down the supporting springs at those corners sufficiently. Thus, only some of the 24 PZT cantilevers were excited. This result suggested to us that the production floor tile should be of a smaller size such that the cover plate will be evenly pressed down by a foot step no matter what location on the plate it lands on.

With step landing on the optimal location #3, the energy conversion efficiency can be examined in the quantitative relation between the amount of the output electrical energy and the input mechanical energy. The input mechanical energy was found from the potential energy stored in a PZT cantilever based on the displacement and effective spring constant by the following equations,

$$E_{Input} = \frac{1}{2} k_{eff} z_0^2, \tag{14}$$

$$k_{eff} = \omega_n^2 M, \tag{15}$$

where k_{eff} represented effective spring constant, z_0 was the tip displacement of a PZT cantilever, ω_n was the resonant frequency of a freely oscillating PZT cantilever, and M was the seismic mass attached to the tip of a freely oscillating PZT cantilever. The resonant frequency of a freely oscillating PZT cantilever was found from the output AC voltage in Fig. 7, which was approximately 10.54 Hz. Fig. 16 demonstrates the measured conversion efficiency with various load resistors; as can be seen, the greatest conversion efficiency was 17.12% at the optimal load resistor of 74.44 kΩ.

In the final test, the energy harvesting floor tile was placed on a passageway in front of a classroom where 45 students had to walk by and step on it. In this scenario, the output voltage and trend of harvestable energy over time were recorded and calculated and are shown in Fig. 17. The amplitudes of the output DC voltage were in the range of 10.15–21.41 V. The different voltage values were not due to the weight of each pedestrian, rather it was due to the pedestrians not stepping on the same location on the cover plate every time as discussed above. The total output energy derived from this experiment was 42.09 mJ. The average energy per one step was approximately 0.93 mJ.

Since the concept of this work is to employ the energy harvesting floor tile in the field of smart city, for providing a sustainable power source to low-power electronic devices, its total output energy was assumed to supply low-power wireless sensor nodes presented in [21,22,23], and shown in Table 2. The supplied energy can power an accelerometer, a capacitive strain gauge, and smoke detecting wireless sensor nodes to operate for approximately 1.60, 70.15, and 8,503.03 s, respectively. These wireless sensor nodes usually oper-

Table 2
Estimation of operational time of a low-power wireless sensor node assumed powered by output energy from actual pedestrian steps.

Reference	Wireless sensor node	Power consumption (mW)	Operational time (s)
Thapanun et al. [21]	Accelerometer	26.31	1.60
Zeiser, R et al. [22]	Capacitive strain gauge	0.6	70.15
Luis, Juan A et al. [23]	Smoke detecting	4.95×10^{-3}	8,503.03

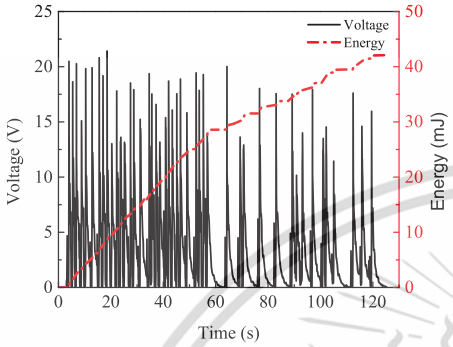

Fig. 17. Output voltage and energy generated by many pedestrians stepping on the energy harvesting floor tile.

ate in both hibernated and active states in order to reduce power consumption; therefore, it is feasible to store the harvested energy in a capacitor during the node's hibernated state for sufficient use in the further duty cycle of data tracking and transmission. It should be noted that the relatively high amount of energy found in this study was from using an optimal resistor as a load. In real applications, some amount of the energy achieved in this experiment will be lost when it is stored in a capacitor as a power source for a wireless device due to self-discharge of the capacitor and leakage current in the electronic components when nobody is stepping on the floor tile. The leakage current can be minimized by optimizing the energy management circuit and using low-power electronic components [24,25].

6. Conclusion and future development

An energy harvesting floor tile with frequency up-conversion mechanism was designed and realized in this study. The frequency up-conversion was achieved by using restoring forces from springs to rapidly separate an iron bar away from a permanent magnet where they were attracted to each other via magmatic force. Too large a displacement of the unimorph cantilever could cause a crack in the piezoelectric layer; this situation was examined then prevented from happening further by using a stopper. The airgap between the permanent magnet and the iron bar strongly influenced the energy generation; the relationship was analyzed by both a Finite Element Method (FEM) and an experiment. When the airgap was large enough to diminish the magnetic force attracting the iron bar to zero, an oscillating PZT cantilever gave the maximum output energy. Validation of the designed mechanism was made with a tile with one unimorph PZT cantilever. The results suggested that even though the PZT cantilever used in this research had a problem of laminated layers between piezoelectric layer and elastic layer peeling off from each other, the prototype was successful with respect to frequency up-conversion mechanism with good energy conversion efficiency. The energy harvesting floor tile was then scaled up to consist of 24 PZT cantilevers and used in a performance evaluation experiment. It was observed that the differences in the curvature of the PZT cantilevers and the large size of energy harvesting floor could reduce the total output energy. The former issue was dealt with by fine-tuning individually the amount of displacement that each cantilever could travel, while the latter issue would be dealt with in a future work by making the floor tile smaller. In an actual test having people walking and stepping on the floor tile for 45 steps, it was found that this number of steps could provide high enough harvested energy to activate a few low-power wireless sensor nodes.

For a future work, we will design a more robust piezoelectric cantilever with no lamination between piezoelectric layer and elastic layer so that no fine-tuning of cantilever displacement will be needed. In addition, another goal is to increase the output energy by optimizing the shape of the piezoelectric cantilever and the size of the energy harvesting floor tile as well as using a higher-energy-output piezoelectric material.

Acknowledgements

Mr. Phosy Panthongsy would like to express his sincere appreciation to the AUN/SEED-Net for the full financial support of his PhD degree education. The authors would like to thank King Mongkut's Institute of Technology Ladkrabang (KMITL) and Synchrotron Light Research Institute (SLRI) for providing excellent research facilities and thank to Mr. Somphong Suphachiaraphan for sharing the useful information on the mechanism design.

References

[1] F. Peano, T. Tambosso, Design and optimization of a MEMS electret-based capacitive energy scavenger, J. Microelectromech. Syst. 14 (2005) 435–529.
[2] P. Glynne-Jones, M.J. Tudor, S.P. Beeby, N.M. White, An electromagnetic, vibration-powered generator for intelligent sensor systems, Sens. Actuators A 110 (2004) 344–349.
[3] D. Shen, S.-Y. Choe, D.-J. Kim, Analysis of piezoelectric materials for energy harvesting devices under high-g vibrations, Jpn. J. Appl. Phys. 46 (2007) 6755–6760.
[4] S. Roundy, P.K. Wright, J. Rabaye, A study of low level vibrations as a power source for wireless sensor nodes, Comput. Commun. 26 (2003) 1131–1144.
[5] S. Roundy, P.K. Wright, A piezoelectric vibration based generator for wireless electronics, Smart Mater. Struct. 13 (2004) 1131–1142.
[6] C.B. Williams, R.B. Yates, Analysis of a micro-electric generator for microsystems, Sens. Actuators A Phys. 52 (1996) 8–11.
[7] H. Kulah, K. Najafi, Energy scavenging from low-frequency vibrations by using frequency up-conversion for wireless sensor applications, IEEE Sens. J. 8 (no. 3) (2008) 261–268.
[8] M. Umeda, K. Nakamura, S. Ueha, Analysis of the transformation of mechanical impact energy to electric energy using piezoelectric vibrator, Jpn. J. Appl. Phys. 35 (5B) (1996) 3267–3273.
[9] M. Umeda, K. Nakamura, S. Ueha, Energy storage characteristics of a piezo-generator using impact induced vibration, Jpn. J. Appl. Phys. 36 (5B) (1997) 3146–3151.
[10] M. Renaud, P. Fiorini, R. van Schaijk, C. Van Hoof, Harvesting energy from the motion of human limbs: the design and analysis of an impact-based piezoelectric generator, Smart Mater. Struct. 18 (2009), 035001.
[11] H. Kulah, K. Najafi, Energy scavenging from low-frequency vibrations by using frequency up-conversion for wireless sensor applications, IEEE Sens. J. 8 (no. 3) (2008) 261–268.
[12] P. Janphuang, R.A. Lockhart, D. Isarakorn, S. Henein, D. Briand, N.F. de Rooij, Harvesting energy from a rotating gear using an AFM-like MEMS piezoelectric frequency up-converting energy harvester, J. Microelectromech. Syst. 24 (June (no. 3)) (2015) 742–754.
[13] M. Pozzi, M. Zhu, Plucked piezoelectric bimorphs for knee-joint energy harvesting: modeling and experimental validation, Smart Mater. Struct. 20 (no. 5) (2011) 055007–055016.
[14] P. Pillatsch, E.M. Yeatman, A.S. Holmes, A piezoelectric frequency up-converting energy harvester with rotating proof mass for human body application, Sens. Actuator A Phys. 206 (2014) 178–185.

[15] H.T. Luong, N.S. Goo, Use of a magnetic force exciter to vibrate a piezocomposite generating element in a small scale windmill, Smart Mater. Struct. 21 (2012), 025017.
[16] Y. Kuang, Z. Yang, M. Zhu, Design and characterization of a piezoelectric knee-joint energy harvester with frequency up-conversion through magnetic plucking, Smart Mater. Struct. 25 (8) (2016), p. 085029.
[17] X. Gao, W.H. Shih, W.Y. Shih, Induced voltage of piezoelectric unimorph cantilevers of different nonpiezoelectric/piezoelectric length ratios, Smart Mater. Struct. 18 (no. 12) (2009) 125018–125025.
[18] L. Gu, C. Livermore, Impact-driven, frequency up-converting coupled vibration energy harvesting device for low frequency operation, Smart Mater. Struct. 20 (March (no. 4)) (2011) 045004–045013.
[19] Tom V. Mathew, Pedestrian studies, Lect. Notes Traffic Eng. Manage. (2014).
[20] P. Janphuang, R.A. Lockhart, D. Isarakorn, S. Henein, D. Briand, N.F. de Rooij, Harvesting energy from a rotating gear using an AFM-like MEMS piezoelectric frequency Up-converting energy harvester, J. Microelectromech. Syst. 24 (June (no. 3)) (2015) 742–754.
[21] Thapanun Sudhawiyangkul, Don Isarakorn, Design and realization of an energy autonomous wireless sensor system for ball screw fault diagnosis, Sens. Actuators A 258 (2017) 49–58.
[22] R. Zeiser, T. Fellner, J. Wilde, Capacitive strain gauges on flexible polymer substrates for wireless, intelligent systems, J. Sens. Sens. Syst. 3 (1) (2014) 77–86, Gottingen.
[23] J.A. Luis, J.A.G. Galán, J.A. Espigado, Low power wireless smoke alarm system in home fires, Sensors 15 (2015) 20717–20729.
[24] A. Miah, Jae Y. Halim, Park, Theoretical modeling and analysis of mechanical impact driven and frequency up-converted piezoelectric energy harvester for low-frequency and wide-bandwidth operation, Sens. Actuator A: Phys. 208 (2014) 56–65, ISSN 0924-4247.
[25] D. Alghisi, S. Dalola, M. Ferrari, V. Ferrari, Triaxial ball-impact piezoelectric converter for autonomous sensors exploiting energy harvesting from vibrations and human motion, Sensor Actuator A: Phys. 233 (2015) 569–581, ISSN 0924-4247.

Biographies

Phosy Panthongsy received the B.Eng. Degree in Electronic Engineering from National University of Laos (NUOL), Laos, in 2014, and the M.Eng. Degree in Computing in Engineering Systems from King Mongkut's Institute of Technology Ladkrabang (KMITL), Thailand, in 2016. He has been a PhD student at Department of Instrumentation and Control engineering, KMITL. His research interests are in the energy harvesting systems, micro power management, and robotics.

Don Isarakorn is currently an Assistant Professor of Electrical Engineering with the King Mongkut's Institute of Technology Ladkrabang (KMITL), Bangkok, Thailand. He is also the Head of the Multi-Scale Electromechanical Systems Laboratory with the Department of Instrumentation and Control Engineering, where he leads the activities on the mechatronic system integration. He received the B.Eng. degree in electronics engineering and the M.Eng. degree in control engineering from KMITL in 2000 and 2003, respectively, and the Ph.D. degree in piezoelectric microelectromechanical systems from the Sensors, Actuators, and Microsystems Laboratory, École Polytechnique Fédérale de Lausanne, Lausanne, Switzerland, in 2011. His main research interests include piezoelectric materials for sensing and actuating applications, energy harvesting systems, robotics, mechatronics, automatic control systems, and biomedical instruments.

Pattanaphong Janphuang received his B.Eng. degree in electrical engineering from King Mongkut's University of Technology Thonburi, Thailand, in 2001, and M.Sc. in micro and nanotechnology from University of Neuchâtel, Switzerland, in 2009 respectively. He obtained his Ph.D. degree in the field of Microsystems and microelectronics from the Institute of Microengineering, École Polytechnique Fédérale de Lausanne (EPFL), Switzerland, in 2014. He is currently a beamline scientist at BL6a: Deep X-ray Lithography and the Chief of User Office Division at SLRI. He has been author or co-author of over 30 papers published in scientific journals and conference proceedings. His research interests include polymeric MEMS, Power MEMS and energy harvesting, and autonomous smart sensing systems.

Kazuhiko Hamamoto, was born in Nagasaki prefecture, Japan in 1966. He received B.D, M.D and Ph.D from Tokyo University of Agriculture and Technology in 1989, 1991 and 1994 respectively. He was assistant professor in Dept. of Communications Eng., Tokai University in 1994, Associate Professor in 1999, and Professor in Dept. of Information Media Technology, School of Information and Tele-communication Eng., Tokai University in 2009 and Currently, he is the Dean of School of Information and Tele-communication Eng., Tokai University. His research interest is information architecture, especially, medical image processing, human interface and virtual reality. He joins IEICE, IEEJ, IEEE, VRSJ, JSST, etc. He is a member of Technical Committee of Medical and Biological Engineering, Society of Electronics, Information and Systems, IEEJ.

2018 15th International Conference on Electrical Engineering/Electronics, Computer, Telecommunications and Information Technology

A Test Bench for Characterization of Piezoelectric Frequency Up-Converting Energy Harvesters

Phosy Panthongsy and Don Isarakorn*
Department of Instrumentation and Control Engineering, Faculty of Engineering
King Mongkut's Institute of Technology Ladkrabang
Bangkok, 10520 Thailand
don.is@kmitl.ac.th

Kazuhiko Hamamoto
Department of Information Media Technology, School of Information and Telecommunication Engineering
Tokai University
2-3-23 Takanawa Minato-ku Tokyo 108-8619 Japan

***Abstract*—This work focuses on the design and realization of a test bench used to characterize the performances of the piezoelectric cantilever for frequency up-converting energy harvesters. A test bench is completed by combining a frequency up-converter with an oscilloscope (Tektronix TD 3032B). The frequency up-conversion mechanism achieves the excitation on a piezoelectric cantilever through an interaction between a permanent magnet and an iron bar. In the mechanism design, the air gap between a permanent magnet and an iron bar is analyzed by Finite Element Method (FEM). After the design is verified, a test bench is fabricated and then validated with experimental study by testing the performances of a PZT-5H bimorph (T220-H4-503X, Piezo Systems, Inc.); the considered performances are resonant frequency, average output power, total output energy and energy conversion efficiency. The experimental results demonstrate that a fabricated test bench is satisfactory.**

Keywords—frequency up-conversion mechanism; finite element analysis; low-frequency vibration energy harvesting

I. INTRODUCTION

Energy harvesting from ambient environment has grown considerably over the last decades due to the rapid development of electronic devices with reduction of power consumption and size. The harvested energy is supplied to power the low-power consumption electronic devices and various types of wireless sensor nodes as the autonomous energy system instead of energy source from batteries, since the use of batteries has the problem on limited energy storage capacity and lifetime. Moreover, the depleted batteries are the toxic waste, the recycle and disposal process of which are very expensive. The main ambient energy harvesting strategies which have been reported are used to harvest energy from solar, temperature gradient, and vibration sources [1-3]. Among them, the vibration energy harvesting has been specially concentrated because the vibration is ubiquitous and easily found in ambient environment such as human body, industrial machines, bridges, and transportation. The vibration energy harvesting devices are commonly based on piezoelectric, electrostatic and electromagnetic transductions [4-6]. Among these transduction methods, the piezoelectric energy harvester has been attracted with the great of interest by many researchers due to its high output energy density, lower profile of structure and simple configuration [7].

Typically, the piezoelectric energy harvester can be mainly divided into resonant and non-resonant types. The resonant type piezoelectric energy harvester is optimum when its resonant frequency matches to the frequency of vibration source. The mismatch between both frequencies results in low power generation efficiency. Thus, the resonant type harvester does not present a good option to the vibration source with low and variable frequency (e.g., the human moment, machinery with low and variable speed rotary, and so on) because the frequency of vibration source is usually variant and much lower than resonant frequency of harvester. To overcome this challenge, the non-resonant type piezoelectric energy harvester has been recently investigated, which is always resonated at high frequency by frequency up-converting mechanism with regardless the input vibration. In the frequency up-converting strategy, piezoelectric cantilever integrated to harvester is induced the initial deflection and then released to freely oscillate at high frequency [8] - [10]. Moreover, the energy conversion efficiency can be much increased, when the piezoelectric cantilever providing a good energy harvesting performance is integrated to the harvester. Therefore, the work relating to the selection of piezoelectric cantilever is concentrated, especially the fabrication of instrumentation for characterize the piezoelectric cantilever performance. Previously, there are some instrumentations that have been reported [11] - [13], however, they are designed for resonant harvesters which do not support to the harvester with frequency up-converting mechanism. Therefore, the aim of this research is to design and fabricate a test bench for characterization of the piezoelectric cantilever based on frequency up-conversion. In this paper, the overall system of a test bench is firstly reported, and then the structural configuration and method for piezoelectric cantilever characterization is given. After that, the validation of a test bench is illustrated. Finally, the conclusion is drawn.

(AUN/SEED-Net, JICA) and NRCT

2018 15th International Conference on Electrical Engineering/Electronics, Computer, Telecommunications and Information Technology

II. OVERALL OF SYSTEM

Following to the operational behavior of piezoelectric energy harvester with frequency up-converting mechanism, a test bench can be designed. Its general system is shown as a block diagram in Fig.1, which consists of an oscilloscope (Tektronix TD 3032B) and a frequency up-converter. The oscilloscope is used to measure the output electricity from piezoelectric cantilever excited by the frequency up-converter. The frequency up-conversion strategy is based on magnetic plucking. As the design, the frequency up-converter is mainly divided into mechanism and control circuit parts. Its mechanism is illustrated in Fig.2. A plastic mass is a connector between tip of piezoelectric cantilever and a permanent magnet. A motor shaft is attached to a snail cam for transforming the rotary motion into the linear motion. When the greatest radial dimension of snail cam rotates to match a follower, a cover plate supported by the springs is pushed down, thus the iron bar attached underneath of a cover plate is moved closer to a permanent magnet at where high magnetic field. Meanwhile, a permanent magnet will bend a piezoelectric cantilever to attach the iron bar via the magnetic attractive force, while the displacement of piezoelectric cantilever is localized by the topper. Therefore, when a snail cam leaves a follower, the spring will suddenly pluck the cover plate up. It rapidly releases the iron bar from permanent magnet, and results in the free oscillation with high frequency of piezoelectric cantilever. As the time interval (t_d) of matching between the greatest radial dimension and a follower without controller is very short, and the permanent magnet cannot obviously attach to the iron bar resulting in inconstant mechanical input and unclear electrical output of harvester. The control circuit is designed to define a longer time interval t_d. The rotation of motor is controlled by using the microcontroller (ATmega32) through an integrated circuit chip (L293D driver motor), while the matching between the greatest radial dimension and a follower is tracked by a limit switch.

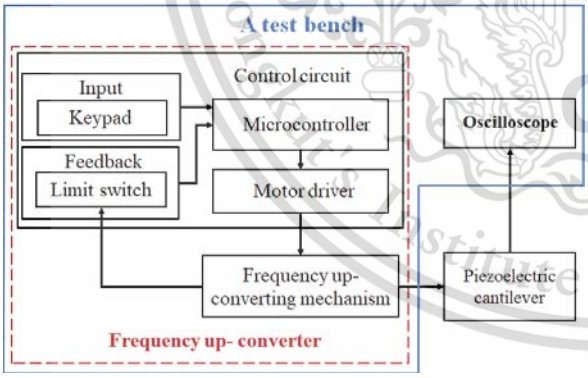

Fig. 1. Block diagram of overall system

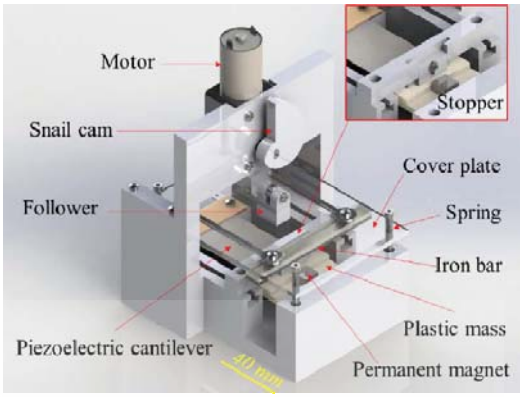

Fig. 2. Mechanism of frequency up-converter

III. STRUCTURAL CONFIGURATION AND CHARACTERIZATION METHOD

In the structural setup of a test bench, an airgap (d_a) between permanent magnet glued on a plastic mass and iron bar should be large enough. If an iron bar is positioned at where high magnetic field density, a permanent magnet will try to attract an iron bar via strong magnetic attractive force, thus the oscillating piezoelectric cantilever can be paused. It causes the unclear experimental results. Therefore, an iron bar should be located at where the magnetic field density equal zero or approximate zero. In this test bench, a 10 x 10 x 0.5 mm^3 permanent magnet (NeFeB-N35) and an 86 x 10 x 2 mm^3 iron bar are used. The airgap (d_a) is considered in 2D simulation using the finite element analysis with a FEMM 4.2 software. In simulation, the magnetic flux density across an iron bar for the different distances of airgap (d_a) were observed. As the results shown in Fig. 3, the magnetic flux density across an iron bar was diminished to approximately zero when the length of air gap (d_a) reaches to 18 mm. Therefore, an iron bar was located at where far from permanent magnet approximately 18 mm.

For characterization strategy, a frequency up-converter was controlled to excite a piezoelectric cantilever with a single pluck. Then, the performance of piezoelectric cantilever was investigated with various resistive loads. The average output power (P_{Avg}) supplied to resistive load since the free oscillation of a piezoelectric began could be found by equation

$$P_{Avg}(t_n) = \frac{1}{t_n}\int_0^{t_n} \frac{V_L^2(t)}{R_L} dt \quad , \tag{1}$$

where $V_L(t)$ is the transient voltage across resistive load and R_L represents the load resistance and t_n is the time since the free oscillation began.

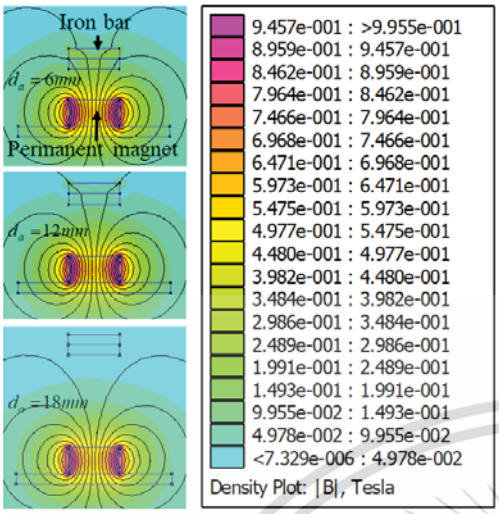

Fig. 3. Simulation results of magnetic flux density across the iron bar

With sampling interval (Δt) of voltage measurement of oscilloscope, the total output energy ($E(t_n)$) is calculated by using the following expression

$$E(t_n) = \sum_{m=1}^{n} \frac{V_L^2(t_m)}{R_L} \Delta t \,. \quad (2)$$

In addition to the average output power and total output energy exhibited above, the energy conversion efficiency also can be determined, which was defined as the ratio between output electrical energy and the input mechanical energy. The input mechanical energy (E_{Input}) is approximately the potential energy stored in a piezoelectric cantilever as given by

$$E_{Input} = \frac{1}{2} k_{eff} z^2 \quad (3)$$

where z is the displacement of piezoelectric cantilever and k_{eff} is the effective spring constant derived from the resonant frequency of piezoelectric cantilever (ω_n) and net weight of mass at the tip of piezoelectric cantilever (M) as

$$k_{eff} = \omega_n^2 M \,. \quad (4)$$

IV. Validation of a Test Bench

The experiment in this section was implemented to validate a test bench by characterizing the performance of a PZT–5H bimorph with a dimension of 0.51 x 31.8 x 63.5 mm^3 (T220-H4-503X, Piezo Systems, Inc.). As the experimental set up shown in Fig. 4, the stopper was used to localize the displacement of a bimorph at 2 mm, and the net weight of mass at the tip of bimorph including a permanent magnet, screw and plastic mass was 12.77 g. Being applied the single pluck with time interval (t_d) of 0.1 s, the performance of a bimorph could be characterized as the results shown in Fig.5. Figure 5 (a) illustrated the generated open circuit voltage. The peak-to-peak voltage was 84.7 V. According to the time period of oscillation (T) in the transient waveform, the resonant frequency of a bimorph was 20.83 Hz; the resonant frequency equals to 1/T. By directly connecting the various resistor to a bimorph, the average output power dissipated in the various resistive loads could be found as shown in the Fig.5(b). The maximum average power of 578.28 µW was observed at optimal load resistance of approximately 99 kΩ. The load resistance was the combined resistance of load resistor and oscilloscope probe in parallel. Figure 5 (c) showed the measured voltage across an optimal load resistor and total energy calculated by using an equation (2). A bimorph could generate the total energy of 537. 33 µJ. The measured energy-conversion efficiency as a function of load was presented in Fig. 5 (d). The greatest conversion efficiency was found to be 32.42 %.

The experimental results above prove that a test bench can be used to characterize piezoelectric cantilever for the piezoelectric energy harvester based on frequency up-conversion.

V. Conclusion

This paper presented a test bench for characterizing the piezoelectric cantilever based on frequency up-conversion. The overall system with operational method was reported. The frequency up-converter based on magnetic plucking was designed to excite the piezoelectric cantilever. The interaction between permanent magnet and iron bar was used to induce the initial deflection in piezoelectric cantilever before letting it to freely oscillate at high frequency. In machanism design, the airgap between permanent magnet and iron bar was optimized using the Finite Element Analysis (FEA). After that, a test bench was fabricated and then validated with experimental study.

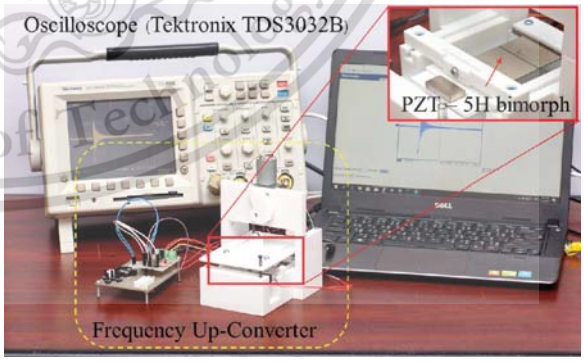

Fig. 4. Experimental setup

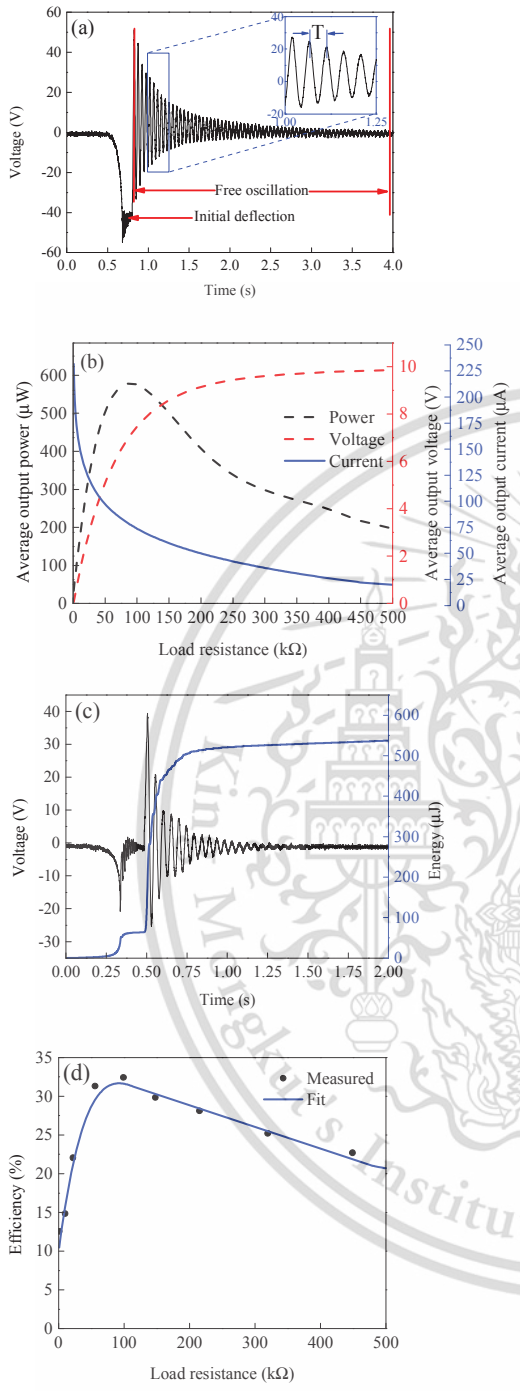

Fig. 5. The characterization results; (a) generated open circuit voltage; (b) average output power, voltage and current across resistive loads; (c) output voltage and total energy across an optimal load resistor; (d) measured energy conversion efficiency

ACKNOWLEDGMENTS

The authors would like to thank the National Research Council of Thailand for financial support. Mr. Phosy Panthongsy would like to acknowledge the AUN/SEED-Net for the full financial support in his PhD degree education.

REFERENCES

[1] D. Brunelli, L. Benini, C. Moser, L. Thiele, "An Efficient Solar Energy Harvester for Wireless Sensor Nodes," *Design, Automation and Test in Europe*, March 2008.

[2] R. J. M. Vullers, R. Van Schaijk, I. Doms, C. Van Hoof, and R. Mertens, "Micro power energy harvesting," *Solid-state Electron.*, Vol. 53, pp.684-693, 2009.

[3] S. P. Beeby, M. J. Tudor, and N. M. White, "Energy harvesting vibration souces for microsystem applications," *Meas. Sci. Technol.*, vol. 17, pp. R175-R195, 2006.

[4] D. Shen, S. –Y. Choe, and D. –J. Kim, "Analysis of piezoelectric materials for energy harvesting devices under high-g vibrations," *Jpn. J. Appl. Phys.*, Vol. 46, pp. 6755-6760.

[5] F. Peano and T. Tambosso, "Design and optimization of a MEMS electret-based capacitive energy scavenger," *J. Microelectromech. Syst.*, Vol. 14, pp. 435-529, 2005.

[6] P. Glynne-Jones, M. J. Tudor, S. P. Beeby, and N. M. White, "An electromagnetic, vibration-powered generator for intelligent sensor systems," *Sens. Actuators, A*, Vol. 110, pp. 344-349, 2004

[7] S. Roundy and P. K. Wright, "A piezoelectric vibration based generator for wireless electronics," *Smart Materials and Structures*, Vol. 13, pp. 1131-1142, 2004

[8] J. Rastegar, and R. Murray, "Novel two-stage piezoelectric-based electrical energy generators for low and variable speed rotary machinery," *in proc. SPIE*, vol. 7288, 2009, pp. 72880B-1-72880B-8.

[9] M. Pozzi, and M. Zhu, "Plucked piezoelectric bimorphs for knee-joint energy harvesting: modeling and experimental validation," *Smart Mater. Struct.*, vol. 20, no. 5, 2011, pp. 055007-055016.

[10] P. Janphuang, D. Isarakorn, D. Briand and N. F. de Rooij, "Energy harvesting from a rotating gear using an impact type piezoelectric MEMS scavenger," *2011 16th International Solid-State Sensors, Actuators and Microsystems Conference, Beijing*, 2011, pp. 735-738.

[11] M. Ferrari, V. Ferrari, D. Marioli, and A. Taroni, "Modeling, fabrication and performance measurements of a piezoelectric energy converter for power harvesting in autonomous microsystems," *IEEE Trans. Instrum. Meas.*, vol. 55, no. 6, pp. 2096–2101, Dec. 2006.

[12] M. Karami, O. Bilgen, D. Inman, and M. Friswell, "Experimental and analytical parametric study of single-crystal unimorph beams for vibration energy harvesting," *IEEE Trans. Ultrason., Ferroelectr., Freq. Control*, vol. 58, no. 7, pp. 1508–1520, Jul. 2011.

[13] J. J. Ruan, R. A. Lockhart, P. Janphuang, A. V. Quintero, D. Briand and N. de Rooij, "An Automatic Test Bench for Complete Characterization of Vibration-Energy Harvesters," in *IEEE Transactions on Instrumentation and Measurement*, vol. 62, no. 11, pp. 2966-2973, Nov. 2013.

The 5th Interneational Conference on Engineering, Applied Sciences and Technology (ICEAST 2019)

Performance and Behavior Analysis of Piezoelectric Energy Harvesting Floor Tiles

Phosy Panthongsy and Don Isarakorn*
Department of Instrumentation and Control Engineering, Faculty of Engineering
King Mongkut's Institute of Technology Ladkrabang
Bangkok, 10520 Thailand
don.is@kmitl.ac.th

Kazuhiko Hamamoto
Department of Information Media Technology,
School of Information and Telecommunication Engineering
Tokai University
2-3-23 Takanawa Minato-ku Tokyo
108-8619 Japan

Pattanaphong Janphuang
Synchrotron Light Research Institute
111 University Avenue, Muang District, Nakhon Ratchasima, 30000
Thailand

***Abstract*—This paper presents the performance and behavior analysis of two unlike piezoelectric energy harvesting floor tiles in which they are functioned with different frequency up-conversion strategies to achieve the high energy conversion efficiency from low and variable-frequency vibration as the human footstep. One of such strategies is to convert the frequency of piezoelectric bimorph up through the magnetic interaction between a permanent magnet and an iron plate, while another one is achieved on that through the mechanical impact between a cover plate and a wall of the floor tile. Experimentally, the floor tiles having one piezoelectric bimorph inside of them are prototyped and then mounted to their individual input-exciting kit to investigate the energy harvesting performance. The input-exciting kits are employed to simulate the human footstep on floor tiles. The results show that the floor tile with frequency up-converting mechanism based on mechanical impact should be a better option for energy harvesting from human footstep due to the low-profile structure and good energy harvesting performance. Moreover, its operational way can result in long-lasting piezoelectric bimorph. When a cover plate is actuated to move down with the velocity of 54.13 mm/s and then released, the floor tile can produce the average power of 0.82 mW at load resistance approximately of 55.68 kΩ.**

Keywords— Piezoelectric energy harvester, frequency up-conversion techniques, energy harvesting floor tiles, low-frequency vibration energy harvesting

I. Introduction

With plenty of vibrations available in the surrounding environment, converting kinetic energy into useable electricity for powering the low-power wireless electronic devices is of much interest. The vibration energy harvesting is possible through three kinds of transduction approaches including electrostatic [1], [2], electromagnetic [3], [4] and piezoelectric [5], [6]. Among them, the piezoelectric energy harvester has received great attention from many researchers and become ubiquitous in a variety of wireless applications (e.g. health monitoring, structure monitoring and industrial process monitoring) due to the simple structure, ease of configuration, high output power and high energy generation efficiency [7]. Its electricity output is commonly provided to power up the aforementioned electronic devices where hard wiring and, furthermore, is used instead of the power source from batteries to avoid several issues such as depleted battery replacement, limited energy storage capacity and toxic waste.

One difficulty in vibration energy harvesting is the low and variable frequency of vibration sources, which usually deviate from the resonant frequency of harvester. The mismatch between both frequencies causes a decrease in energy conversion efficiency. To overcome this problem, the piezoelectric energy harvester combined with frequency up-converting mechanism has been investigated [8]–[10]. The frequency up-converting mechanism is used to deflect the piezoelectric component of harvester initially and then leave it to freely oscillate at high frequency, regardless of the external input vibration. The initial deflection in frequency up-conversion can be performed by non-contact magnetic plucking or mechanical contact. These methods present the best performance depending on the application.

Therefore, the purpose of this paper is to examine the performance and behavior of two energy harvesting floor tiles operated with different types of frequency up-converting mechanism for increasing the efficiency in human footstep energy harvesting. One of frequency up-converting mechanisms induces the initial deflection of piezoelectric cantilever through magnetic plucking and another one is based on a mechanical impact. Following the arrangement of this work, the overall structure and operational stage of both energy harvesting floor tiles is first presented. Their prototypes are then configured for evaluation of energy harvesting performance. After that, the experimental results are discussed and compared. Finally, the conclusion is given.

II. Description of Energy Harvesting Floor Tiles (EHFTs)

A. EHFT Using a Magnetic Plucking Mechanism

The schematic drawing of the EHFT using a magnetic plucking mechanism is shown in Fig. 1(a). The cover plate is placed as a tile surface supported by springs. Its underneath is attached with an iron plate. A base of a piezoelectric bimorph is fixed to the supporter, free end of which is attached to a proof mass glued with a permanent magnet; a proof mass is used to increase the strain in the piezoelectric material, leading an increase in output electricity. When the floor tile is stepped on, the cover plate is pushed down to compress the springs, thus an iron plate is attracted by a permanent magnet at where a cover plate contacts a wall. Closing between iron plate and permanent magnet causes that piezoelectric bimorph is deflected initially as shown in Fig. 1(b). The displacement of piezoelectric bimorph is limited by a stopper to prevent the damage from over bending. Suddenly a foot is moved up away from the floor tile, the springs will push the cover plate up. As the result, the iron plate is rapidly separated from the permanent magnet as illustrated in Fig. 1(c), thus the piezoelectric bimorph is left to freely oscillate at high frequency.

AUN/SEED-Net (JICA) and NRCT

978-1-7281-0067-8/19/$31.00 ©2019 IEEE

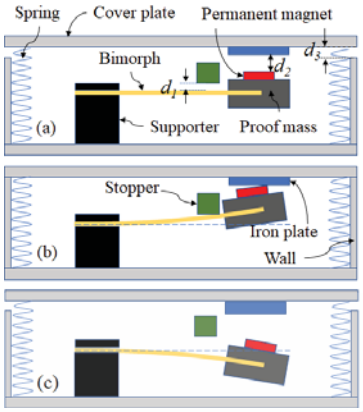

Fig. 1. Structure and operational sequence of the EHFT using a magnetic plucking mechanism; (a) no load; (b) loaded; and (c) unloaded states.

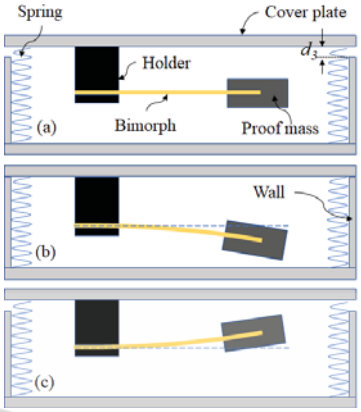

Fig. 2. Structure and operational sequence of the EHFT using a mechanical impact mechanism; (a) no load; (b) loaded; and (c) unloaded states.

B. EHFT Using a Mechanical Impact Mechanism

The structure of the EHFT using a mechanical impact mechanism is depicted in Fig. 2(a). A cover plate is placed on top of the springs. A holder is fixed to the underneath of a cover plate to hold a base of piezoelectric bimorph. A free end of piezoelectric bimorph is attached with a proof mass. During stepping on the floor tile, a cover plate is pushed down to compress the springs and impact a wall as illustrated in Fig. 2(b). The mechanical impact between a cover plate and a wall plucks a proof mass down. Thus, the piezoelectric bimorph is deflected initially in the down direction and then release itself to oscillate freely. In addition, when a floor tile is unloaded as shown in Fig. 2(c), the cover plate is bounced up by the compressed springs. While the cover plate is reaching a top position, a proof mass will be plucked up through the restoring force of springs, making the piezoelectric bimorph deflect initially in the up direction and then let itself to oscillate freely.

III. Experimental Setup and Methods

To investigate the energy harvesting performance and behavior of both EHFTs, the following structures of which were constructed first as a schematic drawing shown in Fig. 3(a) and Fig. 4(a), respectively. The parameters setup was listed in Table I, where d_1 is the gap between a bimorph and a stopper; d_2 is the gap between a permanent magnet and an iron plate; and d_3 is the gap between a cover plate and a wall. The piezoelectric bimorph consists of two piezoelectric layers (PZT-5H) and three elastic layers (RF4). Next, both EHFTs were integrated into their individual input-exciting kit used for simulating the human footstep. The EHFT using a magnetic plucking mechanism was set up as in Fig. 3(b). The snail cam was connected to the shaft of motor. And, the follower was glued on the cover plate. Hence, when a snail cam was driven to pass through the follower, the cover plate could be excited as stepped on by a pedestrian. On the other hand, the EHFT using a mechanical impact mechanism was configured as shown in Fig. 4(b). The footstep was simulated by a pneumatic actuator. At last, both EHFTs were excited for the investigation of the energy harvesting performance and behavior. The exciting ways were designed due to the feature of each EHFT. Operationally, the EHFT using a magnetic plucking mechanism was excited by rotating a snail cam with a fixed angular velocity. And, the EHFT using a mechanical impact mechanism was actuated with several force which could be observed from the moving velocity of a cover plate through an accelerometer (EI-CALC).

Moreover, the produced electricity was examined with various load resistors; herein, the piezoelectric bimorph is connected to a resistor (R_L) in series. The output voltage was measured by an oscilloscope (Tektronix TDS3032B). The average generated power (P_{Avg}) and energy (E) at time t_N can be calculated by using the equations [11]:

$$P_{Avg}(t_N) = \frac{1}{t_N}\int_0^{t_N} \frac{V_L^2(t)}{R_L} dt \quad (1)$$

$$\text{and } E(t_N) = \sum_{n=0}^{N} \frac{V_L^2(t_n)}{R_L} \Delta t_n \quad \text{for N>0,} \quad (2)$$

where a subscript N represents the number of sampled voltages; $V_L(t_n)$ is the voltage across resistive load at time t_n; n = 0,1,2,3…indicates the sampled voltage at a particular time; and Δt_n is the sampling interval. A load resistor leading to achieve the maximum electricity output was used in the characterization of energy harvesting behavior of the EHFTs.

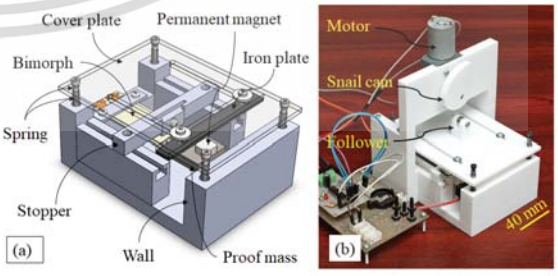

Fig. 3. (a) Schematic drawing of the EHFT using a magnetic plucking mechanism and (b) its experimental setup.

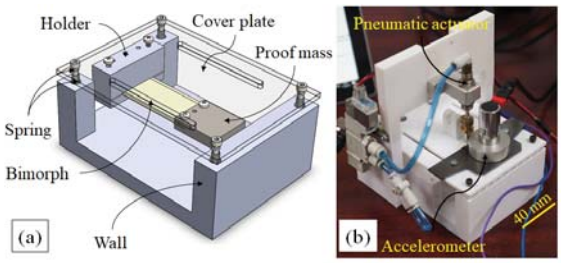

Fig. 4. (a) Schematic drawing of the EHFT using a mechanical impact mechanism and (b) its experimental setup.

TABLE I. PARAMETERS SETUP

Parameters	Dimensions	
	EHFT using a magnetic plucking mechanism	***EHFT using a mechanical impact mechanism***
Piezoelectric bimorph	71.0 x 25.4 x 0.71 mm^3	71 x 25.4 x 0.71 mm^3
Free length of bimorph	48.0 mm	48.0 mm
Mass (tainless steel)	30 x 26 x 6 mm^3	30 x 26 x 6 mm^3
Permant magnet	10 x 10 x 0.5 mm^3	-
d_1	1, 3 and 5 mm	-
d_2	18 mm	-
d_3	4 mm	4 mm

IV. EXPERIMENTAL RESULTS, DISCUSSION AND COMPARISON

In the experimental study of the EHFT using a magnetic plucking mechanism, a snail cam was rotated with a fixed angular velocity of 8 rad/s to pass through the follower. The reason for fixing angular velocity is because the different input excitations have no effect on electricity output for this mechanism. Initially, the gap between a stopper and a piezoelectric bimorph (d_1) was set to 1 mm. This EHFT generated the peak to peak voltage of 39.4 V as shown in the Fig.5. Its free oscillating frequency (f) was found to be 13.88 Hz regarding to the oscillation period (T); f=1/T. By changing the value of load resistor mechanically, the graphs in Fig.6 were obtained. A load resistance of approximately 55.68 kΩ at the maximum power output was chosen for studying the effect of gab d_1 on electricity output. When d_1 was increased from 1 to 3 and 5 mm, as can be seen in Fig.7, the average output power and energy went up significantly from 0.16 to 0.51 and 0.98 mW and 0.42 to 1.26 and 2.37 mJ, respectively.

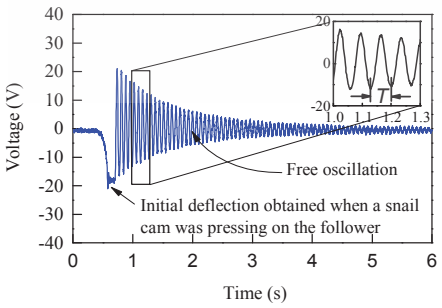

Fig. 5. Output voltage from using d_1 = 1 mm.

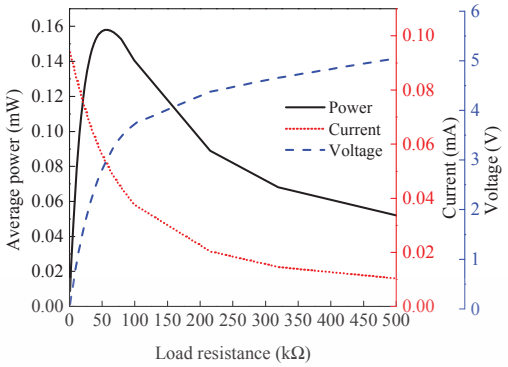

Fig. 6. Average output power with d_1 = 1 mm versus load resistor values.

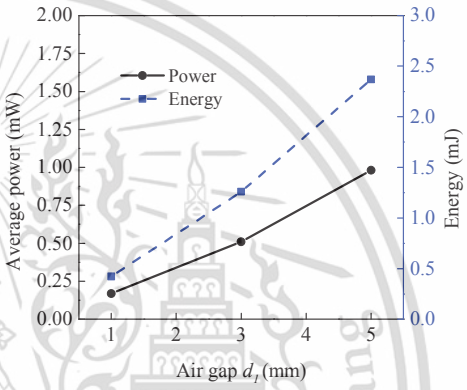

Fig. 7. Average output power and energy with increasing the gap d_1.

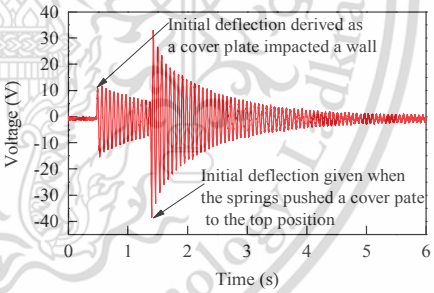

Fig. 8. Voltage generated when the cover pate was moved down with the velocity of 24.50 mm/s.

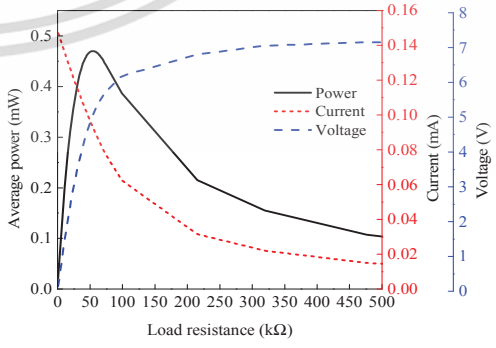

Fig. 9. Average output power across various load resister obtained from pushing the cover plate down with the velocity of 24.50 mm/s.

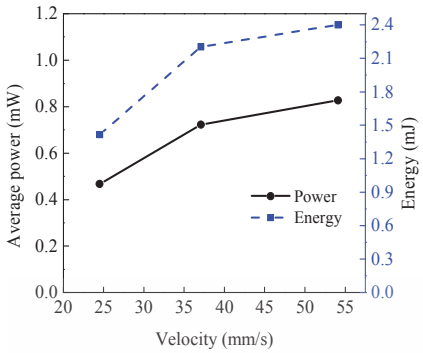

Fig. 10. Average output power and energy as the velocity of a cover plate was increased.

For the EHFT using a mechanical impact mechanism, a cover plate was pushed to move down with the velocities of 24.50, 31.10 and 54.13 mm/s. It assumed that the floor tile was stepped on by several pedestrians having different body weight. The higher velocity is for a heavyweight walker and lower for a lightweight walker. At 24.50 mm/s, this EHFT produced the peak to peak voltage of 71.2 V with a free oscillating frequency of 14.08 Hz as illustrated in Fig.8. The load resistance of approximately 55.68 kΩ could be found at the maximum power as demonstrated in Fig.9, which was further used to investigate the effect of input excitation on electricity output. With making the velocity of a cover plate increase orderly, the average output power and energy rose from 0.47 to 0.72 and 0.82 mW and 0.96 to 1.67 and 2.40 mJ, respectively as plotted in Fig. 10. A slight increase in the amount of electricity where a velocity of the cover plate increase from 31.10 to 54.13 mm/s can rely on the relationship between a plucking proof mass and a reflected piezoelectric bimorph; a proof mass deflected piezoelectric bimorph initially with a bit larger displacement.

Throughout this work it was noticeable that:

• *For the EHFT* using a magnetic plucking mechanism: It had a bit complex structure, which gave the high energy conversion for using a large gap between a stopper and a piezoelectric bimorph. The direct contact between a piezoelectric bimorph and a stopper may cause a decrease in longevity of piezoelectric bimorph. In the energy harvesting, varying force of input excitation, i.e. heavier or lighter walker, had no effect on electricity output. However, the electrical energy was produced only after the cover plate was unloaded, while stepping on the cover plate was for inducing the initial deflection.

• *For the EHFT* using a mechanical impact mechanism: It could be easily configured with a simple structure. The frequency up-converting mechanism was not directly contact on piezoelectric bimorph for inducing the initial deflection, thus piezoelectric bimorph could be long-lasting. In addition, the electricity output was directly proportional to the force of input excitation, the high amount of which was observed at high velocity of a cover plate. Interestingly, the electrical energy can be harvested when the floor tile is loaded and unloaded.

Regarding to the structure profile, operational strategy and energy harvesting performance of both EHFTs, the EHFT using a mechanical impact mechanism is of much interest. It should be better than the EHFT using a magnetic plucking mechanism in term of the long-lasting use and harvesting energy from pedestrian in both crowded and uncrowded areas.

V. Conclusion

Two energy harvesting floor tiles especially aimed to harvest energy from human footstep were proposed in this paper. The different frequency up-conversion techniques used to increase the energy conversion efficiency were depicted. One of these techniques was based on magnetic interaction and another was formed on the mechanical impact. To find the best the floor tile, the comparative study of both floor tiles was implemented. Initially, their prototypes consisting of one piezoelectric inside were fabricated and then evaluated with the input-exciting kit. By considering the experimental results, structure and operational characteristic, the best floor tile could be found at last.

Acknowledgments

The authors gratefully thank to the National Research Council of Thailand for financial support. Mr. Phosy Panthongsy would like to express his sincere appreciation to the AUN/SEED-Net for the fully financial support in his PhD degree education.

References

[1] L. G. W. Tvedt, D. S. Nguyen, and E. Halvorsen, "Nonlinear Behavior of an Electrostatic Energy Harvester Under Wide- and Narrowband Excitation," *J. Microelectromechanical Syst.*, vol. 19, no. 2, pp. 305–316, Apr. 2010.

[2] P. D. Mitcheson, P. Miao, B. H. Stark, E. M. Yeatman, A. S. Holmes, and T. C. Green, "MEMS electrostatic micropower generator for low frequency operation," *Sens. Actuators Phys.*, vol. 115, no. 2, pp. 523–529, 2004.

[3] P. Glynne-Jones, M. J. Tudor, S. P. Beeby, and N. M. White, "An electromagnetic, vibration-powered generator for intelligent sensor systems," *Sens. Actuators Phys.*, vol. 110, no. 1, pp. 344–349, 2004.

[4] L. C. Rome, L. Flynn, E. M. Goldman, and T. D. Yoo, "Generating electricity while walking with loads.," *Science*, vol. 309 5741, pp. 1725–8, 2005.

[5] D. Zhu, S. P. Beeby, M. J. Tudor, and N. R. Harris, "A credit card sized self powered smart sensor node," *Sens. Actuators Phys.*, vol. 169, no. 2, pp. 317–325, 2011.

[6] N. Jackson, R. O'Keeffe, F. Waldron, M. O'Neill, and A. Mathewson, "Evaluation of low-acceleration MEMS piezoelectric energy harvesting devices," *Microsyst. Technol.*, vol. 20, no. 4, pp. 671–680, Apr. 2014.

[7] S. Roundy and P. K. Wright, "A piezoelectric vibration based generator for wireless electronics," *Smart Mater. Struct.*, vol. 13, no. 5, pp. 1131–1142, Aug. 2004.

[8] Y. Zhang and C. S. Cai, "A retrofitted energy harvester for low frequency vibrations," *Smart Mater. Struct.*, vol. 21, no. 7, p. 075007, Jun. 2012.

[9] P. Pillatsch, E. M. Yeatman, and A. S. Holmes, "A piezoelectric frequency up-converting energy harvester with rotating proof mass for human body applications," *Sens. Actuators Phys.*, vol. 206, pp. 178–185, 2014.

[10] Y. Kuang, Z. Yang, and M. Zhu, "Design and characterisation of a piezoelectric knee-joint energy harvester with frequency up-conversion through magnetic plucking," *Smart Mater. Struct.*, vol. 25, no. 8, p. 085029, Jul. 2016.

[11] P. Janphuang, R. A. Lockhart, D. Isarakorn, S. Henein, D. Briand, and N. F. de Rooij, "Harvesting Energy From a Rotating Gear Using an AFM-Like MEMS Piezoelectric Frequency Up-Converting Energy Harvester," *J. Microelectromechanical Syst.*, vol. 24, no. 3, pp. 742–754, Jun. 2015.

เลขที่อนุสิทธิบัตร 14609

อสป/200 - ข

อนุสิทธิบัตร

อาศัยอำนาจตามความในพระราชบัญญัติสิทธิบัตร พ.ศ. 2522
แก้ไขเพิ่มเติมโดยพระราชบัญญัติสิทธิบัตร (ฉบับที่ 3) พ.ศ. 2542
บดีกรมทรัพย์สินทางปัญญาออกอนุสิทธิบัตรฉบับนี้ให้แก่

สถาบันเทคโนโลยีพระจอมเกล้าเจ้าคุณทหารลาดกระบัง

สำหรับการประดิษฐ์ตามรายละเอียดการประดิษฐ์ ข้อถือสิทธิ และรูปเขียน (ถ้ามี)
กฏในอนุสิทธิบัตรนี้

ขที่คำขอ 1803001351

ขอรับอนุสิทธิบัตร 14 มิถุนายน 2561

ะดิษฐ์ นายดอน อิศราภร และ นายโพสี ปานทองสี

สดงถึงการประดิษฐ์ อุปกรณ์ทดสอบคุณสมบัติของเพียโซอิเล็กทริก
โดยใช้วิธีการแบบสั่นต่อเนื่อง

ให้ผู้ทรงอนุ สิทธิและหน้าที่ตามกฎหมายว่าด้วยสิทธิบัตรทุกประการ

ออกให้ ณ วันที่ 16 เดือน พฤศจิกายน พ.ศ. 2561

หมดอายุ ณ วันที่ 13 เดือน มิถุนายน พ.ศ. 2567

(ลงชื่อ).....

(นายดิเรก นุญแท้)

รองอธิบดีกรมทรัพย์สินทางปัญญา ปฏิบัติราชการแทน

อธิบดีกรมทรัพย์สินทางปัญญา

ผู้ออกอนุสิทธิบัตร

พนักงานเจ้าหน้าที่

หมายเหตุ
1. ผู้ทรงอนุสิทธิบัตรต้องชำระค่าธรรมเนียมรายปีเริ่มแต่ปีที่ 5 ของอายุสิทธิบัตร มิฉะนั้น อนุสิทธิบัตรจะสิ้นอายุ
2. ผู้ทรงอนุสิทธิบัตรจะขอชำระค่าธรรมเนียมรายปีล่วงหน้าโดยชำระทั้งหมดในคราวเดียวก็ได้
3. ภายใน 90 วันก่อนวันสิ้นอายุอนุสิทธิบัตร ผู้ทรงอนุสิทธิบัตรมีสิทธิขอต่ออายุอนุสิทธิบัตรได้ 2 คราว มีกำหนดคราวละ 2 ปี โดยยื่นคำขอต่ออายุ ต่อพนักงานเจ้าหน้าที่
4. การอนุญาตให้ใช้สิทธิตามอนุสิทธิบัตรและการโอนอนุสิทธิบัตรต้องทำเป็นหนังสือและจดทะเบียนต่อพนักงานเจ้าหน้าที่

038489

(19) **กรมทรัพย์สินทางปัญญา**
กระทรวงพาณิชย์
เลขที่อนุสิทธิบัตร 14609

(11) **เลขที่ประกาศโฆษณา** 14609
(43) **วันประกาศโฆษณา** 16 พฤศจิกายน 2561
(40) **วันออกอนุสิทธิบัตร** 16 พฤศจิกายน 2561

(12) ประกาศโฆษณาการจดทะเบียนการประดิษฐ์และออกอนุสิทธิบัตร

(21) **เลขที่คำขอ** 1803001351
(22) **วันที่ยื่นคำขอ** 14 มิถุนายน 2561

(51) **สัญลักษณ์จำแนกการประดิษฐ์ระหว่างประเทศ Int.Cl.10**
G01R 29/22, G02F 1/13

(31) **เลขที่คำขอที่ยื่นครั้งแรก**
-

(32) **วันที่ยื่นคำขอครั้งแรก**
-

(33) **ประเทศที่ยื่นคำขอครั้งแรก**
-

(71) **ผู้ขอรับสิทธิบัตร**
สถาบันเทคโนโลยีพระจอมเกล้าเจ้าคุณทหารลาดกระบัง

(72) **ผู้ประดิษฐ์**
นายคอน อิศรากร
Mr.Phosy Panthongsy

(74) **ตัวแทน**
นางสาวณิชยา สืบสุข
ที่อยู่ สถาบันเทคโนโลยีพระจอมเกล้าเจ้าคุณทหารลาดกระบัง
สำนักบริหารงานวิจัยและนวัตกรรมพระจอมเกล้าลาดกระบัง
เลขที่ 1 ซอยฉลองกรุง 1 แขวงลาดกระบัง เขตลาดกระบัง
กรุงเทพมหานคร 10520

(54) **ชื่อที่แสดงถึงการประดิษฐ์** อุปกรณ์ทดสอบคุณสมบัติของเพียโซอิเล็กทริกโดยใช้วิธีการแบบสั่นต่อเนื่อง

(57) **บทสรุปการประดิษฐ์**

อุปกรณ์ทดสอบคุณสมบัติของเพียโซอิเล็กทริกโดยใช้วิธีการสั่นแบบต่อเนื่องตามการประดิษฐ์นี้เป็นอุปกรณ์ที่ออกแบบการทำงานให้คล้ายคลึงกับเครื่องมือหรืออุปกรณ์เก็บเกี่ยวพลังงานจากเพียโซอิเล็กทริกออกแบบกลไกโดยใช้หลักการเพิ่มความถี่ ที่ทำให้เพียโซอิเล็กทริกที่นำมาทดสอบเกิดการสั่น โดยเริ่มที่ความถี่ค่าหนึ่งจนหยุดนิ่ง วิธีนี้ทำให้ได้ลูกสัญญาณ 1 ชุดข้อมูล สามารถนำข้อมูลที่ได้มาวิเคราะห์หาค่าพลังงานและค่ากำลังได้ และหากกลไกทำซ้ำ จะทำให้สามารถวิเคราะห์ค่าความคงทนของเพียโซอิเล็กทริกได้ ทำให้การเลือกใช้เพียโซอิเล็กทริกมีประสิทธิภาพสูงที่สุด

(11) เลขที่ประกาศโฆษณา 14609

ข้อถือสิทธิ

1. อุปกรณ์ทดสอบคุณสมบัติของเพียโซอิเล็กทริกโดยวิธีการแบบสั่นต่อเนื่อง ประกอบด้วย

- โครงสร้างหลักส่วนฐาน (1a) ซึ่งอุปกรณ์ดังกล่าวประกอบเข้ากับโครงสร้างรูปตัวแอล (2) และมีมอเตอร์ (3) ยึดติดเข้ากับโครงสร้างรูปตัวแอล (2) เพื่อทำหน้าที่เป็นต้นกำลังและส่งผ่านลูกเบี้ยว (4) ที่ยึดเข้ากับแกนหมุนมอเตอร์ (3) ให้เคลื่อนที่มากระทบกับแท่น (5a) ที่ภายในบรรจุตลับลูกปืน (6) เพื่อกดให้แผ่นตามลูกเบี้ยว (Follower) (5b) เคลื่อนที่ลง

- โครงสร้างหลักส่วนฐานรูปตัวยู (1b) ซึ่งอุปกรณ์ดังกล่าวประกอบด้วย ฐานรองรับรางคู่ (12) ที่ส่วนบนของฐานรองรับรางคู่ (12) ยึดติดเข้ากับคานหยุด (10) ที่ตำแหน่งกึ่งกลางของคานหยุด (10) มีร่องสำหรับติดตั้งหมุดหยุด (11) และที่ปลายด้านหนึ่งของเพียโซอิเล็กทริก (9) ยึดเข้ากับแผ่นขั้วไฟฟ้า (13a) ที่ประกบรวมอยู่เข้ากับขั้วนำไฟฟ้า (13b) ด้วยน็อตยึดขั้วไฟฟ้า โดยที่แผ่นขั้วไฟฟ้าดังกล่าวจะต่อเชื่อมเข้ากับอุปกรณ์วัดทางไฟฟ้า (16) และที่ปลายอีกด้านหนึ่งของของเพียโซอิเล็กทริก (9) ยึดติดเข้ากับแท่นยึดแม่เหล็ก (15) ซึ่งที่แท่นยึดแม่เหล็กดังกล่าวจะติดเข้ากับแม่เหล็ก (14) เพื่อทำหน้าที่ดูดติดเข้ากับแท่งโลหะเหนี่ยวนำ (7)

โดยมีลักษณะเฉพาะคือ

แผ่นตามลูกเบี้ยว (Follower) (5b) ถูกเจาะใส่น็อต และสวมสปริง (8a) (8b) ทับน็อตอีกชั้นหนึ่ง เพื่อทำหน้าที่รองรับแรงกดและแรงดีด ที่ส่วนบนของแผ่นตามลูกเบี้ยว (Follower) (5b) ยึดติดเข้ากับแท่น (5a) ที่ภายในบรรจุตลับลูกปืน (6) ในตำแหน่งตรงกับจุดกลางที่ลูกเบี้ยว (4) กระทำ ส่วนที่ด้านข้างตามแนวยาวของแผ่นตามลูกเบี้ยว (Follower) (5b) ทั้งสองข้าง ถูกทำให้เป็นร่อง ให้ระยะห่างจากขอบแผ่นถึงร่องมีระยะเดียวกันกับตำแหน่งของฐานรองรับรางคู่ (12) ซึ่งฐานรองรับรางคู่ดังกล่าวจะมีระยะห่างระหว่างกันไม่น้อยกว่าขนาดของแผ่นตามลูกเบี้ยว (Follower) (5b) ที่ด้านล่างของแผ่นตามลูกเบี้ยว (Follower) (5b) มีแท่งโลหะเหนี่ยวนำ (7) ยึดติดเข้ากัน โดยขนาดความยาวของแท่งโลหะเหนี่ยวนำ (7) จะมีขนาดเดียวกันกับขนาดความกว้างของแผ่นตามลูกเบี้ยว (Follower) (5)

แท่งโลหะเหนี่ยวนำ (7) สามารถปรับเลื่อนให้อยู่ในตำแหน่งเดียวกันกับแม่เหล็ก (14) โดยการเหนี่ยวนำทางแม่เหล็กจะเกิดขึ้นระหว่างแท่งโลหะเหนี่ยวนำ (7) ที่ยึดอยู่ใต้แผ่นตามลูกเบี้ยว (Follower) (5b) กับแม่เหล็ก (14) ที่ซึ่งติดอยู่ด้านบนแท่นยึดแม่เหล็ก (15) เมื่อแผ่นตามลูกเบี้ยว (Follower) (5b) ถูกกดลงมาด้วยลูกเบี้ยว (4) ในตำแหน่งต่ำที่สุด แม่เหล็ก (14) จะออกแรงดูดที่เพียงพอจะทำให้ด้านปลายของแผ่น

(11) เลขที่ประกาศโฆษณา 14609

เพียโซอิเล็กทริก (9) ที่มีแม่เหล็ก (14) ติดอยู่ เกิดการงอตัวเข้าหาแท่งโลหะเหนี่ยวนำ (7) และเมื่อแผ่นตามลูกเบี้ยว (Follower) (5) กลับสู่ตำแหน่งเริ่มต้นอย่างรวดเร็ว จะเกิดลักษณะสำคัญทางเทคนิคคือแผ่นเพียโซอิเล็กทริก (9) ดีดกลับไปเป็นความถี่ ในช่วงระยะเวลาหนึ่ง และนำค่าที่ได้มาวิเคราะห์

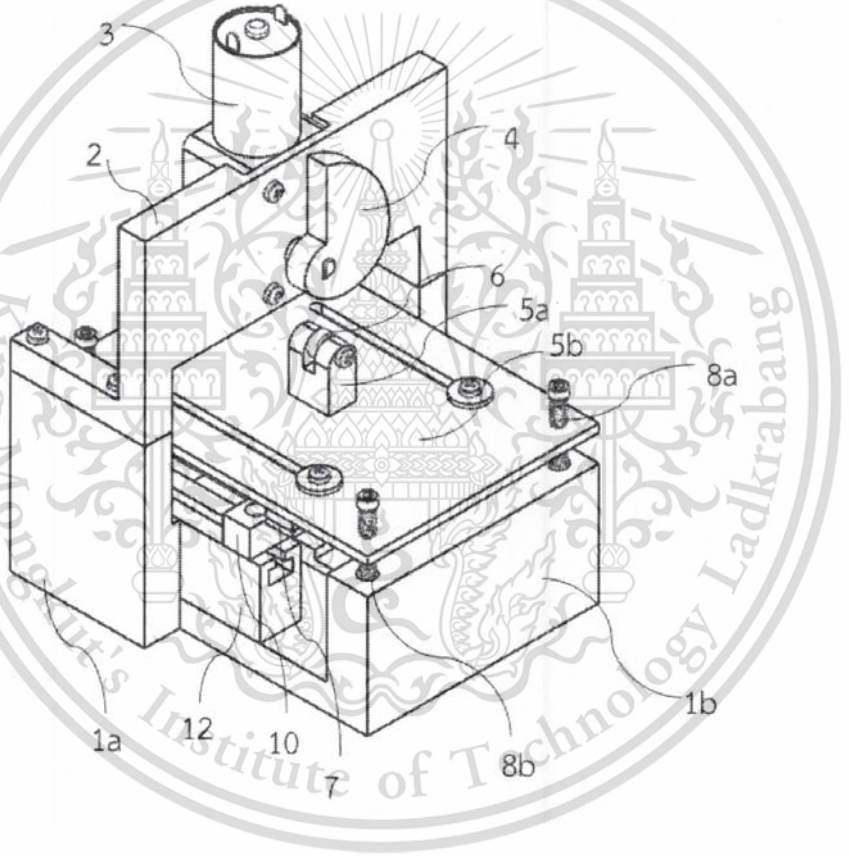

(ข้อถือสิทธิ 3 ข้อ, รูปเขียน 9 รูป)

Author Biography

The author, Phosy Panthongsy was born on September 9, 1992, in Houaphanh, Laos. He received the B.Eng. degree in electronic engineering from National University of Laos (NUOL), Laos, in 2014 and the M.Eng. degree in computing in engineering systems and the Ph.D. degree in electrical engineering from King Mongkut's Institute of Technology Ladkrabang (KMITL), Thailand, in 2016 and 2019, respectively.

When he studied at NUOL, he joined the robotics team at department of electronics and telecommunication engineering. He and his team won the second place of the 9th national robot competition in 2011 followed by the first place of the 10th national robot competition in 2012 and were awarded the first innovation prize by the 3rd job and education fair in 2014.

During his study at KMITL, he received a scholarship from the ASEAN University Network/Southeast Asia Engineering Education Development Network (AUN/SEED-Net) for the completion of master's and doctoral degrees. Moreover, he and his research team were given two awards in 2015: the best innovation award from the 8th science & technology initiative and sustainability awards and the third award from the 10th Thailand Research Expo.

In addition to the awards and honor, he was given the chances to join the exchanging and training programs as follows: the JENESYS 2.0 ASEAN youth exchange program 2013 in Japan (one week), the Short-term Study Program in Japan (SSJP) for the Japanese Fiscal Year (JFY) 2017 under the JICA project (one month) and the long-SSJP for JFY 2018 (four months).

His research interests are in the energy harvesting systems, micro power management and robotics.